Alma Mater Studiorum - Università di Bologna

DOTTORATO DI RICERCA IN

SCIENZE CARDIO NEFRO TORACICHE

Ciclo 35

Settore Concorsuale: 06/E1 - CHIRURGIA CARDIO - TORACO - VASCOLARE

Settore Scientifico Disciplinare: MED/21 - CHIRURGIA TORACICA

PATHOPHYSIOLOGY OF BILE ACID ASPIRATION IN LUNG TRANSPLANT RECIPIENTS

Presentata da: Andreacarola Urso

Coordinatore Dottorato

Gaetano Domenico Gargiulo

Supervisore

Niccolò Daddi

Co-supervisore

Franco D'Ovidio

Esame finale anno 2023

TABLE OF CONTENTS

CHAPTER 1 Pathophysiology of gastro-esophageal reflux aspiration

Pathophysiology and histopathology of reflux aspiration

The globally accepted definition of gastro-esophageal reflux disease (GERD) has been established in the Montreal consensus as the rise of stomach contents being the direct cause of symptoms or complications (Vakil et al., 2006)Vakil et al. 2006. The classification of GERD is subdivided in two major branches: esophageal and extra-esophageal. The esophageal branch, as will be discussed later in this section, involves the most common complications endured upon acute or chronic reflux symptoms, such as belching, dysphagia, chest pain, esophageal adenocarcinoma, ulceration and Barrett's esophagus. The extra-esophageal branch instead refers to the repercussions of the reflux of stomach contents in other organs proximal to the esophagus, such as the larynx, the pharynx, and the lungs.

The acute symptomatology of esophageal GERD often involves discomfort in the chest, perceived as retrosternal heartburn, and the regurgitation or flux of gastric contents to the hypopharynx. While the biochemical composition of the refluxate will be discussed later in this chapter, upon chronic exposure to acidic compounds in the relatively basic microenvironment of the esophagus, three common non-acute manifestations have been identified. Non-erosive reflux disease (NERD) has a prevalence of 60-70% in the patient population and involves typical reflux symptoms without mucosal erosion, which suggests

that this condition often presents with negative endoscopies and pH studies (de Bortoli et al., 2016). Erosive esophagitis (EE), which affects about 30% of the population, instead is the most identified endoscopic abnormality of mucosal erosion. According to the 2017 Lyon consensus, the lesions are often identified in the distal esophagus if of substantial severity, which is described by the Los Angeles classification (grade A-D) (Gyawali et al., 2018). Management of EE is suboptimal as the constant transit of boluses through the esophageal lumen, along with the detrimental acidic reflux does not allow for proper mucosal healing. Indeed, EE lesions lead to the third most common manifestation, which is Barrett's esophagus (BE) (Vaezi et al., 2022). This manifestation involves cellular transitions, within the esophageal lumen, from a stratified squamous to a metaplastic columnar epithelium. As the transitions extend along the lining, BE can lead to the development of esophageal adenocarcinoma (EAC).

The pathophysiology of gastric reflux has been deemed to be a combination of multiple abnormalities within the distal esophageal and proximal gastric region.
Those known as gastric factors, mainly involve abnormalities with gastric emptying, acid build-up, duodenal reflux, and visceral hypersensitivity (Savarino et al., 2020).

The delayed emptying of the stomach has been associated with transient LES relaxations (TLESR) and esophageal reflux, and the lasting proximity of gastric contents to the lower esophageal sphincter may facilitate their retrograde access to the esophagus, as well as increase the concentration of gastric juices for the breakdown of the bolus. Indeed, a pocket of acidic gastric juice is known to be located at the esophagogastric junction, which is proximal enough for no buffering to occur, and can extend into the lower esophageal sphincter in patients with GERD. Thus, the proximity of the pocket increases

the concentration of acid in the esophagus upon reflux, where the stomach pH is approximately 4, the refluxate pH within the esophagus becomes almost 1.7. To be noted, patients with GERD have not been identified as a population with an increased production of stomach acid, though the contribution of duodenal reflux, inclusive of pancreatic enzymes and bile acids, has been acknowledged as a valid contributor. The detrimental effects of gastric reflux acidity have been chiefly related to the common esophago-diaphragmatic dysmotility and sustained esophageal contractions contributing to visceral hypersensitivity (Savarino et al., 2020).

The abnormalities known as esophageal factors comprise decreased salivation and peristalsis and compromised mucosal integrity.

The function of salivation is hydrating and unifying, yet also stimulates esophageal contraction and clearance. Upon deglutition of saliva, known to be relatively basic, peristalsis is activated and any present acid in the esophagus can be diluted (Tripathi et al., 2018). Patients with GERD present with reduced salivation, which would normally contribute 10% of the chemical neutralization of refluxate. Decreased salivation is among many factors affecting esophageal primary and secondary peristalses, which are critical for the removal of esophageal contents refluxed from the stomach. Primary peristalsis is initiated in the hypopharynx upon swallowing and can be understood as a vertical/longitudinal action in the movement of the bolus; while secondary peristalsis is the horizontal or constrictive movement of the esophageal lumen to displace it. Both have the scope to apply distal pressure directing the bolus towards the stomach. Thus, if the role of these contractions is esophageal clearance from ingested food or from refluxed material, it remains unclear whether such dysmotility is a cause or a symptom of GERD.

Alterations in the esophageal mucosa elucidate the possible histopathological abnormalities observed in the various acute and chronic outcomes of GERD. Therefore, it is important to discuss the several barriers affected upon mucosal disruption. First, is a pre-epithelial barrier mostly consisting of basic fluid, likely derived from salivary deglutition and esophageal glands. This layer is disturbed in some patients with NERD and all patients with EE, where its buffering capacity is breached through the lamina propria, where the corrosive acids initiate the dilation of intracellular junctions (DIS) (Tobey et al., 1996).

DIS may present as 'bubbling' (**Figure 1**, black arrows and arrow heads), consisting of a round bubble-like space between cells, or 'laddering' (**Figure 1**, red arrows), consisting of an elongated empty space with sparse extracellular matrix connections between cells (Figure 2) (Yerian et al., 2011). Second, is the basal hyperplasia, which involved the thickening of the basal layer driven by an expansion of the proliferative zone, usually 3-4 cell layers in thickness of 400 microns. Such expansion suggests an uncontrolled growth triggered by the damage and corrosion of acid, yet should not be measured around papillae, as their elongation is considered an additional parameter of mucosal disruption (Vakil et al., 2017). Papillary length is the third affected component of mucosa disruption as they are normally isolated to the lower third of the squamous epithelial cell layer. Upon inflammation and disruption, the squamous mucosa forces itself thorough 50% of the

Figure 1. Dilation of Intracellular Junctions

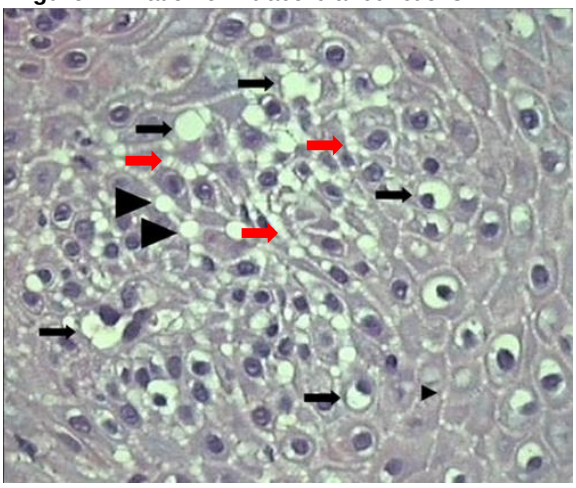

epithelial layer, affecting capillary flow (constriction, push; dilation, pull) and causing red blood cell extravasation (Tripathi et al., 2018).

The prevalence of open and healed wounds is crucial to report as an endoscopic finding as it may aid in the determination and persistence of disease. Open erosions generally are highly populated by leukocytes, which dominate the pro-inflammatory environment between squamous cells, and eosinophils, though unreliably. Necrosis can also be observed on mucosal lesions, along with granulation for forced healing. Healed wounds are instead characterized by the absence of neutrophils and necrosis, but rather the presence of a thin layer of regenerated epithelium. Reporting and monitoring open wounds is incredibly important when trying to prevent infections in patients with GERD. Lesioned epithelium is permissive of pathogen colonization. Commonly seen are *Candida albicans, Escherichia coli, Helicobacter pylori, Clostridium perfringens/difficile,* and other bacteria and viral microorganisms. As we will discuss later in this chapter, infection management is particularly important not only for esophageal and systemic health, but also for the implication pathogens have on the extra-esophageal branch of GERD.

Anatomical aspects associated with reflux aspiration

Under a developmental lens, it is critical to note that the respiratory tract, the stomach and the esophagus share embryonic origin and innervation. The vagal response to the presence of acid in the distal esophagus results in bronchospasms in both healthy individuals and those with underlying respiratory or gastric disease. However, the latter population presents with anatomical alterations which lead to increased reflux and aspiration.

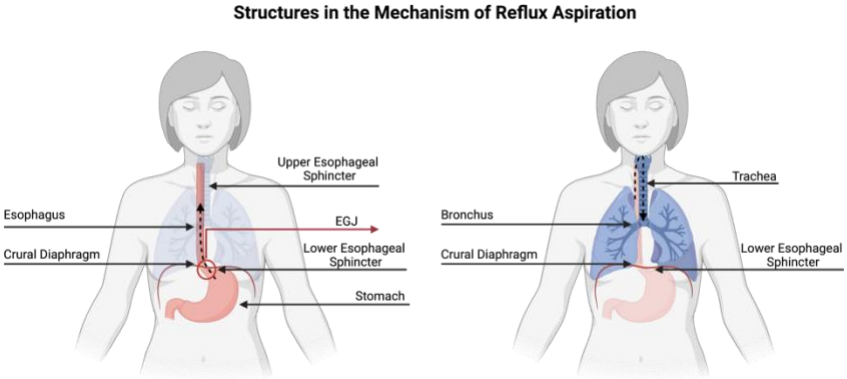

Figure 2. Relevant Gastric and Pulmonary Anatomy

There are crucial mechanical deficiencies which allow for gastric reflux and aspiration. The most prominent in GERD is the reduction of crural diaphragmatic (CD) pressure on the lower esophageal sphincter (LES) located at the esophagogastric junction (EGJ) (Savarino et al., 2020; Fass et al., 2021) (**Figure 2, left**). Thus, the success of the anti-reflux barrier is assured by a combination of factors. The LES is about 2-3 cm in length and is maintained shut by a pressure ranging between 10-30 mmHg, which is variable upon body position, gastric emptying, respiration, abdominal pressure etc. For this reason, most reflux episodes in healthy individuals occur during sleep, as the position of the body affects the pressure on the LES and facilitates the relaxation of the sphincter and the horizontal movement of fluid. However, the difference resides in two details: the acidity of the refluxate, which present as such in 30% of healthy patients, and in 70% of

those GERD; and the integrity of esophageal motility, which in healthy individuals does not allow for the refluxate to reach the proximal esophagus (Fass et al., 2021). Originally, the intrinsic contractile capacity of the LES was considered important in the early diagnosis of GERD via the LES pressure integral (LES-PI); however, this technique has been abandoned as it accounted for a fixed pressure of 20 mmHg, when individuals with different body masses present with different intrinsic LES pressures thus generating confounding results (Hoshino et al., 2011). The currently accepted measurement is the EGJ contractile integral (EGJ-CI), which calculates EGJ vigor, which includes the contractile contribution of both LES and crural diaphragm (CD) , throughout the length of three respiratory cycles (Nicodème et al., 2014). While this technique still requires standardization methods, the most common mechanical failure leading to reflux does not involve the intrinsic pressure of the LES, but rather transient LES relaxations (TLESR). TLESR are induced by CD pressure decrease and gastric tension, as following a substantial meal (Babaei et al., 2008). CD is a crucial barrier against reflux especially in instances of intragastric tension, and its pressure can be altered in the circumstances of neural inhibition, hiatal hernia, and, as elucidated in the next section, pressure differentials within the chest cavity (Fass et al., 2021). In the case of neural inhibition, the CD progressively loses the contractile stimulus leading to TLESR upon strain such as coughing or a full stomach. In the case of hiatal hernias, a space develops between the junction of the CD and the LES which leads to an axial diaphragmatic displacement and persistent refluxing upon swallowing, known as early-retrograde reflux. In the case of pressure differentials, thoraco-abdominal pressure, often observed in lung disease,

affects the contractile potential of the CD, which overrides the absence of a hiatal hernia and the integrity of the LES.

The proximity of the esophagus to the tracheal opening has linked GERD to aspiration, chronic cough and vocal cord dysfunction. Reflux aspiration entails the process of gastric reflux traveling towards the proximal end of the esophagus to then be aspirated into the trachea and reach the airways (**Figure 2, right**). There, the refluxate is expected to cause injury and bronchospasms, exacerbating inflammation and lung disease. Persistent reflux can induce chronic cough as it instigates a broncho-esophageal reflex, also known as a reflex nerve arch, where the irritation of the esophagus caused by the transit of reflux stimulates a bronchospasm in the airway, resulting in difficulty breathing. The upper esophageal sphincter (UES) normally functions as a second asymmetric barrier to prevent the said regurgitation of reflux into the airways. An incompetent UES has been identified in patients with reflux esophagitis and nocturnal asthma. However, as a striated muscle associated with digestion, its tonicity is reduced during sleeping periods, allowing for potential reflux microaspiration, which is also common in healthy individuals (Kahrilas et al., 1987). This barrier mechanism is inefficient in reflux microaspiration, which has been studied in the context of obstructive and interstitial lung pathologies.

Lung disease and reflux aspiration: a binomial reciprocity

While GERD can cause increased morbidity and mortality due to the previously discussed esophageal complications such as EE, BE and EAC, reflux aspiration can also exacerbate pulmonary pathologies by disrupting respiration and the integrity of the airway, and by introducing duodenal and gastric microorganisms (Meyer, 2015; Hsu et al., 2017). While the injurious effects of aspirated gastric contents, reflux episodes have been associated to oxygen desaturations and airway epithelial injury (Wilshire et al., 2013). With technological advances and detection strategies there is increasing evidence that reflux aspiration is associated to obstructive and interstitial lung diseases and their exacerbations. Some examples are idiopathic pulmonary fibrosis (IPF), interstitial lung disease (ILD), chronic obstructive pulmonary disease (COPD), aspiration pneumonia, cystic fibrosis (CF), non-CF bronchiectasis, and chronic lung allograft dysfunction (CLAD) post-transplantation (Lee et al., 2020). However, the discussed developmental link suggesting gastro-pulmonary axis fades the line between causality and consequence.

Reflux has been identified as an important and worsening contributor to IPF and other ILDs (Hershcovici et al., 2011). IPF is canonically considered a progressive idiopathic disorder yet the presence of fibrotic foci in bronchioles have been associated to aspiration episodes, leading to the conclusion that the exacerbation of the disorder might not be entirely idiopathic. Indeed, reflux is present in over 90% of patients diagnosed with IPF. The histologic and sparse alveolar damage, inclusive of subpleural honeycombing and bronchiectasis, suggest particulate trapping and peripheral airway damage which could be plausibly caused by aspirated gastric and pancreatic fluids. In contrast, in other ILDs such as systemic sclerosis (SS) the esophageal involvement is

much clearer and more pronounced (Hershcovici et al., 2011). The pathologic reflux episodes have been linked to the progressive severity of interstitial injury and resulting fibrosis. Thus, the reflux aspiration seen in restrictive lung diseases such as IPF and other ILDs may further reduce the total lung capacity (TLC), by definition already decreased, by accumulating fluid and induce additional scarring. It can be also inferred that the reduced TLC causes pressure differentials in the chest cavity which impact the previously discussed thoracoabdominal pressure gradient, thus inducing altered diaphragmatic contractions leading to retrograde flux.

Similarly, obstructive lung diseases such as asthma and COPD present with prevalent and often inconspicuous GERD. Although breath condensates and sputum show clear presence of pepsin, it has not been directly attributed to aspiration and does not correlate to disease severity or pH decreases, thus might be restricted to the laryngopharynx. However, patients with known pulmonary conditions like COPD, which might affect esophageal function, are often prescribed proton-pump inhibitors (PPI) and β-agonists (Mungan and Pinarbasi Simsek, 2020). PPI may account for the unchanged pH observed in the airway of COPD patients and their bronchoalveolar lavage fluid (BALF), which does not rule out microaspiration (Lee et al., 2020; Mungan and Pinarbasi Simsek, 2020). Indeed, harmed epithelium and increased incidence of aspiration pneumonias have maintained a persistent interest in GERD as contributive to COPD. The most intriguing link between the conditions is the prescription of previously mentioned β-agonists. COPD, being an obstructive disease, is characterized by normal and often increased TLC. The undue pulmonary expansion may have a substantial physiologic effect on the displacement of the CD and the resulting inefficiency of the EGJ. The

competency of the latter is dependent on the respiratory phase and, in the case of hyperinflation, may shift its pressure point thus allowing relaxation on the LES and simultaneously the partial expiration effort may delay esophageal clearance. As in asthma, the vagal and diaphragmatic responses in COPD have the potential to cause reflux episodes.

The notable prevalence of delayed gastric emptying and gastro-esophageal reflux in patients with end stage lung disease, including ILD, COPD and CF candidates for lung transplantation has been described (D'Ovidio et al., 2005b). Typical gastroesophageal reflux symptoms were documented in 63% of patients. In the hyperinflated patients COPD and CF with a flattens and stretched diaphragm the esophageal length was significantly greater than in patients with a restricted end stage lung disease as per patients with pulmonary fibrosis and scleroderma having a cupped and retracted diaphragm. These anatomical differences associated with abnormal esophageal and gastric motility. The lower esophageal sphincter was hypotensive in 72% of patients, and 33% had esophageal body dysmotility. Prolonged gastric emptying was documented in 44%, and 38% had abnormal pH testing. The overall DeMeester score for esophageal acid pH testing was above normal in 32% of patients, and 20% had abnormal proximal esophageal pH probe readings.

In bronchiectasis and CLAD, retrograde flux has been determined by BALF sampling and identification of biomarkers of reflux. Again, CF and non-CF bronchiectasis, lung transplantation, and volume reduction surgeries alter the

mobility, positioning and pressure within the chest cavity (Masuda et al., 2018). In the specific cases of bronchiectasis and lung transplantation, or in the event of CLAD, reflux aspiration has been confirmed through sampling of BALF, which revealed the presence of bile, suggesting duodenal and gastric reflux aspiration (D'Ovidio et al., 2005a, 2006; D'Ovidio and Keshavjee, 2006; Urso et al., 2018, 2021). As discussed in later chapters, the heterogeneous composition of bile is a central in airway injury and dilation, supporting its role as a biomarker for allograft dysfunction and the luminal dilation observed in bronchiectasis (McDonnell et al., 2018).

It is therefore important to consider the reciprocity between GERD and lung disease when assigning causality (Okwara and Chan, 2021). Elements such as intrathoracic pressure, vagal innervation and diaphragmatic displacement affect the tone of both the LES and the UES and predispose the individual to esophageal peristaltic dysfunction. Pulmonary and esophageal diseases may reciprocally inflict severe disorder and complicate patient treatment.

Detailed composition of refluxate

Physical properties of the refluxate

Three main factors determine the outcomes of the retrograde flux and its successive aspiration: the refluxate volume and its composition.

As all individuals present with some form of refluxing episodes, the volume of refluxate has been thoroughly studied to seek for associations with the pathogenesis of GERD. It can be presumed that an elevated amount of reflux would correspond to a higher gravity of disease. Measuring differences in reflux volume is challenging due to the unpredictability of natural reflux episodes in healthy adults and patients with GERD. Several techniques have been employed mostly based on physiologic assumptions. However, these methodologies are not entirely informative of the overall aspiration experience of the patient. They represent single timepoints and do not assess microaspiration episodes experienced beyond the hospital setting or during daytime. The first involves measuring proximal reflux, as a larger volume would be expected to travel more proximally compared to smaller volumes. A difference in exposure has been identified in a study involving 15 adult patients, monitored while supine and upright, where acid volume increased the incidence of proximal migration (Orr, 2000). Additional challenges are imposed with the ultimate dilution of the refluxate with saliva, which interferes with a reliable monitoring of number of daily / nightly reflux episodes and their volume. The second common technique is esophageal scintigraphy which will measure the volume of retrograde transport of a radiotracer such as techeitium-99 over time, which informs on the extent of peristalsis. This method is usually appropriate for early stages of GERD where patients experience initial dysphagia and increasing risk of aspiration, with the scope to track the progression of disease. It is considered an effective method of analysis specifically

upon confirmed diagnosis to determine severity, as it is relatively non-invasive and precise (Chojnowski et al., 2016). The third methodology is esophageal ultrasound to measure esophageal distension, or the increase in cross-sectional area of the esophageal lumen. This methodology also follows the assumption that increased distension, or pressure, on the barriers rhewould be induced by a larger amount of volume. Especially with intraluminal high-frequency ultrasounds (HFU) the distention, size and contents of the esophageal lumen could be easily measured in healthy and pathogenic individuals after swallowing increasing volumes of water (**Figure 3** 1mL-10mL-20mL) (Rhee et al., 2002). This technique has also proven useful for tumor staging and it is considered to be superior to cross-sectional imaging such as CT and MRI, as it shows an N stage (T: tumor invasion, N: lymph node spread, M: metastasis) accuracy of up to 88% compared the scans in the low forties and sixties (Krill et al., 2019).

Figure 3. Esophageal distention with HFU

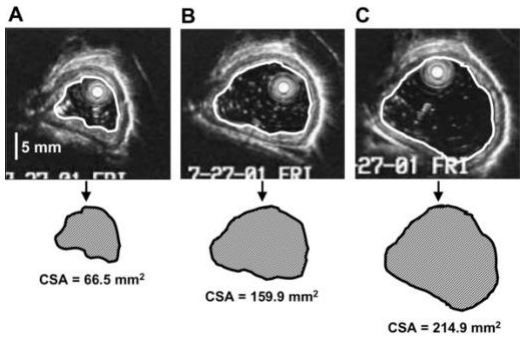

It is important to note that the extent to which refluxate travels may be dependent on other properties besides volume, such as viscosity and pressure. Reduced retrograde flux has been observed with increased viscosity, which impedes rapid and seamless flow against the esophageal barriers and towards the proximal lumen, which is a largely studied concept in enteral nutrition (Tabei et al., 2003). However, a margin of error exists in the calculation of the contribution of

viscosity to prevent overextension and maximal opening of the trans-sphincteric or esophageal lumen, as passive muscle does possess viscoelastic properties, which prompt it to reshape upon the passage of viscous material to reduce flow time (Ghosh et al., 2008). Pressure and gastric fullness also impact the frequency and flow time of gastric reflux. Episodes of reflux and aspiration have been reported more frequently post-prandially rather than upon fasting due to TLESR caused by intragastric pressure (Frankhuisen et al., 2009).

Two additional esophageal properties may affect the transit of refluxate, regardless of its composition and viscosity: peristalsis and tone (Goyal and Chaudhury, 2008). Esophageal clearance has been deemed to be independent of the constituents of the refluxate, however further molecular analyses could be performed to ascertain the irrelevance of receptor-mediated smooth muscle contractions. The role of peristalsis is to respond to the passage of a bolus by decreasing the contractile potential and inducing constriction; thus, the property mainly responds to luminal extension. Patients with GERD and aspiration have been found to have delayed peristalsis compared to healthy controls along with a lengthier interval between a reflux episode and peristaltic clearance (Goyal and Chaudhury, 2008). Vascular structures have interestingly been shown to affect peristalsis, as the surrounding compression of the esophagus potentially limits its extension and disfavors reflux loitering. The concept of compression can also be understood in the context of esophageal tone, which refers to the inherent property of smooth muscle. A more compliant distal esophagus would allow stretching and

contribute to reflux pooling at that point. Instead, increased tonicity is less permissive to pooling and stretching, rather it facilitates the distribution of the refluxate evenly towards the proximal end (Fletcher, 2004).

The properties of the refluxate affect its transit towards the proximal end, which contributes to the generation of a range of symptoms, such as hypersensitivity and aspiration.

Constituents of the refluxate

While physical properties facilitate the spread of the refluxate, its components contribute to the symptomatology of GERD and aspiration, along with the mucosal damage observed.

As discussed in the previous section, gastric pressure from stomach fullness is known to increase the probability of reflux episodes. Simultaneously, ingested food dilutes gastric juices to an acidic pH of 4; and, for this reason, post-prandial states are mistaken to be more prohibitive of acidic reflux. However, the proximity of the acid pocket to the EGJ increases the infusion of undiluted acid through the LES, which can easily reach a pH of 1.5-3.5, inducing the canonical symptomatology of acid reflux such as pronounced retrosternal heartburn. In cases of weak acidity (pH 6-7), similar symptoms are reported yet with increased delay in esophageal bruising, lesions and increased severity of esophagitis. Stomach acids have been linked to all the above symptoms as well as chronic cough. GERD patients exhibit a higher incidence of laryngitis and chronic cough and present with decreased tonicity and pressure in the UES. Physiologically this suggest a mechanism of reflux microaspiration into the airways followed by their constriction to expel the foreign fluids. The latter has been an observation in patients with both acidic (pH <4) and weakly acidic (pH 4-7) reflux. A number of studies have focused on the outcomes of acid neutralization using proton pump inhibitors (PPI) on reflux

symptoms. Importantly, while successful in the increase of reflux pH, PPI treatment does not impede reflux.

Potent proteases also contribute to the mucosal damages observed upon reflux. Pepsinogen is a proteolytic zymogen secreted by chief cells, whose bilobed structure is disrupted at low pH (<6), which activates the inert zymogen generating pepsin. While often referred to as one single protease, the composition of pepsin has been analyzed via high-performance anion exchange chromatography as a collection of isoenzymes, present in different percentages and activated at diverse pH ranges (**Figure 4**) (Bardhan et al., 2012). Pepsin 3B is the most ubiquitous and reactive in human gastric juice, as it preserves its catalytic abilities at a pH of 4.5-5. Upon reflux, pepsin adheres to the protein layer of the epithelium and damage cells from the surface in, or be endocytosed and disrupt their function from the inside out. It depletes the cell's defenses by inducing oxidative stress, disrupting mitochondrial metabolism and interfering with the cell's overall function. Intracellular changes caused by pepsin isoenzymes involve protection and function, such as the reduction in e-cadherin and the repression of the stress protein Sep70 and carbonic anhydrase (CA3) (Johnston et al., 2007). E-cadherin functions as junction protein, maintaining mucosal

Figure 4. Human pepsin isoenzymes

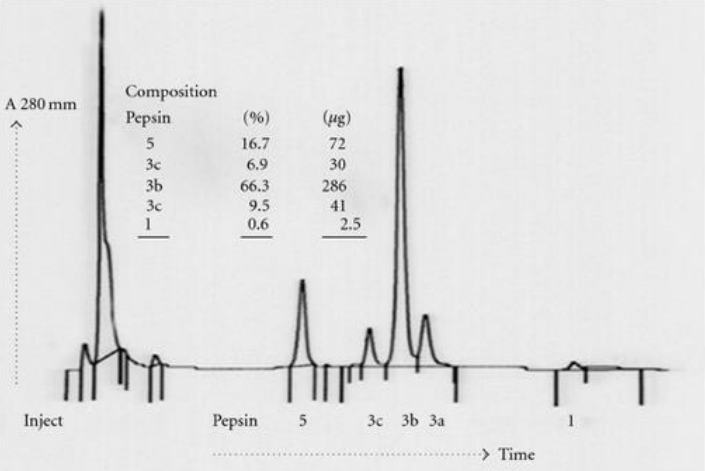

integrity and cellular adhesion; Sep70 is a molecular chaperone assisting in protein folding; and CA3 holds an important role in pH determination facilitating the conversion of carbonic acid to CO_2 and water. Pepsin has long been considered a marker of reflux and of aspiration. The esophageal and airway mucosal damage depend on the length of contact with pepsin and the pH in the microenvironment. Thus, gastric acid and pepsin proteases can certainly be damaging; however, pepsin concentrations must be substantial for it to be considered the main causative agent of mucosal disruption and cellular dysfunction upon reflux and aspiration (Rosen et al., 2012). Indeed, pepsin inhibitors have not been successful treatments for esophageal and airway epithelial injury.

The duodenal component of reflux involves the alkaline pancreatic enzymes and bile acids. Pancreatic enzymes, such as lipase and trypsin, are excluded from the pathology associated to reflux and aspiration, as the potential damage caused by these molecules is close to null due to their inactivity at acidic pH (>6). Thus, they have been deemed to impose no threat in the context discussed. Bile acids, or bile salts, while discussed with greater detail in later chapters, are variable in their structures and emulsifying functions. The physiochemical properties of bile acids allow for cellular entry as well as their actions as ligands for a variety of surface and nuclear receptors. Being stored in the gallbladder, their secretion is in proximity to the pyloric sphincter. While largely alkaline, the damage caused by the antroduodenal motility of these molecules is independent of their pH. Their effect involves solubilizing cellular membrane phospholipids, thus inducing extracellular

spillage of the cell content. In the esophagus bile acids have been identified as dilators of intracellular spaces, reducing transmucosal resistance and increasing permeability in symptomatic patients with or without the evident signs of tissue degeneration observed in esophagitis (Woodland and Sifrim, 2010). As discussed in the following section, while not immediately evident, bile acids have been deemed to be causative of microinsults at the level of both esophageal and airway mucosae.

Aspiration in lung transplant patients

Acid, pepsin and bile acids in lung disease

The organogenetic overlap between esophageal and lung disease allows for limited speculation on how they are respectively causative. Two theories have been proposed to summarize the potential cause-effect relationship between the two organs: the reflux and the reflex pathways (Ruiz de León San Juan, 2018). The reflux theory exposes esophageal dysfunction as causative of retrograde flux, which is aspirated causing airway damage. The reflex theory is based on a vasovagal esophageal-bronchial reflex of the vagus nerve controlling both the LES relaxation and the resulting bronchospasm. As previously noted, the relationship can also be bidirectional, as the esophagus and the lungs share the chest cavity, thus are physically and mechanically connected.

Various non-invasive methodologies can be utilized to measure pepsin in the esophagus and airways, such as salivary analysis and exhaled breath condensate. In several studies, the analysis of bronchoalveolar lavage fluid (BALF) and large airway bronchial washing (LABW) revealed the presence of both gastric and duodenal contents indicating aspiration of reflux. Pepsin aspiration correlated to non-acid events monitored via bronchoscopy and multichannel intraluminal impedance (MII) in patients with asthma and cough. Comparisons between healthy individuals and IPF patients also revealed increased pepsin and bile acids in BALF, which was further elevated in acute disease episodes. Similarly, in COPD it did not

associate with disease severity nor diagnosis of GERD. However, tracheal pepsinogen did show a correlation with increased inflammation and pathogen colonization, yet the contributive effect of corrosive acids and bile salts has not been documented in the study (Liu et al., 2021). Overall, as in esophageal dysfunction, pepsin can be considered a biomarker of retrograde flux.

Bile acids have instead been deemed to have much broader effects than those on the esophageal mucosa. GERD is described as one of the main comorbidities of lung disease (Lee and Ryu, 2018). In patients with aspiration, bile acids were associated to severity of lung function. However, their quantification is complex and expensive: Colorimetric assays along with liquid chromatography mass spectrometry have been used to determine relative concentrations of bile acids in BALF and LABW. While informative of their presence, exact quantification of the refluxed bile acids has been a complicated endeavor as the dilution factor attributed to both saliva, airway mucus and the saline utilized for the washing remain confounding factors (Sweet et al., 2009). Nevertheless, bile acid aspiration has been associated with disruption of the pulmonary mucosal layer (Gipson et al., 2020). A significant decrease in microbiota biodiversity was found in CF children with bile acids above the detectable level (Woods et al., 2021). Decreased oral bacteria and increased opportunistic pathogens colonized IPF, ILD and CF patients with elevated bile acid levels (Allaix et al., 2017; Al-Momani et al., 2022). Mucosal disruption allows for heme breakdown and bilirubin secretion. For this

bilirubin testing, indicative of disrupted tissue, is considered a marker of duodenogastric reflux carrying bile acids.

Reflux episodes in lung transplantation

The deleterious effects of reflux episodes observed in lung disease are considered highly detrimental in the context of lung transplantation. Aspiration is a risk factor of rejection in immunocompromised patients accepting the donor organ (Meyer, 2015). Transplant candidates are likely to present with pre-existing reflux due to the mechanical changes imposed on the diaphragm by the shift in cavity pressure caused by altered lung volume (D'Ovidio et al 2005b). This suggests that differences in intrathoracic physiology may play an important role pre and post allograft. The spontaneous reversal of acid gastroesophageal reflux has been described after lung transplantation possibly following the normalization of the anatomical relationship between the diaphragm and the esophageal LES (D'Ovidio et al. 2008)

When undergoing transplant evaluation, esophageal body peristaltic dysfunction is considered a risk factor for aspiration, leading to potential pneumonia, worsened pulmonary function tests (PFT), increased oxygen requirement and overall lung decline (Okwara and Chan, 2021). However, it is also recognized that transplant patients, not previously diagnosed with GERD, may present with recurrent episodes despite the absence of canonical esophageal symptoms. It remains crucial to maintain wariness and monitor esophageal function and BALF for signs of retrograde flux. MII showed increased and homogeneous success over pH testing in lung transplant recipients frequently

presenting with delayed gastric emptying, thus possibly having alkaline overall pH, which would mask the existence of reflux if relying solely on acidity.

While an established marker of reflux aspiration, studies on GERD and pepsin and lung transplant patients have delivered inconclusive results. Elevated pepsin has been detected in the BALF of lung transplant patients, with highest levels correlating to acute rejection (Stovold et al., 2007). However, these studies did not account for the presence of other macromolecules such as bile acids in the refluxate. Indeed, many groups have disproven the association between pepsin and allograft rejection, showing that while lung transplant patients present with elevated pepsin concentrations in BALF compared to healthy controls, this difference did not correlate with poor outcomes (Blondeau et al., 2008). GERD, measured as acid reflux or according to conventional esophageal damage associated with the pathology, has also not been a reliable factor. In the same study, the vast majority (70%, 32/45) of patients with chronic lung allograft dysfunction (CLAD) presented with detectable bile acids especially in later stages of the syndrome. The correlation between bile acids and allograft dysfunction in lung transplantation has been described by multiple centers and has been associated to inflammatory cascades inclusive of IL-8 cytokine release, which disturb the healing process (D'Ovidio et al., 2005a).

The scope of analyzing BALF for acid and macromolecules was initially to establish the occurrence of reflux aspiration. Aspiration is in turn associated with allograft rejection in lung transplant patients, which shifted the field towards

understanding the role and impact of reflux components. While reflux acidity and aspirated pepsin demonstrate aspiration, they did not correlate with increased incidence of allograft dysfunction. Conversely, elevated bile acid detection has been informative of CLAD progression, thus is considered a marker of aspiration and a risk factor for rejection (Blondeau et al., 2008). The molecular action of bile acids in the airways, along with a monitoring protocol or algorithm to predict CLAD in lung transplant patients, have yet to be established.

In the study detailed herein, we hypothesize 1) a differential contribution of the conjugated and unconjugated BA to the pathogenesis of CLAD and seek to establish a detection window allowing for CLAD prediction in lung transplant patients. As will be evidenced in the first section of Chapter 3, we investigate the longitudinal presence of bile acids in LABW collected at specific intervals post-transplantation. We find that bile acids have dramatic effects on cellular integrity and lipid release, rendering patients more susceptible to tissue damage and opportunistic bacterial infections.

In the second section of Chapter 3 we further hypothesize (2) that bile acids could also act on airway mechanics, stimulating smooth muscle and affecting airway contractility. We investigate the molecular mechanism of all bile acids on murine and human airways.

Overall, the scope of this study is to identify the relevance of bile acids in the progression of allograft dysfunction and identify possible molecular mechanisms contributing to patient morbidity.

CHAPTER 2 Bile acids as ligands in molecular signaling

Origin, composition, and physiological roles

Bile acids (BA) are amphipathic steroidal emulsifiers consisting of a saturated tetracyclic hydrocarbon ring. Their synthesis largely occurs in the liver with the contribution of mitochondrial cytochromes P450. It involves a multi-enzymatic process of cholesterol catabolism, where the rate-limiting step involves the enzyme 7α-hydroxylase, or CYP7A1 in humans (Björkhem et al., 2010; Donepudi et al., 2018). Oxysterols such as 24-hydroxysterol, 25-hydroxysterol and 27-hydroxysterol are also possible substrates for BA synthesis. This process exploits an alternate P450-pathway and lipid metabolizing enzymes, such as CYP46A1, CYP27A1 and CH25H, among others. Oxysterols require the catalyzing action of CYP39A1 and CYP7B1, followed by a series of structural modifications, to be converted to BA intermediates. BA conjugation is considered the most terminal step. It involves the addition of a glycine or taurine amino-group by N-acetyltransferase. This renders the molecules increasingly amphipathic and soluble (Russell, 2003).

Upon meal ingestion, primary BA stored in the gallbladder enter the digestive system. Along the small intestinal tract, these molecules facilitate the

solubilization of monoacylglycerols and fatty acids as well as nutrient reabsorption. Among their beneficial functions are the stimulation of bile flow, the regulation of glucose and the promotion of cholesterol secretion and catabolism (de Aguiar Vallim et al., 2013). BAs control their own synthesis, transport and detoxification along with aiding in the maintenance of a healthy gut microbiome. Recycling BAs is essential to biological processes such as intestinal motility. Their cycle culminates in the ileum where 95% is successfully reabsorbed. The remaining percentage proceeds into the colon and is most often secreted through fecal elimination (Dawson, 2018).

Successful transit of BAs is paramount. While the ileum presents with a moderate absorptive capacity, a functional deficiency or reduced expression of reuptake proteins leads to BA accumulation in the colon damaging its cellular heterogeneity (Mekhjian et al., 1979). Primary BAs that are unsuccessfully reabsorbed in the ileum experience structural modifications catalyzed by anaerobic bacterial enzymes such as 7α-dehydroxylase in the colon (Peleman et al., 2017). The colonic atmospheric conditions have been deemed important in the process of BA oxidation and conversion. Microbial hydrolases generate a prevalently hydrogen-dominated environment, halting BA oxidation, contrasting a nitrogen-dominated environment, which promotes it (Harris et al., 2018; Hylemon et al., 2018). Bile salt hydrolases (BSH) in the large bowel are responsible for the shift in prevalence of secondary and unconjugated BA in the stool (Ridlon et al., 2016). Both may determine the severity of the damage caused by BA (Mikov et al.,

2006). The recurrent colonic biotransformations are associated with hydrophobicity, causing the dissociation of membrane proteins, leakage and alteration of lipid composition (Taranto et al., 2006). This is due to the detergent nature of BA, which exhibit cytotoxic and membranolytic effects upon variation of their critical micelle concentrations (CMC) and hydrophobicity. Thus, hydroxy and dihydroxy BAs are linked to increased toxicity and disruption of membrane profiles (Swann et al., 2011).

Bile acid receptors and their involvement in pathogenesis

The effect of BA on both nuclear and surface receptors has been extensively investigated in a variety of tissues including human intestines and lungs (**Table 1a, Table 1b**) (Keely et al., 2022).

Table 1a. Surface BA Receptors (Urso et al. 2022)

Receptor	Bile Acid	Concentration	Tissue Prep	Response	Effect	Solvent	Ref
G PROTEIN COUPLED RECEPTORS							
TGR5 **(GPR130, GpBAR1)**	DCA OA	1-100µM 100µM	Proximal colon from *tgr5*- WT and KO mice	↑WT KO only 100µM at DCA	5HT and CGRP from EC cells to stimulate peristaltic reflex	0.1% ethanol, Distilled water	(137)
	DCA TLCA CCDC CCDC	100 µM 100 µM, 100 µl rectal enema	DRG neurons innervating colon (mouse) spinal cord (mouse)	↑ ↑ ↑ ↑	increased intracellular Ca^{2+} in subpopulations of neurons (%) DCA ~20%, TLCA~ 25%, CCDC~30% phosphorylated MAP-kinase-ERK-1/2 immunoreactivity (pERK-IR) enhanced in response to colorectal distention	NA saline	(5)
	INT-777 UDCA	10-100 µM 3-60 µM	proximal colon (mouse) 	↑ -	increased transepithelial resistance and reduced short circuit current, reduced with TTX or neuron free preparation weak TGR5 agonist	DMSO	(128)
	LCA, DCA	10 and 30 µM	enteroendocrine cell line, STC-1 cells transfected withTGR5 siRNA cells transfected with TGR5 cDNA	↑ - ↑	promote GLP-1 secretion reduced LCA responses at 10 and 30µM increased LCA responses at 30µM	DMSO	(180)
	range of conjugated & unconjugated BAs UDCA BA mixture	concentration curve 10 mM total BA ~9 mM, 1 mM each	COS-7 monkey kidney cells expressing human or rat TGR5 *in vivo* intraluminal *tgr5*- WT and KO mice	↑ - UDCA BA mix: ↑WT -KO	increased cAMP production rank order of potency LCA>DCA>CDCA UDCA and CA ~20% efficacy at 10µM GLP-1 and PYY release	modified Krebs-Ringer buffer isotonic saline	(162)
	LCA RO5527239 (TGR5 agonist) DCA RO5527239	concentration curve concentration curve	CHO cells transfected with TGR5 STC-1	↑ ↑	increased cAMP production EC_{50}= 457 and 3.6nM E_{Max}~110% both increased cAMP production EC_{50}= 1.59µM and 321nM GLP-1 release EC_{50}= 11µM and 321nM	NA	(200)

MrgprX4	DCA, UDCA CDCA, CA, OA DCA UDCA DCA, t-DCA, UDCA CDCA	2 - 100 µM 10 µM 100 µM 1-2 mM	HEK293 cells DRG from +X4 humanized mice *In vivo* +X4 humanized mice	↑ ↑ ↑	increased $[Ca^2]^+_i$ ~5-6% of +X4 sensory neurons activated by both increased cholestatic itch	water, DMSO or 0.1M NaOH NA	(10)
Muscarinic M2	t-CDCA, g-DCA, t-DCA, t-CA	100 µM	ventricular neonatal rat myocytes	↑	reduced contraction (G_i coupled) (role in TGR5 mediated release of cAMP found to be independent of contraction response)	L-15 media	(20)
	TCA	0-100 µM	ventricular neonatal rat myocytes	partial agonist	radioligand binding, Kd=17µM reduced cAMP production (30% of carbachol response) reduced contraction (0.2 and 1 mM)	DMSOHBSS	(21)
Muscarinic M3	CDCA, LCA, g-LCA, t-LCA, g-DCA, t-DCA, UDCA	30 µM	*ex vivo*, precision-cut lung slices	↓	inhibited acetylcholine contractile responses t-LCA IC_{50} = 3.2 µM	NA	(19)
S1PR2	t-CA, t-DCA, g-DCA, g-CA, t-UDCA	50-100 µM	primary rat hepatocytes	↑	activation of ERK1/2 and AKT	DMSO	(24)
	t-CA	100 µM	MLE		activation of ERK1/2 and AKT cell proliferation and migration	PBS	(25)
FPR	CDCA	25-400 µM	human monocytes human monocytes EFTR cell EFTR cell human monocytes EFTR cell	↓	inhibited monocyte chemotaxis to fMLP IC_{50}= 100 µM inhibited monocyte Ca flux by fMLP inhibited cell migration by fMLP IC50= 125 µM inhibited Ca^{2+} flux by fMLP IC_{50}= 50 µM radioligand fMLP binding IC_{50}= 140 µM	ethanol	(27)
	DCA	25-200 µM 25 µM 5-200 µM	human monocytes and neutrophils	↓	inhibited fMLP induced chemotaxis IC_{50}=100 µM inhibited fMLP induced Ca^{2+} mobilization radioligand fMLP binding	PBS	(26)

Table 1a. Nuclear BA Receptors (Urso et al. 2022)

NUCLEAR RECEPTORS							
FXR	CDCA>DCA and LCA	50 µM Concentration curve for CDCA	CV-1 cells with rat FXR HepG2 cells with human FXR	↑	Transactivation of FXR with luciferase reporter CDCA EC_{50}=50 µM and 10 µM rat and human FXR	ethanol	(38)
	CDCA>DCA and LCA CDCA, g-CDCA, t-CDCA	100µM	CV-1 cells	↑ ↑	Reporter gene assay. Increased CAT activity FRET ligand sensing assay Increased relative fluorescence CDCA EC_{50}=4.5 µM g- and t-CDCA EC_{50}=10 µM	NA	(37)
	CA GW4062 (FXR agonist) CDCA CA DCA LCA OCA	200 mg/kg 100 mg/kg concentration curve 50 µM 20 µM	Mice treated *in vivo* 72 hours prior to tissue harvest Human ileum and colon mucosal biopsies 6h incubation	ileum, jejunum and duodenum ↑ Liver - Ileum ↑ Colon – Comparison with matched con. CDCA	FGF-15 mRNA present in ileum, jejunum and duodenum FGF19 expression EC_{50}= 20 µM 80% of CDCA response 40% 4% 5x greater than CDCA response	NA	(41, 42)
PXR	LCA 3-keto-LCA LCA 3-keto-LCA CDCA CA DCA	concentration curve 100 µM	CV-1 cells with human PXR CV-1 cells with human or mouse PXR and reporter plasmid (Cyp3a23)2-tk-CAT	↑ ↑ ↑ (human) ↑ - - -	scintillation proximity binding assay IC_{50}= 9 and 15 µM reporter gene assay. Increased CAT activity	NA	(50)
	CDCA DCA LCA LCA	100 µM 8mg/day for 4 days, oral gavage	CV-1 cells with human and rodent PXR and reporter plasmids *PXR*- WT and KO mice *in vivo*	↑ ↑ ↑ ↑ WT -KO	reporter gene activity and CYP3A4 reporter gene activity northern blot analysis CYP3A11 mRNA	NA	(48)
VDR	LCA 3-keto-LCA LCA 3-keto-LCA CA, CDCA	concentration curve	HEK293 cells transfected with VDR Monkey kidney COS-7	↑ ↑ -	GAL4-receptor luciferase assay EC_{50}= 8 and 3 µM Competitive binding assay [3H]1,25(OH)2D3 K_i= 29 and 8 µM	NA	(55)
	LCA	0.8 mmol/kg, oral gavage	Ileum tissue of *Vdr* WT and KO	↑ WT - KO	induces mRNA expression of *Cyp24a1*	ethanol and corn oil	(56)

The mechanism of feedback regulation in BA biosynthesis involves the nuclear receptor farnesoid X (FXR). FXR promotes the synthesis of the hormone FGF19, thus is upstream of the negative feedback pathway. FXR is pivotal to epithelial integrity and pro-inflammatory cytokine moderation. Its isoforms ($FXR_{\alpha 1-\alpha 2-\beta 1-\beta 2}$) have been identified in the liver, intestine, lung, adrenals, heart and kidney and mostly in the liver (Zhang et al., 2003; Anisfeld et al., 2005; Inagaki et al., 2006). FXR contributes to the transcription of genes involved in BA and lipid metabolism such as the ileal bile acid binding protein, short heterodimer partner (SHP), phospholipid transfer protein, several transporters and alipoprotein C-II (Wang et al., 2018). The majority of the latter promote BA export or inhibit their synthesis in the liver. Reduced BA synthesis occurs upon their binding to FXR, which activates SHP, a second nuclear receptor. In turn, SHP inhibits the liver receptor homologue-1, a third nuclear receptor responsible for activating enzymes 7α-hydroxylase and sterol 12α-hydroxylase. The ability of BA to affect FXR varies among them. These differences may involve hydrophilicity and inability to enter cells without transporters, or the incompatibility with FXR itself.

The dysregulation of FXR has been tied to chronic intestinal inflammation and visceral hypersensitivity, due to continuous stimulation of peripheral afferent nerves (Mosińska et al., 2018). High fat diets, discouraged in cases of irritable bowel syndrome (IBS), affect FXR activity and BA profile in stool (Portincasa et al., 2017). Increased levels of lithocholic acid (LCA) and DCA disrupt the gut barrier and reduce the amount of fecal ursodeoxycholic acid (UDCA), which is consistently

cytoprotective (Stenman et al., 2013). Thus, high fat diets worsen health in IBS patients, commonly leaning towards increased body weight and obesity, and interfere with FXR-regulated-BA synthesis (Sandhu et al., 2017).

Other nuclear receptors are involved in self-defense mechanisms especially in the enteric system. LCA, secondary unconjugated hydroxyl BA, has been shown to be a ligand of the Vitamin D receptor (VDR) in the gut. Despite vitamin D and its isoforms being the most common ligands of VDR, this receptor is known to be directly and indirectly responsive to a series of xenobiotic and endogenous metabolites, such as BAs (Gombart, 2009). After the structural modifications experienced by BAs in the large intestine, the VDR functions as a high affinity sensor for the extremely toxic LCA. Their binding activates a feed-forward cascade involving the catabolism of LCA by the P450 enzyme CYP3A, initiating a protection mechanism for the colon. Such homeostatic pattern can be clearly deranged by an increased presence of LCA in the large intestine causing a saturation of the pathway. This phenomenon is observed in individuals on high-fat diets or in those patients having severe vitamin D deficiency (Makishima et al., 2002). Moreover, VDR has been implicated in other immunity-related cascades such as the stimulation of cathelicidin, an antimicrobial peptide involved in biliary tract sterility. Select BAs have been shown to increase the VDR protein expression stimulating the release of cathelicidin and the initiation of its bactericidal pathway (D'Aldebert et al., 2009). This receptor is known to be present also in the small and large intestine, and has been shown, upon interaction with ligands such as D_3, to

stimulate a similar release of the cathelicidin peptide (Wang et al., 2004; Gombart et al., 2005). VDR's functionality in the colon could explain its interaction with detrimental BAs and its contributions in gut immunity and protection (Makishima et al., 2002; Adachi et al., 2005; Nehring et al., 2007).

Similar to VDR, an additional nuclear receptor involved in sensing of toxic xenobiotic and endobiotic substances is the pregnane X receptor (PXR). Studies have determined the presence of PXR in the liver and intestines, where BAs mainly circulate, yet discovered a mild expression pattern in other tissues. PXR's participation in BA metabolism consists in the activation of transport genes such as *MRP2* and *Oatp2*, normally responsible for the excretion of toxic molecules via the biliary system across the canicular membrane. In fact, after CYP3A4 hydroxylates BAs, MRP2 and Oatp2 successfully evacuate them. The defense role played by PXR, and its involvement with shuttling molecules for excretion, led to investigations on its direct interaction with BAs (Kliewer et al., 2002). LCA and 3-keto-LCA were shown to successfully bind human PXR and stimulate the expression of transport and detoxification genes (Staudinger et al., 2001). Hence, in patients with cholestasis, state caused by an accumulation of LCA, targeting PXR with a stronger agonist may intensify the expression of detoxification genes, antagonizing the injurious effects of the secondary BA (Xie et al., 2001). Furthermore, the constitutive androstane receptor (CAR) and PXR have been found to serve complementary roles in detoxification of BAs (Lickteig et al., 2016; Klag et al., 2018). Both receptors heterodimerize with the retinoid X receptor,

activate the expression of xenobiotic metabolizing enzymes and promote resistance to hepatotoxicity. Zhang and colleagues have shown a compensatory function served by CAR in response to increased levels of LCA in FXR $^{-/-}$ and PXR $^{-/-}$ null mice. In this case, CAR completely takes over the protective role held by PXR, while CAR $^{-/-}$ null mice livers have been found to be severely compromised and did not survive LCA treatments (Zhang et al., 2004).

Besides affecting stool consistency and passing along with cholestatic disease, BAs can be considered environmental factors exacerbating inflammatory processes or even promoting mucosal dysplasia. Recent studies have associated increased spillage of BAs in the colon, often due to dysregulated reuptake, to the augmentation of adenocarcinomas, encouraging neoplasia (Raufman et al., 2015). Among the membrane receptor subtypes involved are the Muscarinic GPCRs, specifically the M3 conditional oncogenes. These seven-transmembrane receptors have been documented in most smooth muscle tissues among which liver, gut, lung, heart, and uterus. Besides their known cholinergic interactions, M3Rs can be activated by BAs, whose presence in feces has been shown to stimulate the growth of colonic crypt foci (Flynn et al., 2007). Cheng et al. found that M3R expression in normal colonic epithelium differed dramatically from that in colon adenomas, the latter's being strongly increased. Despite their associations to metastatic disease, BA-induced-M3R expression seems crucial to primary colon neoplasia rather than to the sustenance of its progression (Felton et al., 2018). Studies in H508 human colon cancer cell lines expressing M_3-R also show an

increase in inositol phosphate and proliferation, opposed to cell lines not expressing the receptor (Cheng et al., 2002). This could be linked to the change observed in intracellular distribution of M3R, suggesting a transition from a stable plasma membrane localization to a more dynamic functional role in cancer initiation (Cheng et al., 2017). In fact, the aberrant proliferation was subsequently associated to a BA-induced transactivation of the epidermal-growth factor receptor (EGFR), mechanistically catalyzed by matrix metalloproteases (MMPs), parts of membrane-bound complexes, in the colon and the bile duct (AMONYINGCHAROEN et al., 2015). The metalloproteases MMP-1 and MMP-7 display a proportional increase to BA levels post-muscarinic M_3 interaction, showing a compelling pathway of responsiveness (Cheng et al., 2007; Peng et al., 2013; Said et al., 2017).

Responsible for the integrity and health of the large intestine, the colonic epithelium is lined with several layers of protection, both physical and hormonal. Human β-defensins (HβDs) are balancing proteins specific to the colon, selective towards their activity against bacterial populations, and mediators of mucosal inflammation and cytokine release. Amongst the receptors involved in HβD activation is the Takeda GPCR 5 receptor (TGR5), highly expressed in the stomach, ileum and colon, and documented to play a role in the immunity of other tissues. Lajczak et al have shown how increasing levels of the secondary deoxycholic acid (DCA) stimulates TGR5 in the colonic epithelium causing a slow onset secretion of HβD1 and HβD2. These findings suggest that BAs, in this case a secondary

unconjugated specie, may function as triggers of colonic immune defense mediated by TGR5 (Lajczak-McGinley et al., 2020). Moreover, Cipriani and colleagues had previously determined the involvement of TGR5 in intestinal homeostasis. TGR5 knockout mice displayed a significant alteration in colonic histopathology, distribution and maturation kinetics of mucous cells and disruption of the architecture of tight junctions (Cipriani et al., 2011). These, being signs of intestinal inflammation, suggest that TGR5 may indeed serve a protective function especially in detection of excess BAs. Similarly, tight junction alterations, oxidative stress and cellular apoptosis are indicative of gut barrier dysfunction as in obstructive jaundice. Ji et al. found that internal biliary drainage improved intestinal bile flow and concomitantly stimulated the recovery of epithelial cell proliferation as a result of the presence of CDCA upregulating TGR5 (Ji et al., 2017). CDCA, a primary specie contributing to the majority of the BA pool, is a strong ligand of intestinal TGR5 along with LCA, which mainly interacts with TGR5 in the colon. Ward and colleagues have explored the affinity of TGR5 for LCA in colonic epithelium, mainly focusing on secretion and transport functions. BAs are known to stimulate colonic transit of stool and, in their studies, LCA activated TGR5 in rat colonic epithelium while decreasing the secretion of Cl^-. This finding suggests that the receptor may also influence electrolyte transport, important for fluid secretion and eventual stool passing (Ward et al., 2013). BA interaction with TGR5 is actually associated with 5-HT release causing a peristaltic reflex in the colon. In fact, the loss of TGR5 causes a delay in stool evacuation, with the resulting pellets

appearing drier and in reduced amounts (Alemi et al., 2013b). These results are compatible with the electrolyte transport findings, causing a reduction of fluidity in the feces and slower secretion. Besides affecting motility, BAs have also been deemed to induce hyperexcitability of dorsal root ganglia neurons by interacting with TGR5 and generating pruritus. Evidence shows that BAs, in this case DCA, TLCA and oleanolic acid, selectively induce scratching in mice by impacting peripheral sensory nerves. This behavior intensifies with the overexpression of TGR5 and disappears in TGR5 knockout mice (Alemi et al., 2013a).

The clinical implications of the above findings are still to be determined, yet BA interaction with membrane and nuclear receptors may indeed affect neural responses and intestinal microbiota.

Bile acids and ion channels

Numerous studies in various tissues have reported that BA presence leads to the dysfunction of ionotropic receptors, leading to fluid accumulation due to the inhibition of sodium absorption and increased potassium secretion (Volpe and Binder, 1975; Freel et al., 1983; Moschetta et al., 2003). In the context of lung diseases such as CF, ion exchange is incredibly important for the control of salt concentration in airway surfactant. The cystic fibrosis transmembrane conductance regulator (CFTR) protein is responsible for the chloride and sodium intracellular exchange. In the intestine, inhibition of CFTR has been studied in the context of BA-induced diarrhea (BAD), where the primary BA chenodeoxycholic acid (CDCA) activates CFTR and promotes electrolyte and fluid secretion (Duan et al., 2019; van de Peppel et al., 2019). Similarly, in the airway, the taurine conjugated secondary BA TDCA has been also found to modulate chloride secretion in Calu-3 airway epithelial cells at low concentrations, allowing for ion transport and increased pump current (Hendrick et al., 2014). As primarily intestinal molecules, most studies on bile acids and ion channels have been performed on the family of the epithelial sodium channel degenerin (ENaC/DEG), which includes acid sensing sodium channels (ASIC), the FMRFamide-activated sodium channel, and the BA-sensitive sodium channel (BASIC).

The ENaC/DEG family is of particular interest due to the relevance of these channels in the human lung (Wiemuth et al., 2014). It is expressed in the apical

membrane of epithelia and mediates fluid volume by regulating sodium absorption. Though, even applied to the basal membrane, BA are able to activate ENaC/DEG, likely through nuclear transit and FXR. Lithocholic acid (LCA) has been shown to transcriptionally regulate the channel in a sustained yet delayed fashion, regardless of its exposure location. The ENaC/DEG has been described as a heterotrimeric channel composed of several protein subunits (α, β, γ, δ) arranged as $\alpha\beta\gamma$ or $\delta\beta\gamma$, and a degenerin site for channel gating. In humans, conjugated BA such as TCDCA, TDCA and TCA have substantial effects on both $\alpha\beta\gamma$ and $\delta\beta\gamma$ configurations while non-conjugated BA only stimulate $\delta\beta\gamma$. Yet, the effect of BA on these channels has been shown to be related to the facilitation of channel opening, thus to the degenerin site. Indeed, a single point mutation of the degenerin impeded BA action on ENaC/DEG generated current, establishing channel gating as the functional target of BA in the airway (Ilyaskin et al., 2016, 2017). In contrast, the epithelial action of the synthetic ursodeoxycholic acid (UDCA) on ENaC/DEG channels has been described in the airway as beneficial. Both normal and CF epithelia showed reactivity to UDCA and increased airway surface liquid rather than dehydration, which implies a therapeutic potential of UDCA (Mroz and Harvey, 2019).

The contribution of BA on the actions of ASIC and BASIC is still of great interest in intestinal studies showing a similar degenerin-mediated regulation of channel activity and current flow as observed in the airways (Ilyaskin et al., 2017, 2018).

TDCA has been shown to engage in transient hydrogen bonding with the external vestibule of the channel, affecting flux and ion concentrations intra/extracellularly if bound to the specific G433 site located around the pore (Ilyaskin et al., 2017, 2018). The effects on BASIC are not as potent or as specific as those on ASIC, as they require substantially higher concentrations resulting in minor alterations (Lenzig et al., 2019).

The above introduction to BA origin, composition and physiological role led us to hypothesize that aspirated BA from duodenogstroeophageal fluid impact airway mechanics and alter patient morbidity after lung transplantation. In the following chapter, the first section will delineate the clinical portion of this study, which involved investigating the presence and differential role of the conjugate and unconjugated BA in the airways of lung transplant recipients. We established set timepoints for BALF was collection and assaying to determine the concentration and effect of BA aspiration in lung transplant patients.

The second section will further examine the role of BA as molecular ligands with receptor-mediated effects. We tested this hypothesis by engaging in a systematic study of murine and human airway contractility upon exposure to a panel of the 13 known BA both ex-vivo and in-vivo.

CHAPTER 3 Bile acids in the human and murine airways

BA as markers of aspiration and determinants of clinical outcomes in lung transplantation

As discussed in Chapter 1, duodeno-gastro-esophageal reflux (DGER) is a known factor associated with an increased risk of CLAD development and recurrent micro-aspiration. BA are known to impact macrophage responses (Hofmann; Pols et al., 2011a), alter surfactant lipids and innate immunity molecules, such as SP-A and SP-D (D'Ovidio et al., 2006), and associate with airway infections (D'Ovidio et al., 2005b; Pols et al., 2011b). Presence of BA in large airway bronchial washings (LABW) or bronchoalveolar lavages (BAL) has been associated with poor lung transplant outcomes, particularly at 3-months after transplantation (D'Ovidio et al., 2005c, 2006; D'Ovidio and Keshavjee, 2006; Blondeau et al., 2008; Ahmed et al., 2019). Anti-reflux procedures in patients with GER have shown the greatest benefit for survival and freedom from CLAD, especially if performed within 3 months post-transplant (Cantu et al., 2004). However, little is known on the role of individual aspirated BA species, which are characterized by different solubility and lipophilicity profiles according to the pH of the environment, and their effect on the lung (KULLAK-UBLICK et al., 2000). Chenodeoxycolic acid (CDCA) in particular, has been shown to reduce cell viability, and enhance reactive oxygen species production (Wu et al., 2009; Zhangxue et al., 2012). Despite its low toxicity and hydrophobicity, CDCA increases cell permeability and facilitates decay of epithelial markers (Su et al., 2013). In this section we will explore our first hypothesis which considers *the differential*

contribution of BA subspecies to the pathogenesis of CLAD and seek to establish a detection window allowing for CLAD prediction in lung transplant patients. We find that patients undergoing BA aspiration incur increased morbidity and mortality and identify a preventive surveillance timepoint post-transplantation.

Materials and Methods

Human subjects. Clinical information and biological samples from routine follow-up testing were prospectively collected from 111 consecutive recipients (2009 through 2013). The protocol was created with adherence to the Institutional Review Board of the Columbia University Medical Center. Informed consent was obtained from each patient for use of excess LABW.

Sample collection. Large airway bronchial washes (LABW) of 20 mL saline solution injected in the lower lobe bronchus of the transplanted lung without wedging the bronchoscope were collected during routine surveillance bronchoscopies at 3, 6, 9 and 12-months after transplantation in the outpatient setting. Samples were immediately spun down (450 RCF at 4C for 8 min) for supernatant collection, and aliquots were snap-frozen at −80° C and stored for evaluation.

Clinical assessments. CLAD development was monitored by routine pulmonary function tests and defined as a permanent forced expiratory volume (FEV1) drop more than or equal to 20% from the average of the two best post-transplant FEV1 measured at least 3 weeks apart with absent clinical confounders, as per International Society of Heart and Lung Transplant guidelines. For the purpose of this study, recipients were required to have been post-transplant for at least 6 months before CLAD diagnosis. Clinical information was updated to January 2020, including development of CLAD, and survival and analyses assessed time from transplant to event. A secondary outcome of interest was the rate of bacterial airway infections during the first year after transplant, which were

defined positive bacterial cultures of the combined BAL and LABW clinical specimen obtained by surveillance or therapeutic bronchoscopy.

Targeted metabolomics. Liquid chromatography tandem mass spectrometry for 13 bile acids. 100µl of BW were used straight and spiked with deuterated internal standard at a level of 5nM and were mixed with ten volumes of methanol. After incubation at 4◦C for 15min, the mixture was centrifuged, and the organic layer was transferred to a LCMS vial and evaporated under nitrogen stream. The extracted compounds were resuspended in 55% methanol containing 5mM ammonium formate for further analysis. LC-MS/MS analysis was performed using a API 4000 triple quadrupole mass spectrometer (ABSCIEX, Foster City, CA) equipped with an electrospray ionization source and integrated to an Eksigent Ultra LC 100 system. Instrumentation control, data acquisition and quantitation were done using Analyst 1.6 software. Chromatographic separation was performed on a Phenomenex Kinetex C18 column (50x2.1mm, 1.7u, 100A) maintained at 40◦C and a flow rate of 200ul/min. The initial flow conditions were 40% Solvent A (water containing 5mM ammonium formate) and 60% Solvent B (Methanol containing 5mM ammonium formate). Solvent B was raised to 80% linearly over 8min, increased to 97% in 2min and returned to initial flow conditions by 12 min with a total run time of 15min. The mass spectrometer was operated under selective reaction monitoring (SRM) mode with negative electrospray ionization. The lower limits of quantitation for the bile acids, defined as the lowest concentration with an accuracy and precision <20% ranged from 1nM to 10nM. Values below the lower level of quantification, but above the lower level of detection were assigned the arbitrary value of half the lower level of quantification. Intra-

assay precision for the measured bile acids ranged from 3.57%-5.63% and an intra-assay accuracy from 94.3% to 105.6%. The assay showed an inter-assay precision for bile acids ranging from 1.66% to 4.13%. All BA were LCMS grade and purchased from Sigma Aldrich (St Louis, MO).

Targeted lipidomics. Lipidomic analysis for 26 lipid families inclusive of 250 lipids was conducted in all samples. Lipid extracts were prepared from 300µl of LABW sample using a modified Bligh Dyer procedure , spiked with appropriate internal standards, and analyzed using a 6490 Triple Quadrupole LC/MS system (Agilent Technologies, Santa Clara, CA). Glycerophospholipids and sphingolipids were separated with normal-phase HPLC using an Agilent Zorbax Rx-Sil column (inner diameter 2.1 x 50 mm) under the following conditions: mobile phase A (chloroform:methanol:1 M ammonium hydroxide, 89.9:10:0.1, v/v) and mobile phase B (chloroform:methanol:water:ammonium hydroxide, 55:39.9:5:0.1, v/v); Flow rate of 0.5 ml/min; 95% A for 0.5 min, linear gradient to 30% A over 5 min, liner gradient to 25% A over 1.5 min, linear gradient back to 95% A over 0.5 min and held for 4 min for column re-equilibration. Sterols and glycerolipids were separated by reverse-phase HPLC using an Agilent Zorbax Poroshell 120 EC-C18 column (2.1 x 50 mm) with an isocratic mobile phase consisting of chloroform:methanol:100mM ammonium acetate, 100:100:4, v/v; Flow rate of 0.5 ml/min for 6min. Quantification of lipid species was accomplished using multiple reaction monitoring (MRM) transitions that were developed in earlier studies in conjunction with referencing to appropriate internal standards: PA 14:0/14:0, PC 14:0/14:0, PE 14:0/14:0, PG 15:0/15:0, PI 16:0/16:0, PS 14:0/14:0, BMP 14:0/14:0, APG 14:0/14:0, LPC 17:0, LPE

14:0, LPI 13:0, Cer d18:1/17:0, SM d18:1/12:0, dhSM d18:0/12:0, GalCer d18:1/12:0, GluCer d18:1/12:0,LacCer d18:1/12:0, D7-cholesterol, CE 17:0, MG 17:0, 4ME 16:0 diether DG, D5-TG 16:0/18:0/16:0 (Avanti Polar Lipids, Alabaster, AL).

Cytokine assays. BW samples were also assayed for cytokines. To measure the cytokines in the BW samples they were shipped on dry ice to Eve Technologies (Calgary, AB, Canada). The NEW-Discovery Assay Human Cytokine Array 48-Plex (HD48) was used to measure the following media analytes: sCD40L, EGF, Eotaxin, FGF-2, Flt-3 ligand, Fractalkine, G-CSF, GM-CSF, GROα, IFNα2, IFNγ, IL-1α, IL-1β, IL-1ra, IL-2, IL-3, IL-4, IL-5, IL-6, IL-7, IL-8, IL-9, IL-10, IL-12 (p40), IL-12 (p70), IL-13, IL-15, IL-17A, IL-17E/IL-25, IL-17F, IL-18, IL-22, IL-27, IP-10, MCP-1, MCP-3, M-CSF, MDC (CCL22), MIG, MIP-1α, MIP-1β, PDGF-AA, PDGF-AB/BB, RANTES, TGFα, TNFα, TNFβ, VEGF-A.

Statistical analyses. Continuous and categorical data were compared using a Mann-Whitney (or a student's t-test on variables with a normal distribution) or chi-squared test, respectively. Concentrations of BA among different samples was analyzed by a one-way ANOVA using a mixed-effects model to account for repeated measures. BW lipid levels and cytokine levels were compared to BA levels using a Pearson's correlation test and significance in the setting of multiple testing was defined using the Benjamini-Hochberg method. Continuous variables and outcomes were tested using linear regression. Time-to-event rates were calculated using the Kaplan-Meier method and compared using a log rank test. In order to examine the association between BA levels and outcomes of interest (CLAD and mortality), a Cox proportional hazards model was used. Variables of interest

with a $p<0.25$ in the univariable analysis were included in the multivariable model. All data was complete without missing entries. Differences were considered statistically significant for $p<0.05$. All statistical analyses were performed using Stata version 14.0 (Stata Corp, College Station, TX).

Results

Airway BA are present in post-transplant patients. At least one BA was detectable in 226/240 (94.2%) BW samples from recipients. Among those with detectable BA, values ranged from 0.5-30,461 nM, with a median of 9.5 nM (**Table 1**). **Figure 1A** shows the levels of BA assayed at various time points during the first year after transplant. BA were present in 90% (45/50) of samples from recipients at 3 months post-transplant. The range of total BA ranged from 0-149.8 nM with a median of 7.8 nM [25^{th} -75^{th} percentile: 1.8-19] (**Table 1**). Primary BA were present in 48.9% (22/45) of positive samples, whereas secondary BA were present in 46.7% (21/45) of positive samples. Samples containing only primary BA were 42.2% (19/45) of the pool, contrasting a 0% (0/45) for samples containing only secondary BA. Conjugated species were present in 98% (44/45), while unconjugated in 62.2% (28/45). The breakdown of BA per species showed the primary conjugated glycocholic acid (GCA) as the most widely present, with a median of 1.2 nM, followed by glycochenodeoxycholic acid (GCDCA). **Figure 1B-D** illustrates the overall trend per sampling timepoint for recipients with 1, 2, ≥3 samples.

	BA concentration			BA percent from total		
	Median (nM)	Range (nM)	IQR (nM)	Median (%)	Range (%)	IQR (%)
Total BA	7.9	0-149.8	[1.8-19]	100	-	-
Unconjugated	2.5	0-86.9	[1.7-11]	28.2	0-100	[0-63.3]
Conjugated	3.1	0-67.4	[1.3-9.9]	71.8	0-100	[36.7-100]
Primary	0	0-81.9	[0-5]	0	0-80.4	[0-28.8]
CA	0	2.5-54.2	[0-2.5]	0	0-37	[0-14.3]
CDCA	0	5-27.7	[0-5]	0	0-80.4	[0-18.5]
Secondary	0	0-26.6	[0-2.5]	0	0-90.9	[0-31.6]
LCA	0	5	[0]	0	0-90.9	[0]
DCA	0	2.5-16.6	[0]	0	0-35.4	[0-9.6]
HDCA	0	5	[0]	0	0-28.6	[0]
UDCA	0	5	[0]	0	0-38.5	[0]
Primary conjugated	2.5	0-67.4	[1-9.3]	2	1-3	[1-3]
TCA	0	1.25-8.6	[0-1.3]	0	0-100	[0-11.7]
GCA	1.2	0.5-46.9	[0.5-3.4]	19.6	0-100	[7.5-42]
TCDCA	0	0.5-4.2	[0-0.5]	0	0-23.4	[0-1.7]
GCDCA	0.5	0.5-33.5	[0-2.5]	14.7	0-91.1	[0-25.4]
Secondary conjugated	0	0-32	[0-1.3]	0	0-71.4	[0]
TLCA	0	1.25	[0]	0	0-47.2	[0]
TDCA	0	1.25-32	[0]	0	0-71.4	[0]
GDCA	0	0.5-3.6	[0]	0	0-12.7	[0]

Table 1. Descriptive statistics for 13 bile acid detected in bronchial washes of post-transplant recipients.*BA: bile acids, IQR: interquartile range, CA: cholic acid, CDCA: chenodeoxycholic acid, LCA: lithocholic acid, DCA: deoxycholic acid, HDCA: hyodeoxycholic acid, UDCA: ursodeoxycholic acid, TCA: taurocholic acid, GCA: glycocholic acid, TCDCA: taurochenodeoxycholic acid, GCDCA: glycochenodeoxycholic acid, TLCA: taurolithocholic acid, TDCA: taurodeoxycholic acid, GDCA: glycodeoxycholic acid.*

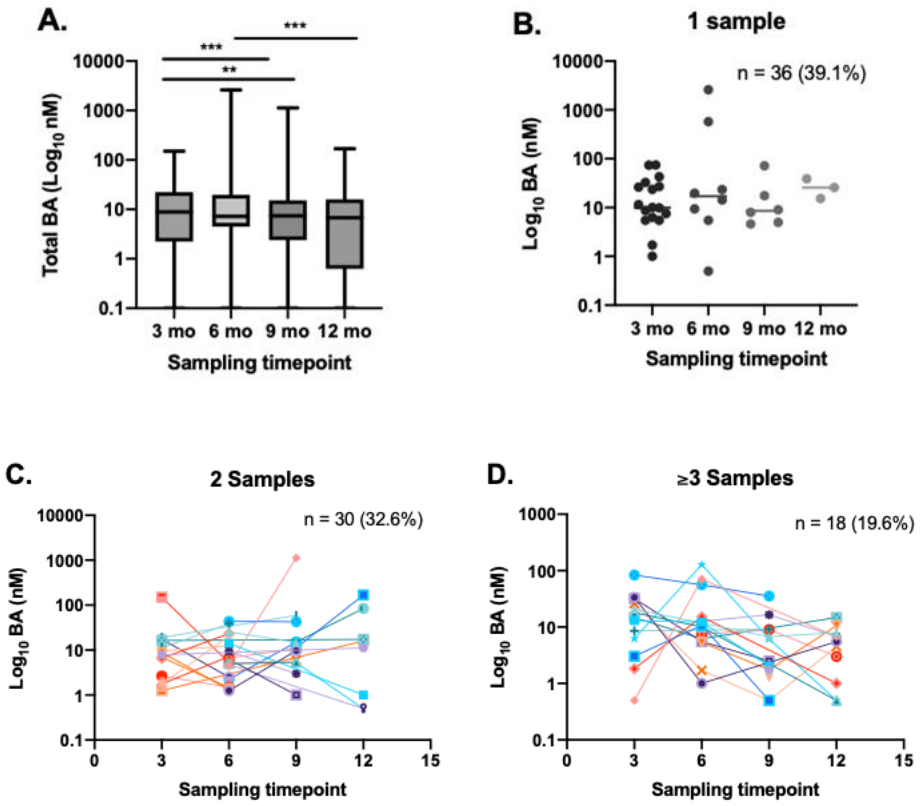

Figure 1. *Overall BA levels and time-points post-transplant.*

Recipients (n=50)	Low BA(n=35)	High BA(n=15)	p-value
Bilateral Tx	19 (54%)	9 (60%)	0.709
CMV Mismatch	9 (26%)	2 (13%)	0.333
Sex (Female)	11 (31%)	8 (53%)	0.427
Sex Mismatch	10 (29%)	6 (40%)	0.427
LAS at transplant*	44.4 [39.9-49.9]	44.3 [35.7-61.6]	0.695
Time (months) from Tx to bronchoscopy	3 [2.5-3.4]	3.1 [2.2-3.6]	0.700
Fundoplication	5 (14%)	1 (7%)	0.447
Before transplant	0 (0%)	1 (7%)	
After transplant	5 (14%)	0 (0%)	
pH testing			0.686
GER	13 (37.1%)	7 (46.7%)	
Normal	8 (22.9%)	2 (13.3%)	
Not performed	14 (40%)	5 (33.3%)	
Age*	58 [43-63]	59 [49-63]	0.873
PGD 2-3 at 72h	7 (20%)	3 (20%)	1.000
Disease			
CF	9 (26%)	3 (20%)	0.665
COPD	5 (14%)	7 (47%)	0.014
ILD	21 (60%)	5 (33%)	0.084
Acute Rejection	1 (7%)	0	0.522
Airway Bacteria infection	9 (26%)	9 (60%)	0.02
Donor			
Age*	25 [21-45]	38 [23-48]	0.207
Sex (female)	9 (26%)	6 (40%)	0.312
Smoking	10 (29%)	3 (20%)	0.527

Table 2. *Donor and recipient characteristics according to levels of bile acids in bronchial wash collected at the 3-month bronchoscopy.* BA: bile acids, CMV: cytomegalovirus, Tx: transplant, LAS: lung allocation score, GER: gastroesophageal reflux, PGD: primary graft dysfunction, CF: cystic fibrosis, COPD: chronic obstructive pulmonary disease, ILD: interstitial lung disease. *Continuous variables are presented as median [interquartile range]

High total BA levels and greater proportion of conjugated BA at 3-months after transplant predict earlier CLAD and reduced survival. BW samples were divided and analyzed according to tertiles of the sum of all assayed BA. Approximately 35% (78/226) of samples with detectable BA belonged to the highest tertile, which was defined by a total concentration of BA of ≥16.57nM.

At the 3-month post-transplant surveillance bronchoscopy, 30% (15/50) of samples presented with high levels of BA, similar to the 6-months timepoint in which 28% (13/47) of BW samples presented high levels of BA. A gradual decrease was observed between the combined 9 and 12-month timepoints, with a 20% (13/64) of samples reaching higher concentrations. For purpose of early identification of patients at high risk of adverse outcomes and based on prior literature we decided to focus on the 3-month time point which included 50 patients for further analyses. **Table 2** show the recipient and donor characteristics of the patients with BW collected at 3 months grouped according to BA levels. BA were defined high and low according to highest tertile which was comparable to that calculated on the entire sample collection (≥16.57nM). Recipients with higher BA concentrations in the BW after transplant showed an increased risk for earlier CLAD development and reduced survival (**Figure 2**). Higher BA concentrations at 6, 9, and 12 months also showed increased risk for earlier death, while only at 9 months for earlier CLAD development (**Figure 2**).

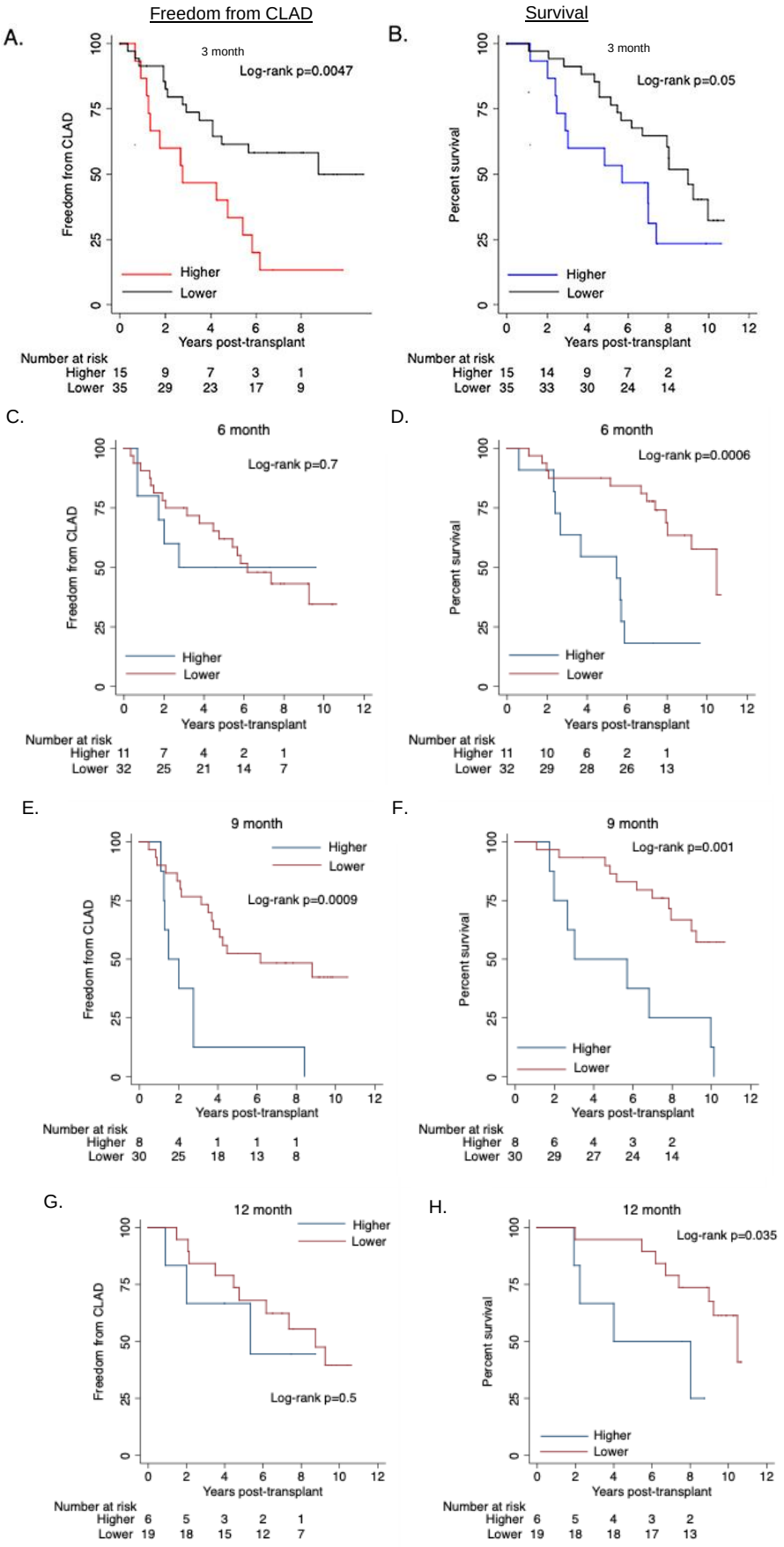

Figure 2. *Higher BA levels consistently predict adverse outcomes and mortality after transplantation.*

On univariable analysis, BA concentration had an increased hazards for CLAD (HR: 2.67, 95% CI: 1.23-5.77, p=0.013) and mortality (HR: 2.24, 95% CI: 1.02-4.91, p=0.044). A high BA concentration was an independent risk factor for CLAD after adjusting for other known risk factors (**Table 3**). A similar trend was seen for mortality, although it did not reach statistical significance. When exploring the role of BA species, recipients that developed CLAD within 3 years post-transplant showed greater percentage of conjugated BA over total BA in the post-transplant BW (median: 56.7% [30.4%-87%] vs 100% [86.5%-100%], p=0.009). After dividing the percentage of conjugated BA of the total BA into tertiles (<33.3%, 33.3-67.3%, and ≥67.3%), recipients with a high percentage (≥67.3%) were compared to those with a low percentage (<67.3%). Reduced freedom from CLAD and survival was observed on recipients that had a higher percentage of conjugated BA (**Figure 3A--B**). Both a high concentration as well as a high proportion of conjugated BA were independent predictors of CLAD and mortality after adjustment for other covariates (**Table 4** showing a synergistic effect on these outcomes) (**Figure 3C-D**). Greater hazards for CLAD development (adjusted HR: 20.35, 95% CI: 4.98–83.2, p<0.001) and for mortality (adjusted HR: 11.35, 95% CI: 3.18–40.53, p<0.001) were observed in recipients with high total BA and high proportion of conjugated BA. On univariable analysis, CLAD and overall mortality was associated with the concentration of conjugated primary BA species detected in the BW samples post-lung transplant, as shown in **Table 5**. The cause of death in recipients with higher BA levels showed a trend towards an increased rate of CLAD and bacterial pneumonia (**Table 6**, 33.3% versus 63.6%; p=0.11).

CLAD		HR	95% CI		p-value
	High BA	3.81	1.51	9.63	0.005
	Fundoplication[1]	1.47	0.42	5.12	0.545
	Gender mismatch	0.78	0.28	2.15	0.631
	Double lung-Tx	1.33	0.45	3.95	0.605
	LAS	1.00	0.97	1.03	0.944
	CMV mismatch	2.36	0.77	7.18	0.131
	Recipient age	1.04	0.97	1.11	0.237
	Donor age	1.01	0.98	1.04	0.558
	PGD 2-3 at 72 h	0.42	0.12	1.41	0.16
	Donor smoking	1.12	0.44	2.84	0.81
Mortality		**HR**	**95% CI**		**p-value**
	High BA	2.95	1.10	7.90	0.031
	Fundoplication[1]	0.65	0.12	3.52	0.621
	Gender mismatch	1.16	0.45	3.00	0.765
	Double lung-Tx	1.54	0.56	4.19	0.403
	LAS	1.04	1.01	1.06	0.016
	CMV mismatch	2.57	0.76	8.63	0.128
	Recipient age	1.01	0.95	1.08	0.71
	Donor age	1.02	0.99	1.05	0.2
	PGD 2-3 at 72 h	0.44	0.12	1.56	0.204
	Donor smoking	0.83	0.32	2.18	0.705

Table 3. *Cox proportional hazards multivariable model for CLAD and mortality among patients with samples at 3 months after lung transplant*. CLAD: chronic lung allograft dysfunction, HR: hazards ratio, CI: confidence interval, BA: bile acid, LAS: lung allocation score, CMV: cytomegalovirus, PGD: primary graft dysfunction. Model stratified by recipient diagnosis. [1]Fundoplication performed prior to CLAD development.

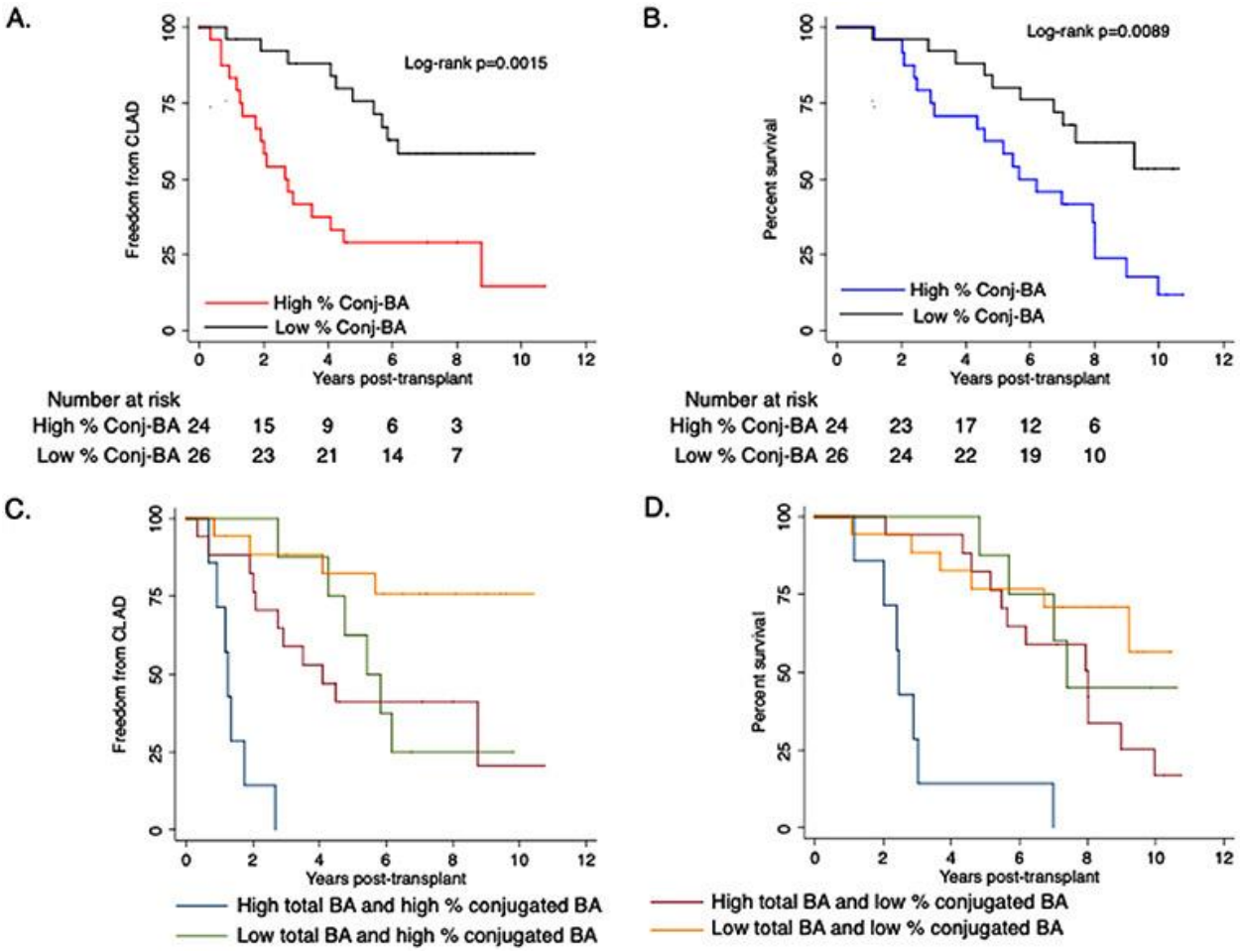

Figure 3. *Patient survival post-exposure to high or low concentrations of conjugated BA.*

CLAD	**HR**	**95% CI**		**P value**
High % PC-BA	5.55	1.74	17.67	0.004
High total BA	5.52	1.96	15.55	0.001
Fundoplication	2.09	0.59	7.40	0.253
Gender mismatch	0.80	0.24	2.65	0.716
Double lung transplant	1.55	0.44	5.44	0.49
LAS	1.00	0.96	1.04	0.978
CMV mismatch	1.03	0.32	3.32	0.966
Recipient age	1.05	0.98	1.11	0.165
Donor age	1.00	0.96	1.03	0.925
PGD 2-3 at 72 h	0.77	0.19	3.07	0.711
Donor smoker history	1.40	0.53	3.67	0.493
Mortality	**HR**	**95% CI**		**P value**
High % PC-BA	2.56	0.79	8.25	0.117
High total BA	4.08	1.45	11.46	0.008
Fundoplication	0.96	0.26	3.47	0.948
Gender mismatch	1.59	0.60	4.20	0.351
Double lung transplant	1.24	0.38	4.00	0.72
LAS	1.04	1.01	1.07	0.009
CMV mismatch	1.65	0.50	5.43	0.408
Recipient age	1.02	0.96	1.08	0.612
Donor age	1.01	0.98	1.05	0.483
PGD 2-3 at 72 h	0.67	0.15	3.05	0.606
Donor smoker history	1.31	0.48	3.58	0.596

Table 4. *Cox proportional hazards multivariable model including high BA and high percentage of conjugated BA tested at 3-months after lung transplant.* HR: hazards ratio, CI: confidence interval, BA: bile acid, LAS: lung allocation score, CMV: cytomegalovirus, PGD: primary graft dysfunction. Model stratified by recipient diagnosis

A.

CLAD		HR	95% CI		p-value
Primary		1.01	0.99	1.03	0.372
	CA	1.02	0.98	1.05	0.317
	CDCA	1.02	0.95	1.10	0.546
Secondary		1.04	0.97	1.11	0.278
	LCA	1.06	0.86	1.31	0.59
	DCA	1.04	0.91	1.19	0.584
	HDCA	1.10	0.89	1.36	0.374
	UDCA	1.10	0.89	1.36	0.38
Primary conjugated		1.03	1.01	1.06	0.001
	TCA	1.36	1.15	1.60	<0.001
	GCA	1.06	1.02	1.10	0.007
	TCDCA	1.76	1.20	2.59	0.004
	GCDCA	1.05	1.01	1.09	0.009
Secondary conjugated		1.04	0.98	1.11	0.189
	TLCA	1.42	0.69	2.94	0.342
	TDCA	1.04	0.97	1.11	0.256
	GDCA	1.16	0.72	1.87	0.55

(continued)

(continued)

B.

Mortality		HR	95% CI		p-value
Primary		1.02	0.99	1.04	0.209
	CA	1.03	0.99	1.06	0.128
	CDCA	1.02	0.94	1.11	0.567
Secondary		1.02	0.95	1.10	0.559
	LCA	1.17	0.94	1.45	0.169
	DCA	1.03	0.91	1.18	0.618
	HDCA	0.92	0.69	1.23	0.591
	UDCA	1.04	0.82	1.32	0.743
Primary conjugated		1.05	1.02	1.07	<0.001
	TCA	1.05	0.88	1.26	0.571
	GCA	1.09	1.04	1.15	<0.001
	TCDCA	2.27	1.56	3.32	<0.001
	GCDCA	1.06	1.02	1.10	0.003
Secondary conjugated		1.06	1.00	1.13	0.07
	TLCA	1.19	0.55	2.57	0.661
	TDCA	1.06	1.00	1.13	0.07
	GDCA	1.01	0.58	1.79	0.962

Table 5. *Univariable hazards for primary outcomes by bile acid species**)***

	Low BA (n = 18)	High BA (n = 11)
CLAD	6 (33.3%)	2 (18.2%)
CLAD & Bacterial Pneumonia	6 (33.3%)	7 (63.6%)
CLAD & Fungal Pneumonia	2 (11.1%)	0 (0%)
CLAD & Viral Pneumonia	1 (5.6%)	0 (0%)
Malignancy	3 (16.7%)	2 (18.2%)

Table 6. *Recipient cause of death according to bile acid levels at 3 months.* BA: bile acids, CLAD: chronic lung allograft dysfunction.

*BA aspiration predict bacterial airway infections***.** Higher levels of BA in BW at 3-months had a significant increase in positive bacterial cultures (**Table 7-8**). The level of BA at 3-months also correlated with an increased rate of positive bacterial cultures within the first-year post-transplant (**Figure 4A**). This was mostly related to significant correlation with conjugated bile acids by univariable analysis (**Table 9, Figure 4B**). After adjusting for baseline risk factors (**Tables 3-4**) using multivariable regression, conjugated BA levels remained an independent predictor (Beta coefficient: 0.77; 95% CI: 0.28–1.26; p= 0.003) for positive cultures within the first-year post-transplant.

Bile Acid Levels in bronchial washes at 3 months after Lung Transplant and Bacteria			
	No Bacteria	**Bacteria**	**Total**
Low Bile Acids	26 (74%)	9 (26%)	35 (70%)
High Bile Acids	6 (40%)	9 (60%)	15 (30%)
	32 (100%)	18(100%)	50 (100%)

χ^2 =5.4; p=0.02

Table 7. *Bile acid levels associate with airway infections*

Bile Acid Levels in Bronchial Washes at 3 months after Lung Transplant and Type of Bacteria		
	Low Bile Acids (9 /35)	**High Bile Acids (9/15)**
Pseudomonas	4 (11.1%)	3 (20%)
Klebsiella	2 (5.6%)	1 (6.7%)
E.Coli	1 (2.8%)	1 (6.7%)
Enterobacter	0 (0%)	1 (6.7%)
Stenotrophomonas	0 (0%)	1 (6.7%)
Staphylococcus Aureus	2 (5.6%)	2 (13.4%)

Table 8. *Bacterial cultures by bile acid levels.*

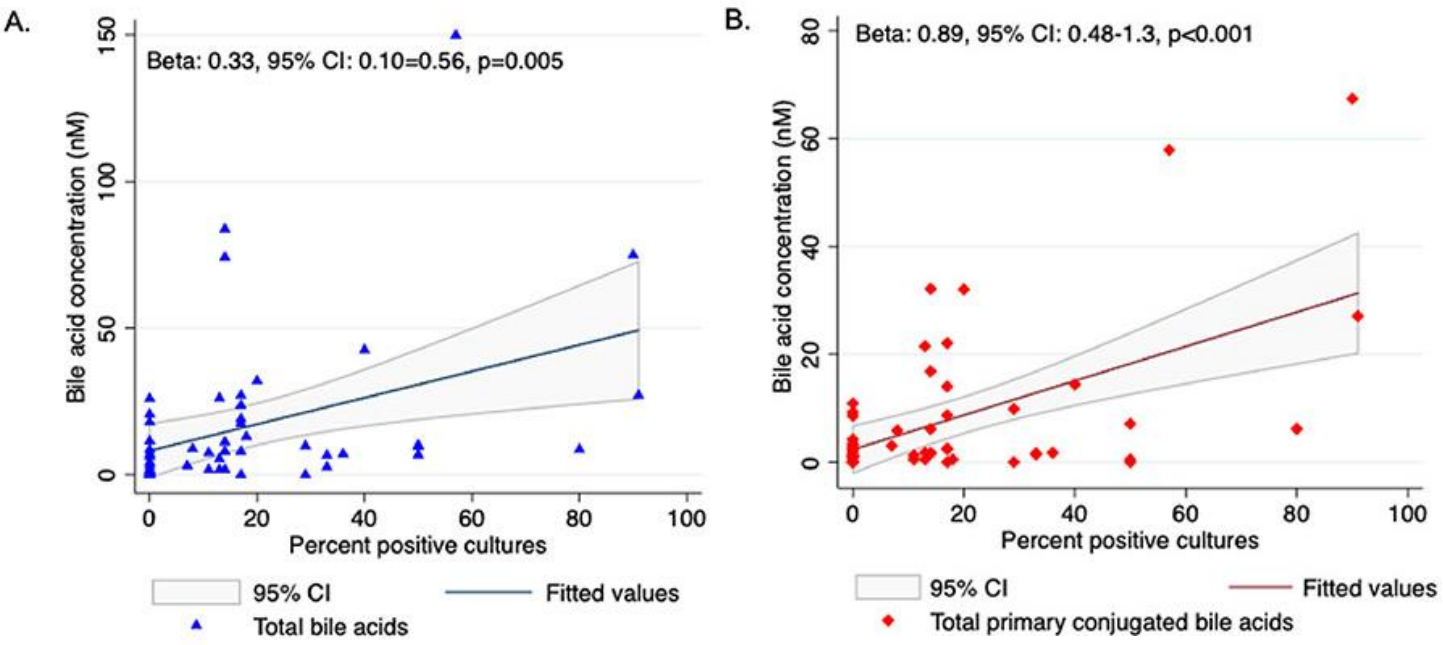

Figure 4. *Total and primary conjugated bile acids in BW are associated with an increased rate of pulmonary infections during the first year after transplant.* The total (A) and primary conjugated bile acid (B) levels in BW at 3-months post-transplant were compared to the percentage of positive airway cultures during the first year post-transplant using linear regression.

	Beta	95% CI		P value
Primary	0.40	-0.12	0.91	0.128
CA	0.64	-0.11	1.39	0.094
CDCA	0.82	-0.68	2.31	0.277
Secondary	0.50	-0.95	1.94	0.494
LCA	4.79	0.93	8.65	0.016
DCA	-0.42	-3.03	2.19	0.748
HDCA	-0.29	-5.20	4.62	0.906
UDCA	0.47	-3.97	4.91	0.832
Primary conjugated	0.89	0.48	1.30	<0.001
TCA	0.90	-3.48	5.27	0.682
GCA	1.72	0.96	2.48	<0.001
TCDCA	7.01	-0.36	14.39	0.062
GCDCA	1.17	0.37	1.97	0.005
Secondary conjugated	-0.18	-1.64	1.28	0.803
TLCA	0.32	-15.05	15.69	0.966
TDCA	-0.17	-1.66	1.31	0.816
GDCA	-0.90	-11.06	9.26	0.86

Table 9. *Univariable correlation by percent of positive bacterial cultures during the first-year post lung transplant by concentration of each BA species.*

Aspirated primary conjugated BA correlate with an increased concentration of airway lipids and cytokines. A correlation between total BA and airway lipid and cytokine changes was observed in the 3-month post-transplant BW, particularly in the presence of primary conjugated BA (**Figure 5A-B**). Significant correlations between primary conjugated BA and lipids were identified for cholesterol ester (CE; *r*=0.57, p=<0.001), sphingomyelin (SM; *r*=0.61, p<0.001), dihydrosphingomyelin (DhSM; *r*=0.65, p<0.001), monsialodihexosylgangloside (GM3; *r*=0.48, p<0.001), phosphatidic acid (PA; *r*=0.33, p=0.018), phosphatidilcholine (PCe; *r*=0.62, p<0.001, phosphatidylethanolamine (PEP; 0.42, p=0.002), phosphatidylinositol (PI; *r*=0.4, p=0.004), ether lysophophatidylcholine (LPCe; *r*=0.3, p=0.035), lysophosphatidylethanolamine (LPEp; *r*=0.31, p=0.028), lysophosphatidylinositol (LPI; *r*=0.34, p=0.015), and *N*-acyl-phosphatidyl serine (NAPS; *r*=0.35, p=0.012) (**Figure 5A**).

A similar pattern of correlation was noted between proinflammatory cytokines and primary conjugated BA, although the strength of the correlation was in general weaker. In particular, the primary conjugated BA TCDCA, strongly correlated with IL-8 (*r*=0.48, p=0.001), IL-1α (*r*=0.64, p<0.001), IL-1ß (*r*=0.65, p<0.001), IL-18 (*r*=0.64, p<0.001), IL-10 (*r*=0.64, p<0.001), IL-13 (*r*=0.63, p<0.001) (**Figure 5B**). Further, high percentage of TCDCA was also an independent predictor of CLAD (HR: 2.57, 95%CI: 1.07-7.26, p=0.035) and mortality (HR: 3.8, 95% CI: 1.44-10.44, p=0.008). Presence or absence of airway bacterial infection in general did not affect the levels of lipids or cytokines (**Table 10-11**).

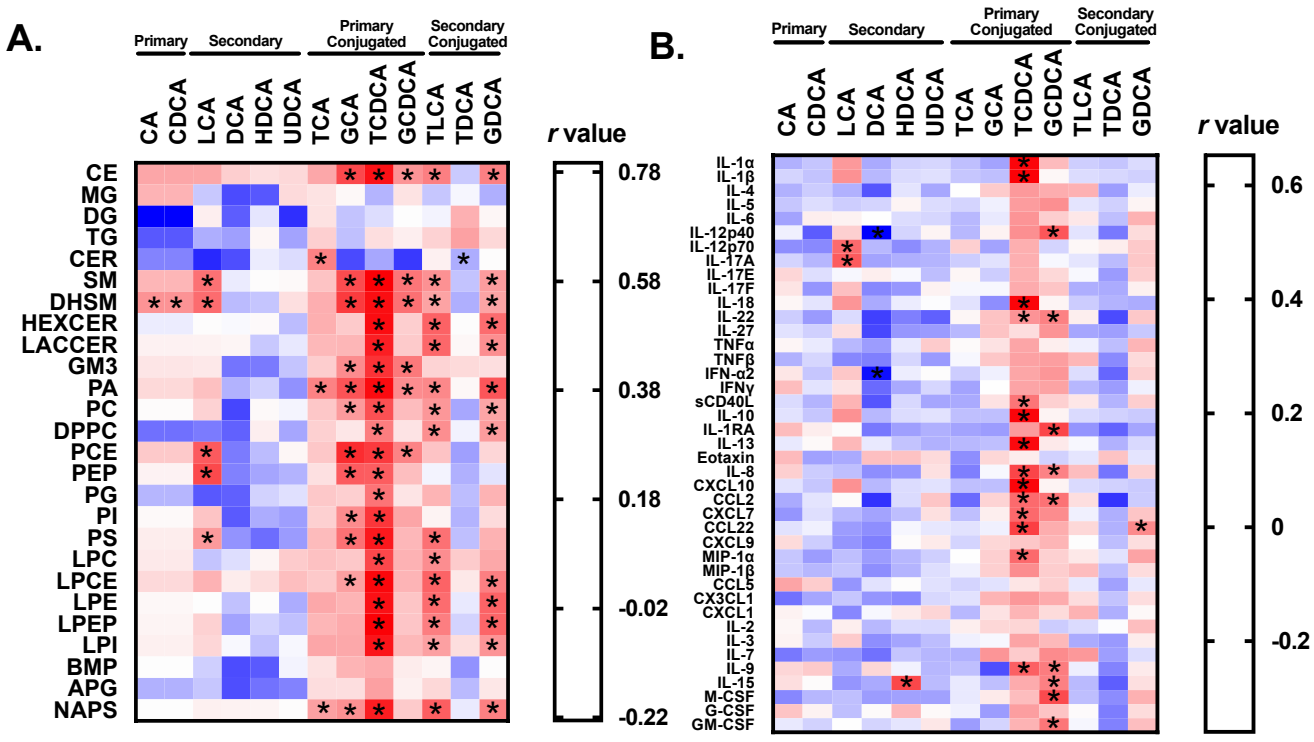

Figure 5. *Association of airway lipid and bile acid subtypes from BW samples at 3 months post-transplant.* The BW concentrations of each bile acid specie and lipids (A) and cytokines (B) were compared using Pearson's correlation. The heatmaps show the *r* value as shown in the legend. The asterisk denote p<0.05 after a Benjamini-Hoschberg correction. Lipid abbreviations - CE: cholesteryl ester, DG: diacylglycerol, TG: triacylglycerol, CER: ceramide, SM: sphingomyelin, dhSM: dihydrosphingomyelin, HEXCER; hexosylceramide, LACCER: lactosylceramide, PA: phosphatidic acid; PC: phosphatidyl choline, PCe: ether phosphatidylcholine, PE: phosphatidylethanolamine, Pep: plasmalogen phosphatidylethanolamine, PG: phosphatidylglycerol, PI: phosphatidylinositol, PS: phosphatidylserine, LPC: lysophosphatidylcholine, LPCe: ether lysophosphatidylcholine, LPE: lysophosphatidy lethanolamine, LPEp: plasmalogen lysophosphatidy lethanolamine, LPI: lysophosphatidylinositol, BMP: bis(monoacylglycero)phosphate, NAPS: N-acylphosphatidylserine. CA: cholic acid, CDCA: chenodeoxycholic acid, LCA: lithocholic acid, DCA: deoxycholic acid, HDCA: hyodeoxycholic acid, UDCA: ursodeoxycholic acid, TCA: taurocholic acid, GCA: glycocholic acid, TCDCA: taurochenodeoxycholic acid, GCDCA: glycochenodeoxycholic acid, TLCA: taurolithocholic acid, TDCA: taurodeoxycholic acid, GDCA: glycodeoxycholic acid.

	Negative cx for bacteria (n=33)			Positive cx for bacteria (n=17)			
	Median	**IQR**		**Median**	**IQR**		**P value**
CE	3.90	2.38	10.63	8.73	5.26	19.52	0.034
MG	5.55	3.76	7.58	6.34	3.42	13.74	0.992
DG	45.01	19.4	64.94	33.73	23.82	42.41	0.180
TG	2.63	1.74	6.51	3.00	2.36	3.59	0.910
CER	0.01	0.00	0.12	0.01	0.00	0.07	0.976
SM	1.79	1.13	3.27	2.51	1.82	3.29	0.187
DHSM	0.01	0.00	0.01	0.01	0.00	0.01	0.201
HEXCER	0.02	0.01	0.03	0.02	0.01	0.03	0.878
LACCER	0.63	0.34	1.44	1.16	0.43	5.61	0.179
GM3	0.15	0.08	0.26	0.12	0.07	0.18	0.264
PA	0.23	0.11	0.31	0.26	0.19	0.33	0.187
PC	10.59	5.09	13.41	12.02	7.44	13.04	0.443
DPPC	6.64	4.26	9.69	9.19	6.38	10.45	0.311
PCE	1.86	0.84	2.56	2.26	1.69	2.81	0.104
PEP	0.32	0.03	0.78	0.32	0.17	0.53	0.830
PG	2.21	0.88	4.91	2.31	1.21	3.93	0.878
PI	3.05	1.71	6.48	3.61	2.26	4.64	0.894
PS	0.22	0.05	0.56	0.22	0.12	0.60	0.351
LPC	0.67	0.29	1.08	0.60	0.37	0.95	0.862
LPCE	0.12	0.10	0.18	0.15	0.12	0.21	0.215
LPE	0.07	0.02	0.16	0.14	0.06	0.20	0.104
LPEP	0.16	0.03	0.37	0.22	0.12	0.31	0.373
LPI	0.30	0.23	0.41	0.30	0.28	0.38	0.735
BMP	0.01	0.00	0.04	0.02	0.01	0.03	0.187
APG	1.81	0.67	3.49	1.95	1.35	4.75	0.559
NAPS	0.01	0.01	0.03	0.02	0.01	0.02	0.419

Table 10. *Comparison of percentage of individual lipids among samples with a negative or positive bacterial culture.* Cx: culture, IQR: interquartile range, CE: cholesteryl ester, DG: diacylglycerol, TG: triacylglycerol, CER: ceramide, SM: sphingomyelin, dhSM: dihydrosphingomyelin, HEXCER; hexosylceramide, LACCER: lactosylceramide, PA: phosphatidic acid; PC: phosphatidyl choline, PCe: ether phosphatidylcholine, PE: phosphatidylethanolamine, Pep: plasmalogen phosphatidylethanolamine, PG: phosphatidylglycerol, PI: phosphatidylinositol, PS: phosphatidylserine, LPC: lysophosphatidylcholine, LPCe: ether lysophosphatidylcholine, LPE: lysophosphatidy lethanolamine, LPEp: plasmalogen lysophosphatidy lethanolamine, LPI: lysophosphatidylinositol, BMP: bis(monoacylglycerol)phosphate, NAPS: N-acylphosphatidylserine.

	Negative cx for bacteria (n=33)			Positive cx for bacteria (n=17)			
	Median	IQR		Median	IQR		P value
IL-1α	35.98	9.65	101.97	70.05	53.45	140.90	0.163
IL-1β	1.95	0.84	7.39	5.32	1.63	11.59	0.226
IL-4	0.14	0.06	0.27	0.29	0.06	0.37	0.156
IL-5	0.13	0.05	0.79	0.08	0.05	0.34	0.760
IL-6	9.78	0.91	33.35	12.49	8.28	37.85	0.182
IL-12p40	3.29	1.57	5.84	2.55	1.57	4.50	0.614
IL-12p70	0.07	0.04	0.20	0.07	0.04	0.11	0.389
IL-17A	0.01	0.01	0.01	0.01	0.01	0.01	0.919
IL-17E	0.01	0.01	0.38	0.01	0.01	0.18	0.545
IL-17F	0.10	0.01	0.37	0.09	0.03	0.24	0.627
IL-18	2.33	0.40	17.79	4.37	1.36	11.79	0.529
IL-22	2.32	0.01	15.31	9.63	2.80	18.87	0.129
IL-27	0.01	0.01	5.50	0.01	0.01	0.01	0.437
TNFα	1.21	0.09	2.65	2.22	1.10	4.00	0.103
TNFβ	1.28	0.07	2.36	2.23	0.99	5.08	0.098
IFN-α2	1.23	0.46	2.88	1.23	0.62	1.80	0.640
IFNγ	0.02	0.01	0.22	0.06	0.01	0.45	0.242
sCD40L	0.50	0.01	1.96	1.96	1.16	3.06	0.060
IL-10	0.10	0.05	0.21	0.15	0.10	0.31	0.122
IL-1RA	59.72	14.18	358.37	268.40	96.68	425.62	0.073
IL-13	0.01	0.01	2.67	0.01	0.01	3.18	0.871
Eotaxin	3.61	2.31	7.62	11.15	6.58	25.73	0.008
IL-8	2.33	0.40	17.79	4.37	1.36	11.79	0.527
CXCL10	41.59	5.85	99.45	36.86	12.34	62.75	0.924
CCL2	609.06	236.28	1178.48	438.54	153.12	1102.91	0.298
CXCL7	4.03	2.02	7.47	1.80	0.01	2.84	0.075
CCL22	5.90	0.97	14.95	5.41	2.85	17.14	0.482
CXCL9	347.42	144.98	736.70	705.38	364.99	984.25	0.118
MIP-1α	3.23	0.01	14.66	8.55	3.94	30.71	0.208
MIP-1β	5.82	1.66	16.15	8.76	5.94	16.62	0.203
CCL5	13.07	2.70	60.24	45.66	21.78	91.91	0.031
CX3CL1	4.51	0.01	13.75	7.01	0.85	16.28	0.685
CXCL1	1379.40	27.56	3131.09	1454.42	955.88	2200.36	0.729
IL-2	0.01	0.01	0.01	0.01	0.01	0.01	0.919
IL-3	0.01	0.01	0.01	0.01	0.01	0.01	0.858
IL-7	0.72	0.01	4.86	1.01	0.01	3.51	0.764
IL-9	0.54	0.01	1.16	0.62	0.56	0.88	0.429
IL-15	1.55	0.38	4.10	2.77	0.61	7.41	0.361
M-CSF	243.93	101.31	477.62	193.11	131.73	452.53	0.949
G-CSF	23.70	1.50	90.86	40.06	10.25	236.86	0.156
GM-CSF	1.26	0.01	3.23	2.15	0.01	3.26	0.562

Table 11. *Comparison of cytokine concentrations among samples with a negative or positive bacterial culture.* IQR: interquartile range, IL: interleukin, CSF: colony stimulating factor, IFN: interferon.

Discussion

With the advantages brought by quantitative mass spectrometry assays for BA and lipidomics, this study explores the presence of aspirated BA subspecies in the airways of lung transplant recipients and their association with clinical outcomes. We investigated changes of bronchial airway lipids in association with aspirated BA. Our findings confirm the role of aspirated BA as risk factors for lung transplant recipient outcomes at 3-months post-transplant (D'Ovidio et al., 2005c, 2006; Zhang et al., 2020), provide individual quantitation of all BA species, and propose a novel data on conjugated BA species serving as specific diagnostic elements. Conjugated BA in high proportions were independent risk factors for poor outcomes such as bacterial infections and magnified the risk for earlier CLAD development and reduced survival. Lastly, BA levels correlated with changes in free airway surface lipids and surfactant phospholipids, along with inflammatory cytokines. Despite our study being limited to a single center investigation with a small sample size, it confirms and provides incremental knowledge over the recently published multicenter study by Zhang et al., which also showed significant clinical correlations only with the conjugated specie they tested at the 3-month time point over other timepoints (Zhang et al., 2020).

Circulating BA concentrations in healthy humans have been deemed to range low micromolar units with no correlation with airway concentrations (García-Cañaveras et al., 2012). Aspirated BA are subject to dilution of the refluxate with saliva, airway mucus, and volumes added during bronchoscopies for sample collection (D'Ovidio et al., 2005c). To accommodate for this, we captured a more proximal airway contamination through BW assuming a potentially greater yield in BA detection. We show that the BA composition in

the airways adheres to that reported in the gastro-intestinal tract, where primary conjugated BA dominate the environment (Hofmann 1999), yet in lower concentrations (Table 1). This study has shown particular relevance for TCDCA. The unconjugated form of this primary bile acid, CDCA, has been previously implicated in cellular damage, permeability and increased reactive oxygen species (Wu et al., 2009; Zhangxue et al., 2012; Su et al., 2013). The conjugation with taurine adds a sulfonic acid functional group to the molecule, increasing its acidity and solubility. The gut-originating strong acid is neutralized by PPI treatment, but the solubility and penetrability properties remain. There is no evidence of *de novo* synthesis of BA in the pulmonary epithelium (Zhao et al., 2014), and secondary BA are specifically produced in the intestines by anaerobic bacteria (e.g. *Clostridium difficile*) as derivatives of primary BA. These observations fortify the concept of a gut-lung axis in the context of micro-aspiration, and our data showing secondary and conjugated BA in BW samples is confirmatory of retrograde reflux aspiration pathophysiology (Ma et al., 2021).

Micro-aspiration following reflux involves gastro-enteric content transit through the esophagus into the airways. The canonical diagnostic approach involves performing distal esophageal pH testing, which does not reveal a significant relationship with aspiration, resulting in under-diagnosis (D'Ovidio et al., 2005c). In addition, data from our group has previously shown that proximal, but not distal, esophageal pH testing associates with micro-aspiration. As observed in the multicenter study published by Zhang et al, the transient nature of micro-aspiration can result in failure to diagnose reflux and renders distal esophageal pH testing unreliable (Zhang et al., 2020). This potential unreliability incites the preventive prescription of PPIs, which successfully address the pH of the

refluxate but not the remaining abnormalities associated with aspirating molecules of duodeno-gastric origin (Tamhankar et al., 2004). Therefore, minor reflux episodes in a dysfunctional esophagus can still result in undetected retrograde micro-aspiration, especially in the context of nocturnal events occurring while the patient is supine and the upper esophageal sphincter is relaxed (Kahrilas et al., 1987). These observations question whether the clinical practice of distal esophageal pH testing and pH correction altogether might suffice in the context of a newly grafted organ and led us to exclude pH testing from this study.

Differences in the high versus low levels of BA were noted according to the underlying recipient disease. Most recipients with interstitial lung disease had lower levels of BA, while a larger proportion of the COPD recipients had high levels. This observation may appear in contrast with the known prevalence of GER in interstitial lung disease and in idiopathic pulmonary fibrosis. However, little is known on BA aspiration in restrictive or obstructive lung disease. Further, the timing of normalization after the transplant of the diaphragmatic function on the gastro-esophageal high-pressure zone has not been studied in the different recipient populations. This may provide a protective effect towards aspiration as spontaneous reversal of acid GER at 3 months after lung transplantation has been described.

Type II pneumocytes and goblet cells provide *de novo* synthesis of surfactant lipids that coat the alveoli and airways. These lipids reduce surface tension and provide the first innate defense barrier against environmental insults (Ingenito et al., 2000). Type II pneumocytes, respond to injury by secreting free lipids into the distal airspaces of the lungs (Romero et al., 2015). Our data shows that elevated BA levels strongly correlate

with free airway membrane lipids and tensioactive surfactant lipids (van Meer et al., 2008). Previous studies have associated BA to surfactant dysfunction modulated by an increase in the enzyme phospholipase A2 (PLA2). Hence, the damage induced by BA to the surfactant layer may facilitate increased alveolar permeability, the formation of foam cells resulting in lung toxicity and fibrotic injury (de Luca et al., 2009; Herraez et al., 2014). Indeed, BA microaspiration in children with cystic fibrosis associated with progressive structural changes indicative of their involvement in tissue damage (Caparrós-Martín et al., 2020). As a follow up, our speculation is that the higher levels of free lipids in the airway resulting from aspiration of primary conjugated BA in particular aggravates lung function over time (Figure 5A, Figure 2). This is supported in our results by the increased concentrations of lipids and the poor clinical outcomes. The correlation pattern observed in our cytokine assay which, also confirmed the specific contribution of primary conjugated BA, in particular TCDCA, as a predictor of transplant outcomes associated to inflammatory cytokine dysregulation. Consistently with the BA and lipid assays, reported cytokines were also measured in BW samples to investigate the effect of BA in the bronchial district. In a state of innate defense instability and surface lipid damage, the impact of released inflammatory cytokines can be potentially deleterious to the organ. Inflammation caused by the presence of IL-1β may further jeopardize the structural recovery of the organ by stimulating apoptotic pathways and cell content release. These findings are supported by previous association of retrograde micro-aspiration affecting the epithelial barrier through a reduction of surfactant protein A, C, and D (SP-A, SP-C and SP-D), leading to lower antimicrobial activity facilitating the establishment of bacterial

and fungal populations (D'Ovidio et al., 2005c, 2006; Verleden et al., 2011; Neujahr et al., 2014).

Microorganismal presence post-aspiration has been previously documented in intensive care patients where gram-negative bacteria mostly of gastric origin were associated with bilirubin in the lower respiratory tract (Dumoulin, 1982; Inglis et al., 1993). As part of the adverse outcomes of aspiration, we noted that BW with positive cultures for bacteria of pulmonary and gastric origin associated with greater levels of BA (Figure 4). Pols et al. showed that BA exert immunomodulatory effects by inhibiting macrophage activity and inflammation, which is important during infection (Pols et al., 2011a). Further, primary conjugated BA in our study were identified as independent risk factors for airway infection during the first year after transplant, confirming that the noxious effects of BA aspiration may favor airway infection and colonization (Reen et al., 2016). We further noted that cause of death showed a trend of increased rate of CLAD and bacterial pneumonia in patients with higher BA levels at 3-months after transplantation (Table 6). Whether BA are biomarkers of aspiration and causative agents is question of ongoing research.

Confirmed retrograde aspiration generally advocates for resolutive anti-reflux procedures such as fundoplication (D'Ovidio et al., 2005c, 2006; Zhang et al., 2020; Leiva-Juárez et al., 2021). It is common practice to treat all recipients with PPI irrespective of a diagnosis of GER, while anti-reflux surgery is performed only in recipients with documented GER and with evidence of drop in lung function without other attributable cause. PPIs function to neutralize the gastric pH and consequently the pH of refluxate at the expense of its antibacterial effects. A non-acidic microenvironment promotes the colonization of bacteria

in the stomach and consequently in the lung post- reflux aspiration (Biswas Roy et al., 2018; Leiva-Juárez et al., 2021). Therefore, the presence in the airways of recipients of bacteria and possibly of related pathogen-associated molecular patterns and damage-associate molecular patterns causing inflammation may also be exacerbated by the antacid therapeutic regimens.

In conclusion, our findings confirmed that aspirated BA are risk factors for long-term poor outcomes including reduced freedom from CLAD and survival in lung transplant recipients. Further, we identified conjugated BA as a potentially important diagnostic and prognostic element in the workup of aspiration. We showed that aspirated conjugated BA are associated with a derangement in airway surface and surfactant lipids, inflammatory cytokines and also pose a risk for infections. There is certainly more to discover about this gut-lung axis and the mechanistic role of BA in all the results discussed in order to reach conclusions on potential precision medicine treatment and management strategies. Hence, our findings stimulate the establishment of multicenter studies investigating the role of BA species as markers of retrograde aspiration and risk factors for pulmonary dysfunction which may in the long-term open the field to additional patient-specific therapeutic options.

BA as molecular ligands in airway contractility

As discussed in Chapter 2, BA signaling is known to be regulated by two main receptors: the nuclear FXR and the surface TGR5. Other groups have indicated the participation of BA in pathways mediated by cholinergic muscarinic receptors, highly relevant in bronchoconstriction, ciliary movement and mucus clearance. Thus, this section will address our initial hypothesis stating that *BA hold differential physiological roles in airway mechanics*.

Materials and Methods

Chemicals. A pH-buffered Hank's Balanced Salt Solution (sHBSS) was prepared by diluting a 10X HBSS stock (Thermo Fisher Scientific, Waltham, MA) and supplementing with HEPES (20 mM) and NaOH to obtain pH 7.40 in the final solution. Bile acids (BAs) were purchased from Millipore-Sigma (St. Louis, MO). The following BAs were used and their abbreviation and chemical purity is indicated in parenthesis: primary BAs included cholic acid (CA, ≥98%), glycocholic acid (GCA, ≥97%), taurocholic acid (TCA, ≥95%), chenodeoxycholic acid (CDCA, ≥97%), glycochenodeoxycholic acid (GCDCA, ≥97%), taurochenodeoxycholic acid (TCDCA, ≥95); and secondary BAs included lithocholic acid (LCA, ≥95%), glycolithocholic acid (GLCA, ≥95%), taurolithocholic acid (TLCA, ≥97), deoxycholic acid (DCA, ≥98%), glycodeoxycholic acid (GDCA, ≥97%), taurodeoxycholic acid (TDCA, ≥95%) and ursodeoxycholic acid (UDCA, ≥99%). The specific TGR5 agonist (TC-G 1005) was from Tocris (Minneapolis, MN). BAs and TC-G 1005 were dissolved in dimethylsulfoxide (DMSO, MilliporeSigma) to prepare stock solutions 1,000-fold their final concentration and stored at -20°C. These stocks were diluted in sHBSS the same day of the experiment, and the final concentration of BAs did not exceed 0.1 mM. Acetyl- choline (ACh), 5-hydroxitriptamine (5-HT), atropine, and tetrodotoxin were obtained from MilliporeSigma and dissolved in deionized water to prepare stock solutions at least 1,000-fold their final concentration. These stock solutions were stored at -20°C and diluted in sHBSS on the same day of the experiment. Caffeine (MilliporeSigma) was dissolved directly in sHBSS at a final concentration of 20 mM on the day of the experiment. The pH of the sHBSS containing diluted BAs and/or drugs at their final concentrations was 7.40.

Ethical approval. Animal studies were approved by the Columbia University Animal Care and Use Committee (AC-AAAT6472). Human lungs were provided by an Organ Procurement Organization agreement with the Lung Transplant Program at New York-Presbyterian/Columbia University Irving Medical Center, and these studies were approved by the Institutional Review Board (IRB-AAAR2681).

Preparation of mouse and human precision-cut lung slices. Mouse lung slices were prepared as described previously (Mukherjee et al., 2013). Briefly, male C57BL/6 mice (Charles River, MA) were maintained in our animal facility with free access to food and water under a 12-h light cycle. Approximately 12-wk-old mice of both sexes were euthanized with sodium pentobarbital (120 mg/kg ip), the chest cavity was opened, and the lungs were inflated with 1.3 mL of 2% agarose (low-melting point agarose, Thermo Fisher Scientific) in sHBSS (37°C) and ~0.2 mL of air. The agarose in the lungs was gelled by placing the mouse at 4°C for 20 min. Lungs and heart were removed from the animal, and the lung lobes were cut in 130-μm-thick slices using a tissue slicer (Compresstome VF-300, Precisionary Instruments, Greenville, NC) in a laminar flow cabinet under sterile conditions.

Human lungs from 18 – 60-yr-old donors of both sexes with no documented lung disease were collected and brought to the laboratory within 4–12 h of harvest. The lungs were warmed by submersion in sHBSS at 37°C, and two lobes were cannulated through the main bronchi. The lung lobes were inflated by instilling ~1 liter of 2% agarose in sHBSS at 37°C using constant positive pressure, and gentle manipulation of the tissue was applied to facilitate homogeneous distribution of the agarose. Agarose infusion was terminated when the lung periphery reached a firm consistency upon gentle pressure. The inflated lungs were immediately transferred to ice-cold sHBSS and kept at 4°C for 1 h to allow agarose solidification. Small cubical pieces (~1.5 mL) of agarose-inflated lungs were cut from peripheral regions and mounted in the tissue holder of the compresstome as per manufacturer's instructions. The lung tissue was sectioned in 150- μm-thick slices and transferred to sHBSS.

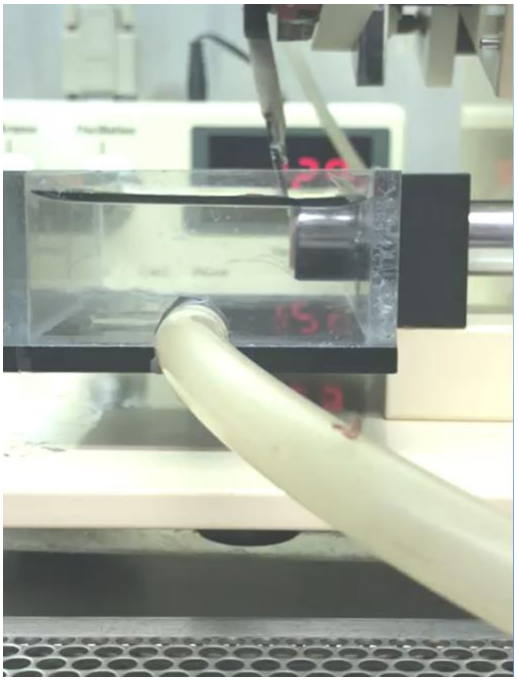

Precision-cut lung slices (PCLS) from both human and mice, containing small terminal airways, were transferred to 60-mm Petri dishes containing 10 mL of low-glucose Dulbecco's Modified Eagle Medium (DMEM, Thermo Fisher Scientific) supplemented with antibiotics and were incubated for 10– 16 h at 37°C and 10% CO2 in a cell culture incubator. PCLS selected for the experiments contained airways with a lumen diameter of 100–250 μm, completely lined by active ciliated epithelial cells and fully attached to the surrounding lung parenchyma.

Measurement of the contractile response of airways. The contractile response of airways in PCLS was measured using phase-contrast video microscopy as previously described (Mukherjee et al., 2013). Briefly, PCLS were mounted on a cover glass in a custom-made perfusion chamber and held in place with a small sheet of nylon mesh with a narrow opening to allow for airway imaging. Perfusion of the PCLS was performed by dripping solution at one end of the chamber and removing it by suction at the opposite end by means of a custom-made, gravity-fed, computer-controlled perfusion system consisting of eight syringe tubes connected to individual electronic solenoid valves (The Lee Company, Westbrook, CT) and to an 8-way manifold. The PCLS were continuously superfused with one of the solutions at ~800 μL/min, and solution changes were made by switching between solutions at preprogrammed times. Exposure of PCLS to two or more drugs/ chemicals (e.g., ACh + TLCA) was made by superfusing a single solution containing all drugs/chemicals at the final concentration. The chamber was placed on the stage of an inverted phase-contrast microscope and lung slices were imaged with a ×10 objective. Digital images were recorded to a hard-drive in time lapse (0.5 Hz), using a CCD camera, frame grabber, and image acquisition software (Video Savant, IO Industries, Ontario, Canada). The airway cross-sectional luminal area (lumen area) was calculated from each image using a custom-written script in Video Savant that

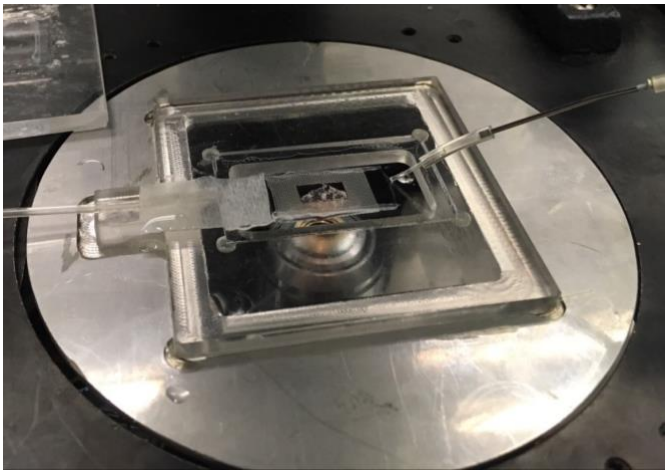

distinguishes the airway lumen from the surrounding tissue. The lumen area was normalized to the initial area (before stimulation) and the changes in lumen area were plotted versus time using graphics software. To study the effects of BAs on airways pre-constricted with cholinergic stimuli, we choose ACh because it is the natural agonist for muscarinic receptors in airway smooth muscle cells. In contrast to other cholinergic agonists such as methacholine, ACh is sensitive to inactivation by acetylcholine esterase that is active in the PCLS. However, under our experimental conditions of continuous superfusion of PCLS, the airways are exposed to fresh ACh and able to maintain a sustained constriction until ACh washout.

Electrical field stimulation-induced contractions of guinea pig trachea. The effect of selected BAs on proximal airway contractions elicited by electrical field stimulation (EFS) was evaluated in guinea pig tracheal rings as previously described (Jooste et al., 2005). Briefly, Hartley male guinea pigs were euthanized with 100 mg/kg ip sodium pentobarbital, and the tracheas were removed and then dissected into closed rings consisting of two cartilaginous rings from which mucosa, connective tissue, and epithelium were removed. The tracheal rings were sus- pended in wire myograph organ baths containing physiological salt solution (composition: 118 mM NaCL, 5.6 mM KCl, 0.5 mM CaCl2, 0.2 mM MgSO4, 25 mM NaHCO3, 1.3 mM NaH2PO4, and 5.6 mM D-glucose) with 10 μM indomethacin (dimethyl sulfoxide vehicle, final concentration of 0.1%). After equilibration, the guinea pig tracheal rings were precontracted twice with a range of ACh concentrations (0.1 μM to 1 mM) to obtain a series of contractile responses from no constriction to maximal constriction. After extensive ACh washout with buffer exchanges,

the resting tension was reset at 1 g. EFS was delivered via two platinum electrodes situated on opposite sides of the preparation and separated ~0.8 cm. The electrical signal was generated using a Grass RPS 107 stimulator (Grass-Telefactor) and consisted of trains of pulses, each with a duration of 0.5 ms and frequency of 32 Hz. Each train duration was 5 s and repeated every 80 s. After waiting a minimum period of 60 min, and when the EFS- induced contraction force had become constant, cumulative doses of BAs were added to the baths to determine the 50% inhibitory con- centration (IC50) of BA at inhibiting EFS-induced contractions. The effect of BAs on the EFS-induced contraction was expressed as a percentage of the EFS-induced force before BAs were added.

Inositol phosphate assays. [^{3}H] inositol phosphate synthesis was measured using the method of Wedegaertner et al. (Wedegaertner et al., 1993) with some modifications, as we previously described (Hotta et al., 1999). Briefly, we used immortalized human airway smooth muscle cells stably transfected to express the human M3 muscarinic receptor, as we described earlier (Townsend et al., 2014). These cells were grown in 24-well plates in media M199 with 10% FBS, 1 ng/mL FGF, 0.25 ng/mL EGF, 0.17 μM insulin, 6.9 nM transferrin, 3.9 nM selenium, and antibiotics (100 U/mL penicillin, 100 μg/mL streptomycin, and 0.25 μg/mL amphotericin B) until they reached confluence. Subsequently, the medium was replaced with DMEM containing 10 μCi/mL myo-[^{3}H] inositol (specific activity 20 Ci/mmol; Perkin Elmer, Waltham, MA) on the day before the assay. The next day, the loading media was aspirated, and the wells were washed twice with 500 μL warm (37°C) assay buffer (sHBSS supplemented with 10 mM LiCl). Assay buffer (300 μL) was added to each well, and cells were pretreated for 15 min at 37°C with

increasing concentrations of GCDCA, TLCA, or vehicle (0.1% DMSO). Cells were then left untreated (basal inositol phosphate synthesis) or were stimulated with 0.15 μM ACh for 30 min at 37°C. The reaction was terminated by the addition of 330 μL of cold methanol. Then, 660 μL of chloroform was added, and the samples were transferred to an Eppendorf tube. The phases of the samples were separated by centrifugation at 820 *g* for 10 min at 4°C. Four hundred fifty microliters of the upper aqueous phase were transferred to a new glass tube. Cold 50 mM formic acid (300 μL) and 100 μL of 3% ammonium hydroxide were added, and total [^{3}H] inositol phosphates were separated from free myo-[^{3}H] inositol by chromatography and quantified by liquid scintillation.

RT-PCR of TGR5 expression in lung slices. PCLS from TGR5 knockout (KO) and wild-type (WT) mice were prepared as described above and stored at -80°C. Total RNA was obtained from these PCLS using Trizol Reagent, and cDNA was synthesized using Super- Script VILO reagents (Thermo Fisher Scientific). Two micrograms of RNA were used for each 20 μL RT-PCR reaction. PCR was then performed (40 cycles) using 1 μL of cDNA product. All primer sets were designed to flank at a large intron to avoid confounding amplification of genomic DNA. Two-step PCR was used with a denaturing temperature of 94°C for 10 s and an annealing/extension temperature of 68°C for 1 min. Mouse whole brain served as a positive control, and PCR reaction mixtures devoid of cDNA served as RT-PCR negative controls. All reagents were from Life Technologies (Carlsbad, CA).

Quantitative RT-PCR of muscarinic receptors expression in peripheral airways. PCLS of 350 μm in thickness were prepared from C57BL/6 mice and incubated overnight in a cell culture incubator as described above. Peripheral airways in cross-section were micro-dissected from PCLS under a dissecting microscope (Nikon, Japan), using a pair of 20G needles to detach them from the surrounding lung parenchyma. Special care was taken to assure that the peripheral airways were also separated from the adjacent pulmonary arteries. A total of ~15 micro-dissected airways from each mouse were collected in a 0.5 mL conical tube containing 100 μL of lysis buffer. In addition, a sample of mouse brain cortex was prepared in parallel. The latter served as a calibration reference for the expression of muscarinic receptors. Total RNA was isolated using the Arcturus PicoPure RNA Isolation Kit (ThermoFisher) according to the manufacturer's recommendations. RNA purity and quantity were measured using the NanoDrop One (ThermoFisher). Complementary DNA synthesis was performed with SuperScript VILO cDNA Synthesis Kit (ThermoFisher) following the manufacturer's recommendations and using 200 ng total RNA in a final volume of 20 μL. Quantitative RT-PCR was performed with the mouse primers shown in Table 1, and amplification was carried out using the PowerSYBR Green PCR Master Mix (ThermoFisher) and the 7500 Real-Time PCR System (ThermoFisher) following manufacturer recommendations. The relative expression of the muscarinic receptor subtypes was calculated using the double- delta Ct method (Livak et al 2001) with glyceraldehyde 3-phosphate dehydrogenase (GAPDH) as the reference gene and mouse brain as the calibrator sample.

In vivo airway resistance and lung compliance testing. In vivo airway resistances were assessed using a flexiVent FX1 module with an inline nebulizer (SciReq, Montreal, QC, Canada), as previously described (Townsend and Emala, 2013), using BA-sensitized and non-sensitized (vehicle controls) WT mice. After intraperitoneal anesthesia with pentobarbital (50 mg/kg), paralyzed with intraperitoneal succinylcholine (10 mg/kg), and tracheostomized for ventilation (tidal volume: 10 mg/kg, 150 breaths/min). Airway resistance was measured through increasing concentrations of nebulized methacholine. Each nebulization period was 10 s with a 50% duty cycle using a 4- to 6-µm nebulizer. EKG and temperature monitoring was performed throughout the experiment. Central airway resistance values (Rn), pressure-volume (PV) loops, and lung compliance (Crs) for each mouse at each methacholine dose represent an average of three forced oscillatory measurements. Data were compared between groups by assessing the area under the methacholine cumulative dose-response curve.

Cytokine analysis. Aliquots of BAL supernatants were stored at -80°C. Cytokine concentrations in BAL supernatants were quantified with the Mouse Cytokine Proinflammatory Focused M31-plex Discovery Assay (Eve Technologies), which quantifies Eotaxin, G-CSF, GM-CSF, IFNγ, IL-1α, IL-1β, IL-2, IL-3, IL-4, IL-5, IL-6, IL-7, IL-9, IL-10, IL-12p40, IL-12p70, IL-13, IL-15, IL-17A, IP-10, KC, LIF, LIX, MCP-1, M-CSF, MIG, MIP-1α, MIP-1β, MIP-2, RANTES, TNFα, and VEGF-A; TGFβ 3-plex, which quantifies TGFβ1 TGFβ2 and TGFβ3; MMP 5-plex, which quantifies MMP-2, MMP-3, MMP-8, proMMP-9, MMP-12; using a bead-based multiplexing technology also known as addressable laser bead immunoassay.

Cryosectioning and Histology. All histology preparation of lung sections has been completed by the Histology Core located at Columbia University Medical Center (New York, USA). Hematoxylin and eosin (H&E) and Masson's Trichrome stained sections were evaluated blindly and a numerical scale was used to quantify aberrant changes. The severity of organizing pneumonia was assessed and allotted a score from 0 to 2, using a predetermined scale (normal lung= 0; mild = 1; severe = 2); inflammation was also assessed and allotted a score from 0-3, using a predetermined scale (negative= 0; focal inflammation with 1 or 2 minute foci with less than 100 inflammatory cells in any focus =1; greater than 2 minute foci and/or more than 100 inflammatory cells plus/minus organizing pneumonia or reactive pneumocytes = 2; more or extensive inflammation and organizing pneumonia = 3). After examination of the whole section, mean values of the duplicate analysis of a blind observer were compared between groups. For overall treatment observations all lung lobe scores were averaged and a non-numerical assessment was communicated.

Statistics. Statistical values are expressed as mean ± SE. Student's *t* test or one-way analysis of variance (ANOVA) followed by Dunnett's Test comparisons were used to evaluate the significance be- tween means from two or more groups, respectively.

Results

Select BAs relax human and mouse peripheral airways precontracted with ACh. To study the effects of BAs on peripheral airways, we exposed PCLS to 30 μM TLCA for 8 min and found no changes in airway lumen area of either human or mouse PCLS (**Figure 1A,D**). A concentration of 30 μM was selected to test the efficacy of the BAs on the contractile responses of the airways based on the affinity of BA receptors with EC50 in the range of 0.1 μM to 20 μM and previous reports investigating the signaling functions of BAs in other organs and systems (Chiang and Ferrell, 2019) as well as our concentration- response curves presented later in this work. Then we tested whether TLCA had any effects on airways precontracted with 0.3 μM ACh, which induces submaximal airway constriction (Parks et al., 1999). ACh reduced the luminal area of human and murine airways by 48.4 ± 8.2% and 59.3 ± 4.5%, respectively. The subsequent addition of 30 μM TLCA, in the continuous presence of 0.3 μM ACh, caused airway relaxation in both human and mouse airways, as evidenced by the significant increase in airway lumen area. However, this TLCA-induced airway relaxation occurred at slower rates in human airways than in mouse airways (maximal relaxation rates were 2.6 ± 0.4%/min and 15.4 ± 1.8%/min, respectively; $P < 0.001$; unpaired *t* test) and reached 36.9 ± 3.7% and 51.0 ± 4.1% after 10 min of TLCA expo- sure, respectively. TLCA-induced relaxation was reversible upon TLCA washout, as the airways re-contracted by superfusing the solution containing ACh alone, although mouse airways re-contracted faster than human airways (**Figure 1B,E**). The subsequent washout of ACh increased the airway lumen area nearly to the resting condition in both human and mouse airways, indicating that the overall integrity and

functional state of the airways was maintained following the exposure of the PCLS to ACh and TLCA. To investigate the action of other BAs on airway reactivity, we performed similar experiments with select BAs on human airways and with the complete panel of 13 BAs on mouse airways. We found that, like TLCA, the other BAs tested caused no significant changes in the basal lumen area of unstimulated airways (**Table 2**). However, in airways precontracted with 0.3 μM ACh, some BAs (all BAs tested at 30 μM) caused relaxation, whereas others had no significant effects (**Figure 1C,F**). All secondary conjugated BAs (TLCA, GLCA, TDCA, and GDCA), the primary unconjugated BA CDCA, and the secondary unconjugated BAs LCA and UDCA induced significant relaxation in mouse airways precontracted with ACh (**Figure 1F**). In contrast, the primary BAs CA, GCA, TCA, GCDCA, and TCDCA and the secondary BA DCA did not have significant effects. Because of limited availability of human lungs for these experiments, we only tested TLCA, GDCA, and CA in human airways. As in mouse airways, TLCA and GDCA significantly relaxed human airways precontracted with ACh, whereas CA had no significant effects (**Figure 1C**). Altogether, these results suggest that BAs have no significant effects on unstimulated airways in PCLS, yet several BAs induce strong relaxation on airways contracted by ACh. Furthermore, the similar effects of BAs in human and mouse airways indicate that the mouse is a suitable model to study the role and mechanisms of BAs in the peripheral airways. Accordingly, some of our subsequent studies were performed on mouse models because of the ease of tissue preparation and availability.

GENE	ACCESSION ID	PRIMER PAIRS	cDNA size (bp)	gDNA size (bp)
CHRM1	NM_007698	F: AGGCCCCCGGAGAAGCACTGAA R: AGCCCCTTCCTCCAGTCACAAGATT	104	13,508
CHRM2	NM_203491	F: CGCTCGCTCCCAAACCGGTCCAA R: GTGTTCAGTAGTCAAGTGGCCAAAGAAACAT	136	134,554
CHRM3	NM_033269	F: GCTCAGTGGACTGTGGATTGAGTGAACCATA R: GAATGTCACGTGCTTGGTCACTTGGTCAGAA	114	102,469
AIRWAY 3	NM_008084	F: CCGTAGACAAAATGGTGAAGGTCGGTGTGAA R: CAATGAAGGGGTCGTTGATGGCAACAAT	120	1,954

Table 1. *Sequence-specific primers for mouse muscarinic receptor subtypes M1, M2, and M3 and GAPDH*

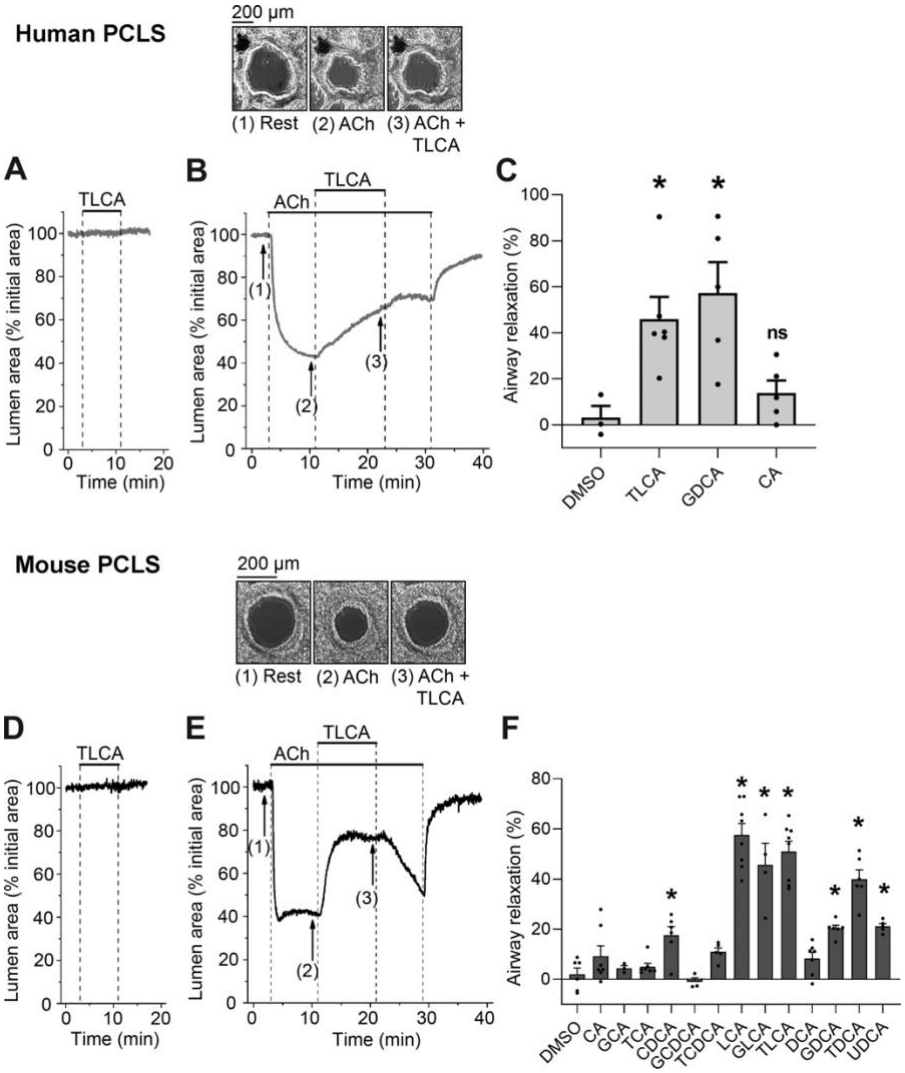

Figure 1. *Bile acids (Bas) induce relaxation of human and mouse peripheral airways precontracted with ACh. A* and *D*: representative traces showing expo- sure of human and mouse precision-cut lung slices (PCLS) to 30 μM taurolithocholic acid (TLCA) in HBSS. TLCA induced neither constriction nor relaxation of unstimulated (resting) airways. *B* and *E*: images and traces showing the changes in cross- sectional lumen area of peripheral airways in human and mouse PCLS constricted with 0.3 μM ACh and relaxed with 30 μM TLCA in the continuous presence of ACh. Drugs were continuously superfused at the times indicated by the lines on top of the traces; HBSS alone was superfused otherwise. The representative images were obtained at the times indicated by numbers below the traces. *C* and *F*: summary showing the relaxation induced by the indicated BAs (tested at 30 μM) or by 0.1% DMSO of airways preconstricted with ACh. Data were obtained from experiments similar to those shown in *B* and *E*: relaxation was calculated by dividing the lumen area value 10 min after BA addition by the lumen area value after ACh but before BA addition. Data are means ± SE of 3–5 PCLS from 3 human lungs or 6–8 PCLS from 3 mice; **P* < 0.05 vs. DMSO, ANOVA with post hoc Dunnett's test.

Concentration-dependence of TLCA- and CDCA-induced relaxation in ACh-precontracted airways.

To better understand the effects of BAs on airway relaxation, we precontracted mouse airways with ACh and subsequently exposed them to repetitive challenges with increasing concentrations of TLCA or CDCA. As shown in **Figure 2**, both TLCA and CDCA induced a concentration-dependent airway relaxation that was reversible upon BA washout. TLCA-induced airway relaxation was 21.0 ± 7.4% at 1 μM, increased gradually up to 80.2 ± 2.3% at 30 μM, and had an inhibitory concentration fifty (IC50) of 3.2 ± 0.6 μM (**Figure 2C**). CDCA was less potent than TLCA to relax ACh-precontracted airways and did not reach saturation at the maximal concentration tested (100 μM). Consequently, we did not calculate the maximal relaxation and IC50 values for CDCA. Since the effects of TLCA were readily reversible and maximal at 30 μM, we choose this BA at this concentration for our subsequent studies to investigate the action mechanisms of BA in the peripheral airways. Similarly, a concentration of 30 μM was used to investigate the effects of the different BAs tested in the studies presented earlier in Fig. 1.

BA	HUMAN	MURINE
DMSO	-2.6 ± 2.7	-1.9 ± 0.2
CA	-5.3 ± 1.8	-0.5 ± 0.3
GCA	ND	-1.3 ± 0.7
TCA	ND	0.4 ± 0.4
CDCA	ND	-1.7 ± 1.0
GCDCA	ND	-0.4 ± 0.4
TCDCA	ND	0.1 ± 0.5
LCA	ND	-0.2 ± 3.2
GLCA	ND	6.4 ± 1.2
TLCA	-2.7 ± 3.7	1.0 ± 0.5
DCA	ND	-1.1 ± 0.5
GDCA	-5.2 ± 1.4	-0.6 ± 0.4
TDCA	ND	-0.3 ± 0.4
UDCA	ND	-0.2 ± 0.4

Table 2. *BAs induce neither contraction nor relaxation in unstimulated (resting) airways.* Values are means ± SE of 3-5 precision cut lung slices (PCLS) from 3 human lungs or 6 – 8 PCLS from 3 mice. Summary of decrease (+) or increase (-) in airway lumen area (%) induced by exposure of the PCLS to bile acids (BA; tested at 30 μM) or 0.1% DMSO (vehicle) in human and mouse peripheral airways at rest. The data were obtained from experiments similar to those shown in Fig. 1, *A* and *D*. There were no significant differences between groups; α = 0.05, one-way ANOVA. CA, cholic acid; CDCA, chenodeoxycholic acid; DCA, deoxycholic acid; GCA, glycocholic acid; GCDCA, glycochenodeoxycholic acid; GDCA, glycodeoxycholic acid; LCA, lithocholic acid; ND, not determined; TCA, taurocholic acid; TCDCA, taurochenodeoxycholic acid; TDCA, taurodeoxycholic acid; TLCA, taurolithocholic acid; UDCA, ursodeoxycholic acid.

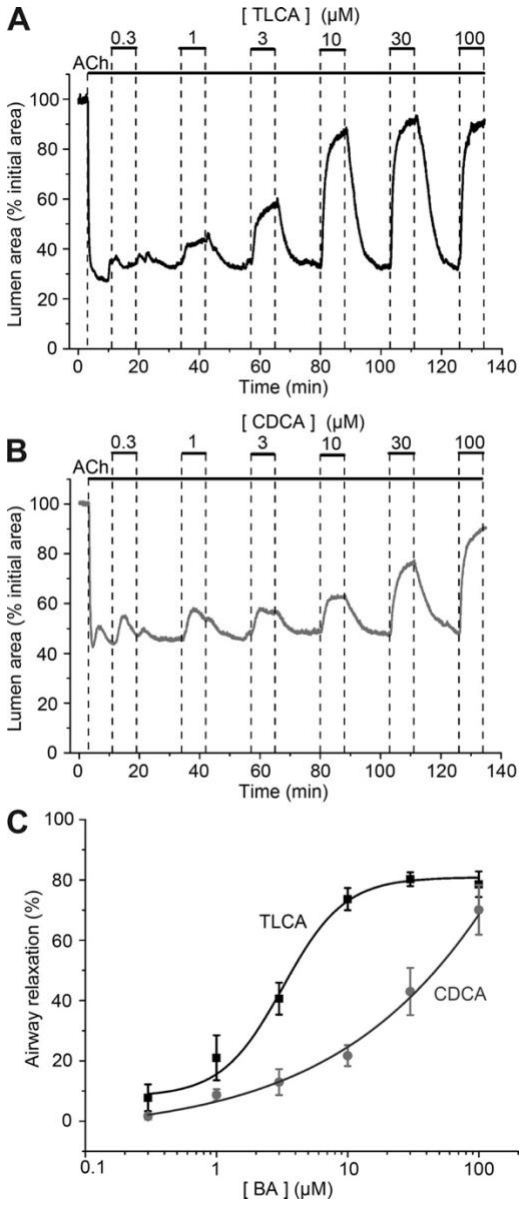

Figure 2. *Taurolithocholic acid (TLCA) and chenodeoxycholic acid (CDCA) induce concentration-dependent relaxation of ACh-precontracted airways with different potencies*. *A* and *B*: representative traces of changes in airway lumen area of mouse precision-cut lung slices (PCLS) contracted with 0.3 μM ACh and exposed to gradual increases in concentration of TLCA or CDCA, as labeled above each trace. *C*: summary of airway relaxation as a function of TLCA or CDCA concentrations, obtained from experiments similar to those shown in *A* and *B*. Data are means ± SE of 5–7 PCLS from 3 mice. BA, bile acid.

TLCA inhibits EFS-induced, endogenous ACh-mediated constrictions in guinea pig trachea rings. To corroborate that TLCA inhibits cholinergic responses of the airways, we investigated the effects of this BA on the muscle force generated by isolated guinea pig tracheal rings in response to electrical field stimulation (EFS). We first confirmed that EFS-induced airway constriction was mediated by endogenous ACh-release from parasympathetic nerve terminals using tetrodotoxin and atropine. These agents inhibit neuronal sodium channels preventing neural release of acetylcholine and postsynaptic muscarinic receptors in the airway smooth muscle, respectively. As shown in **Figure 3A**, both tetrodotoxin and atropine rapidly and completely inhibited EFS-induced transient contractions, confirming the cholinergic nature of this response. Next, we found that TLCA dose-dependently attenuated the magnitude of the transient airway smooth muscle contractions induced by EFS. In contrast, the primary BA GCDCA had a non-statistically significant effect at any concentration tested (**Figure 3B-C**). Thus, these findings in proximal airways are consistent with those obtained in PCLS and support the hypothesis that TLCA, but not primary BAs, inhibits cholinergic airway constriction.

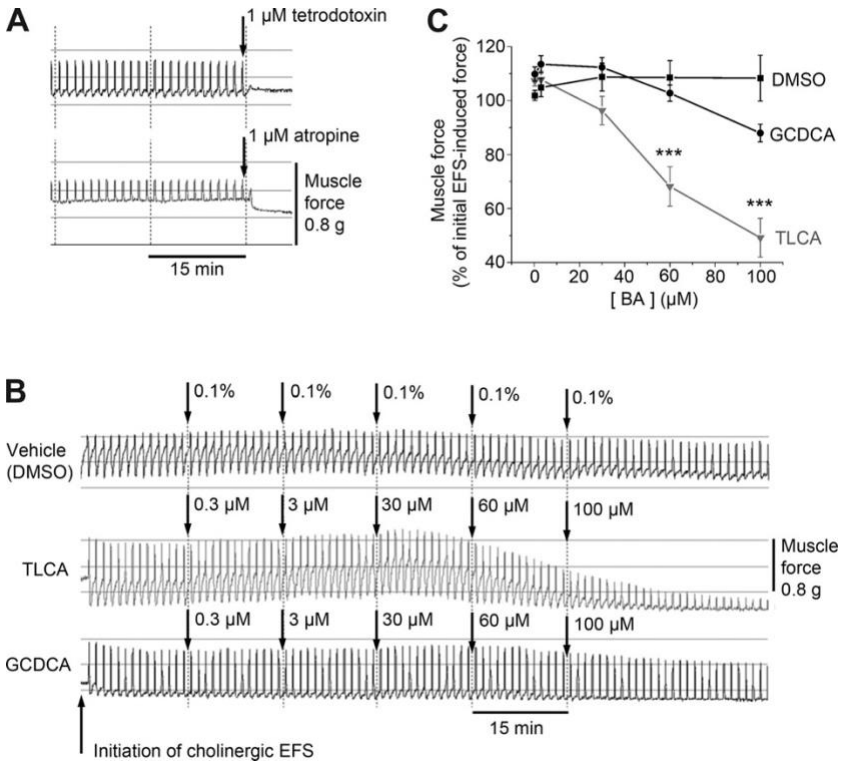

Figure 3. Taurolithocholic acid (TLCA) inhibits muscle force induced by electrical field stimulation (EFS) and mediated by endogenous release of acetylcholine in guinea pig trachea rings. *A* and *B*: representative traces show the inhibitory effects of 1 µM tetrodotoxin and 1 µM atropine (*A*) as well as vehicle (0.1% DMSO) and increasing concentrations of TLCA or glycochenodeoxycholic acid (GCDCA) (*B*) on EFS-induced transient airway constrictions. *C*: summary data show the concentration-dependent inhibition of EFS-induced airway constriction caused by TLCA and GCDCA. Data are means ± SE of $n = 6$ from 3 animals; ***$P < 0.001$ with respect to DMSO (ANOVA with post hoc Dunnett's test).

TLCA specifically inhibits airway constriction induced by ACh but not by other noncholinergic bronchoconstrictors. Since TLCA and other BAs relaxed airways pre-constricted with ACh, we tested whether TLCA would also prevent airway constriction induced by ACh and by other noncholinergic bronchoconstrictors. To this aim, we tested constriction before and after exposure to TLCA, DMSO (negative control), and atropine, a muscarinic receptor antagonist (positive control for ACh stimulation). For these experiments we chose the noncholinergic bronchoconstrictors 5-hydroxitriptamine (5-HT) and caffeine because they induce narrowing of mouse peripheral airways independently of muscarinic receptor activation, as previously demonstrated (Parks et al., 1999). Furthermore, to test the effects of TLCA on 5-HT-induced airway constriction, we choose 0.3 μM as the testing 5-HT concentration because it induces a submaximal airway constriction. As shown in **Figure 4A**, an initial control exposure to 0.3 μM ACh induced an airway contraction that was reversed by ACh washout. Subsequent exposure to 30 μM TLCA did not have an effect on airway luminal area alone but strongly inhibited the contraction induced by a second exposure to ACh. On average, the airway constriction induced by the second ACh stimulus was 50.4 ± 11.2% of that induced by the first stimulus in slices exposed to TLCA, whereas it was 107.3 ± 7.9% in slices exposed to DMSO and -3.1 ± 2.3% in slices exposed to atropine (**Figure 4B**). Importantly, a similar constriction induced by the first and second ACh stimulation before and after DMSO exposure indicates that there is no desensitization of ACh receptors in our experimental conditions and that the reduced ACh-induced airway constriction after exposure to TLCA was not due to such mechanism. In contrast to the inhibitory effects of TLCA and atropine on ACh-induced airway constriction, the results in **Figure 4C–F** show that neither of these inhibitors prevented

the constriction induced by 0.3 μM 5-HT or 20 mM caffeine. These results suggest that TLCA specifically inhibits airway constriction triggered by cholinergic stimulation and that this BA had lower efficacy and potency than atropine.

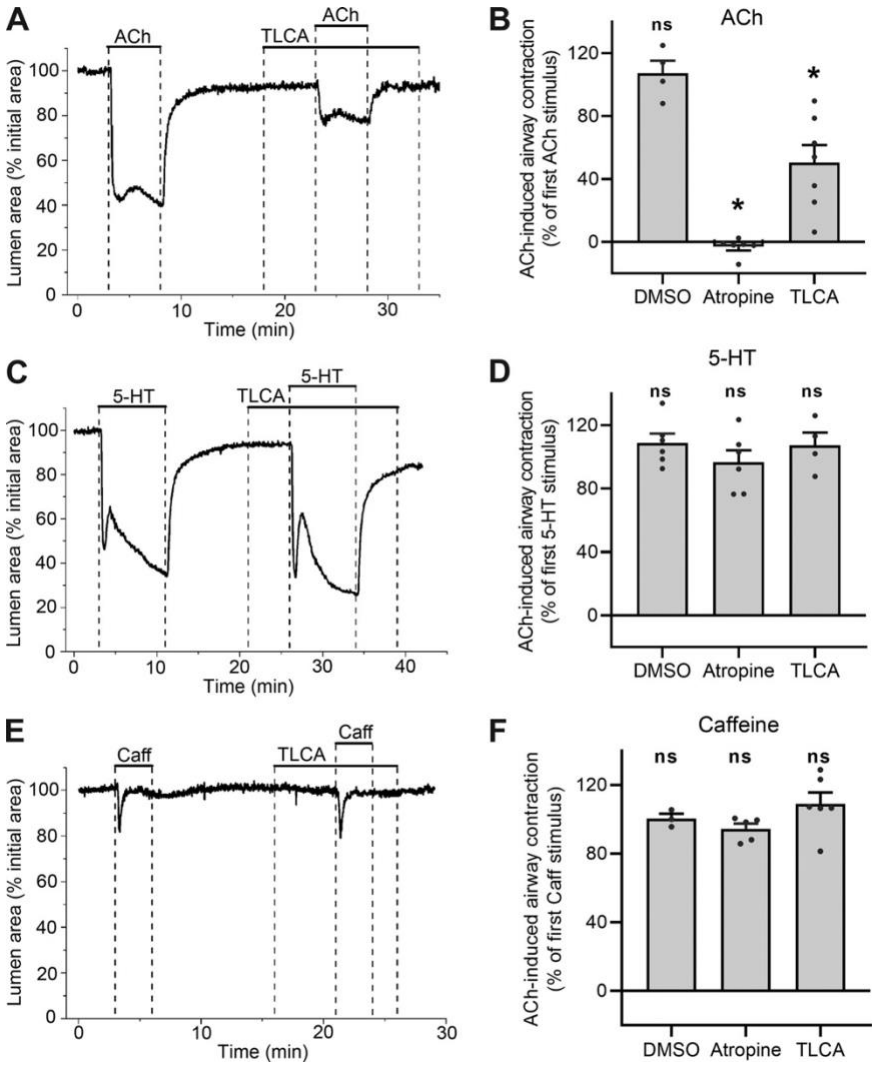

Figure 4. *Pre-exposure of airways to taurolithocholic acid (TLCA) specifically inhibits cholinergic bronchoconstriction. A*, *C*, and *E*: representative traces showing airway constriction induced by exposure of mouse precision-cut lung slices (PCLS) to 0.3 μM ACh (*A*), 0.3 μM 5-hydroxitriptamine (5-HT) (*C*), or 20 mM caffeine (Caff) (*E*) before and after exposure to 30 μM TLCA as labeled above traces. TLCA preexposure reduced the magnitude of airway constriction induced by ACh but not by 5-HT or caffeine. *B*, *D*, and *F*: summary data of the effects of 0.1% DMSO (control), 1 μM atropine (cholinergic antagonist), and 30 μM TLCA preexposure on airway contraction induced by ACh (*B*), 5-HT (*D*), or caffeine (*F*), obtained from similar experiments to those shown in the representative traces on the *left*. Data are means ± SE of 5– 8 PCLS from 3 mice and represent the proportion of the airway contraction induced by second bronchoconstrictor exposure (post-inhibitor addition) with respect to the first exposure (previous to the inhibitor). *$P < 0.05$ (paired *t* test) when testing differences between the first and second constrictions for each agent.

Primary BAs do not affect airway constriction induced by noncholinergic agonist 5-HT. Since primary BAs are the most abundant in lung transplant patients with DGER aspiration (Mertens et al., 2011; Urso et al., 2018), we further investigated whether these BAs have any effects on airway contractility. We pre-exposed the peripheral airways in mouse PCLS to the noncholinergic contractile agonist 5-HT and subsequently added the primary BAs (or DMSO as a control). We used 5-HT at a concentration that produces a submaximal airway constriction as previously described (Parks et al., 1999). As shown in **Figure 5**, the addition of primary BAs had little effect on 5-HT-induced airway constriction, and these effects were not significantly different from those induced by the vehicle (DMSO). These results suggest that primary BAs have neither relaxing nor potentiating effects on 5-HT-induced airway contraction.

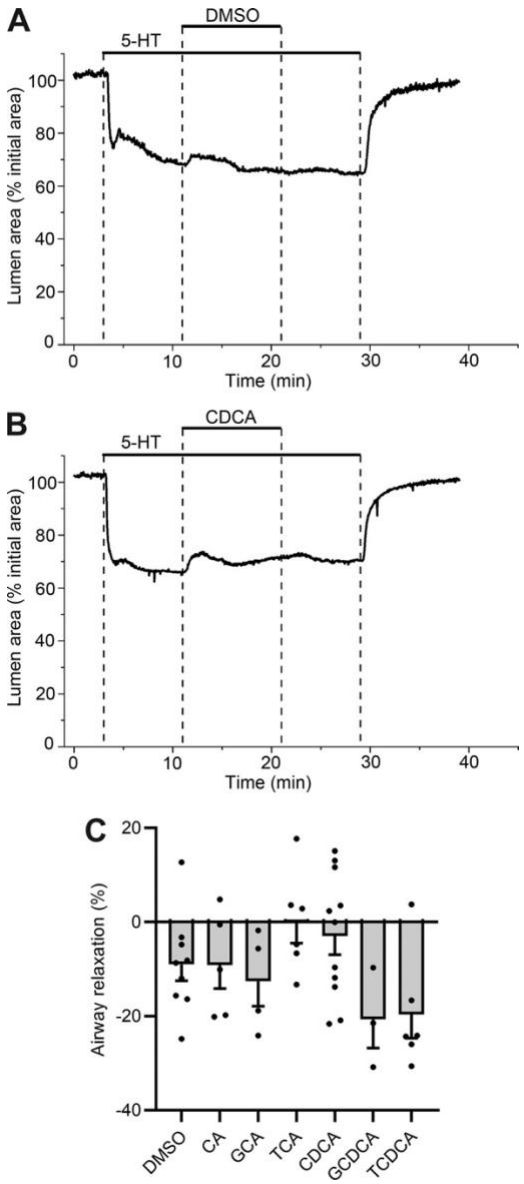

Figure 5. Primary bile acids (BAs) do not affect 5-hydroxitriptamine (5-HT)- induced peripheral airway contraction. *A* and *B*: representative traces show the contractile responses of peripheral airways to 5-HT and subsequent addition of 0.1% DMSO (control) (*A*) or 30 μM chenodeoxycholic acid (CDCA) (*B*). *C*: summary of airway relaxation induced by the primary BAs and DMSO (control). Data are means ± SE of 5–10 precision-cut lung slices from 3 mice; there were no significant differences between DMSO and the primary BAs, α = 0.05 (one-way ANOVA). CA, cholic acid; GCA, glycocholic acid; GCDCA, glycochenodeoxycholic acid; TCA, taurocholic acid; TCDCA, taurochenodeoxycholic acid.

TGR5 does not mediate TLCA-induced relaxation of ACh-precontracted airways. TGR5 is the major BA-specific G protein coupled receptor mediating the acute signaling effects of BAs in several organs and systems (Thomas et al., 2008; Bunnett, 2014; Fiorucci et al., 2018) To test whether TGR5 mediates the effects of TLCA on the airways, we first studied the effects of TC-G 1005, a potent activator of TGR5, on airways precontracted with ACh. Since TC-G 1005 has an EC50 of 6.2 nM for the activation of mouse TGR5 (Duan et al., 2012), we used 30 μM TC-G 1005 in our assays to assure that we were using a concentration that was high enough to stimulate TGR5 in our PCLS preparation. We found that 30 μM TC-G 1005 did not cause significant relaxation, whereas TLCA strongly and significantly relaxed ACh-precontracted airways in experiments performed in parallel (**Figure 6**, *A* and *B*). These results suggest that TGR5 does not play a role in smooth muscle relaxation in peripheral airways. Second, we studied the effects of TLCA on ACh-precontracted airways in PCLS prepared from homozygote *Tgr5*$^{-/-}$ knockout (*Tgr5*-KO) mice (kindly donated by Dr. Higuchi at Columbia University Medical Center) and from wild-type control mice. Using PCR, we confirmed that TGR5 receptors were absent in the lung slices from TGR5-KO mice but present in those from WT mice (n = 6 slices from 3 mice). However, we found that TLCA caused a similar airway relaxation in both TGR5-KO and WT mice (**Figure 6**, *C* and *D*) suggesting that the TLCA-induced airway relaxation was not mediated by TGR5.

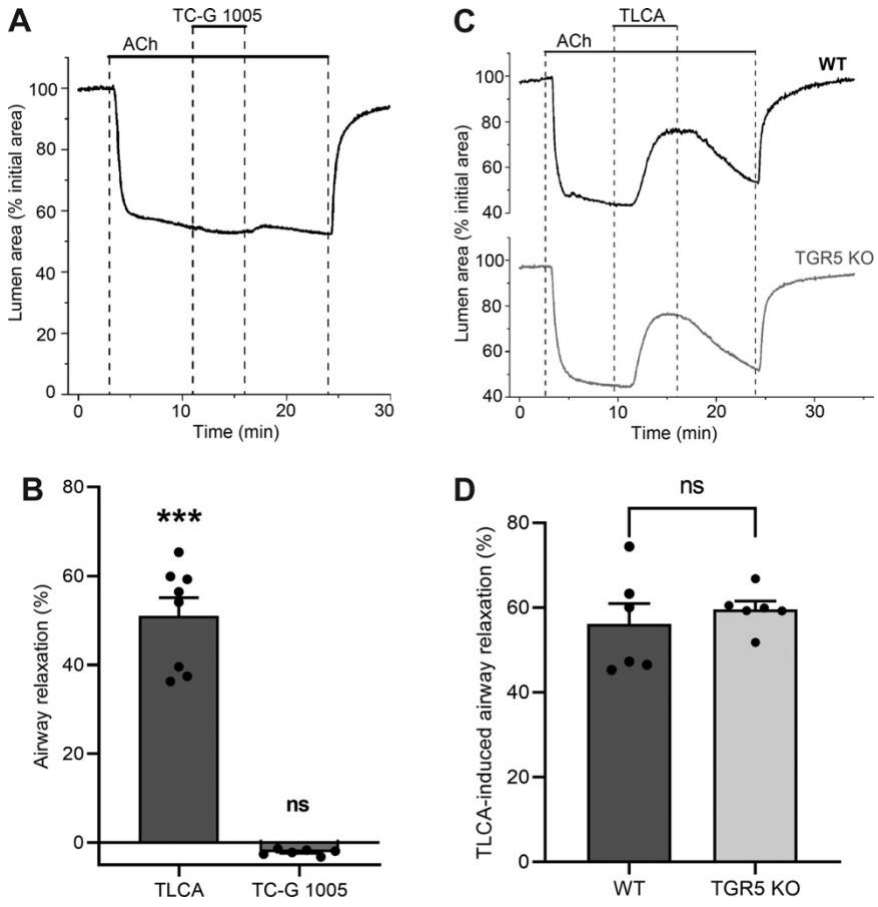

Figure 6. Takeda G protein-coupled receptor 5 (TGR5) does not mediate taurolithocholic acid (TLCA)-induced relaxation of ACh-contracted airways. *A*: representative trace of changes in airway lumen area in mouse precision-cut lung slices (PCLS) exposed to 30 μM TC-G 1005 in the continuous presence of 0.3 μM ACh. *B*: summary of airway relaxation induced by 30 μM TC-G 1005 and 30 μM TLCA tested in experiments similar to those shown in *A*. Data show mean ± SE from 6-8 PCLS from 3 mice. ***$P < 0.001$, paired *t* test, ACh alone vs. ACh + treatments. *C*: representative traces showing airway constriction induced by 0.3 μM ACh and relaxation induced by 30 μM TLCA in PCLS obtained from both TGR5-knockout (KO) and wild- type (WT) mice. *D*: percentage of TLCA-induced relaxation of ACh-contracted airways in both wild-type and TGR5-KO mice. Data show mean ± SE of 6 PCLS from 3 mice in each group; nonsignificant (NS), $P < 0.05$, unpaired *t* test.

TLCA inhibits ACh-induced inositol phosphate synthesis in human airway smooth muscle cells overexpressing M3 receptors. Altogether, our results in ex vivo tissue preparations strongly suggest that the inhibitory effects of TLCA on airway contraction are specific for cholinergic agonists and are not mediated by TGR5 and support the alternative hypothesis that TLCA may specifically inhibit muscarinic receptor activation to cause airway relaxation. To evaluate this hypothesis, we used human airway smooth muscle cells stably overexpressing M3 muscarinic receptors to study the effects of TLCA on ACh-induced inositol phosphate synthesis. We found that TLCA but not GCDCA concentration-dependently inhibited the ACh-induced inositol phosphate synthesis (**Figure 7**). These results support the hypothesis that TLCA may interact with muscarinic M3 receptors in airway smooth muscle to cause inhibition of inositol phosphate synthesis and airway relaxation. The contrasting outcomes between TLCA and GCDCA also indicate that the effects of BAs on inositol phosphate synthesis are consistent with their effects on airway relaxation in PCLS.

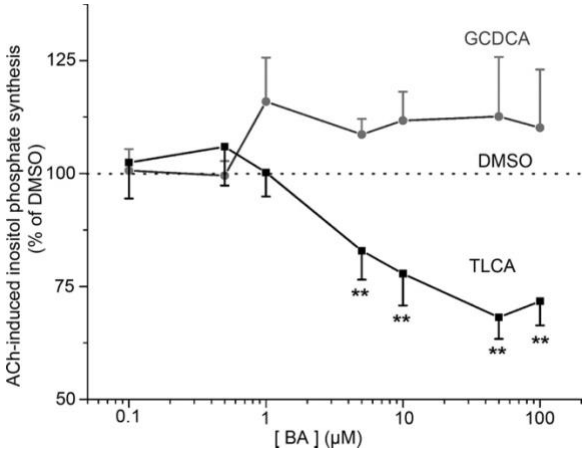

Figure 7. *Taurolithocholic acid (TLCA) inhibits ACh-induced inositol phosphate synthesis in cultured human airway smooth muscle cells overexpressing muscarinic M3 receptors.* Inositol phosphate synthesis was measured in response to 30 min of stimulation with 0.15 μM ACh in [^{3}H]-myo-inositol- loaded cells and preincubated with either TLCA, glycochenodeoxycholic acid (GCDCA; 0.1 μM to 100 μM), or vehicle (0.1% DMSO) for 15 min before the addition of ACh. Data are means ± SE of n = 6. **P < 0.01 with respect to DMSO (ANOVA with post hoc Dunnett's test). BA, bile acid.

Expression of muscarinic receptor subtypes M2 and M3 in mouse peripheral airways. To confirm the expression of muscarinic receptors M2 and M3 in the peripheral airways, we micro-dissected airways from mouse PCLS and performed quantitative RT-PCR using sequence-specific primers (**Table 1**). We found that the expression of M2 and M3 receptors in the peripheral airways was ~0.018-fold that in brain cortex (**Table 3**). In contrast, M1 receptor expression in peripheral airways was not accurately detectable.

	M1	**M2**	**M3**
BRAIN	20.19 (1.0)	22.94 (1.0)	22.27 (1.0)
AIRWAY 1	34.61 (0.0)	29.0 (0.03)	30.18 (0.0)
AIRWAY 2	NA	29.93 (0.02)	30.52 (0.01)
AIRWAY 3	34.36 (0.0)	30.38 (0.015)	28.78 (0.03)
AIRWAY 4	34.68 (0.0)	29.85 (0.02)	28.80 (0.03)
AIRWAY 5	34.93 (0.0)	29.83 (0.02)	28.66 (0.02)
AVG (1-5)	(0.0)	(0.02)	(0.018)
SE	(0.0)	(0.003)	(0.004)

Table 3. *Relative expression of muscarinic receptor subtypes (M1 to M3) in mouse peripheral airways* Quantitative RT-PCR data shown are CT values followed by the fold difference (in parentheses) in gene expression ($2^{-\Delta\Delta}$ CT) obtained with the $\Delta\Delta$CT method using *GAPDH* as the reference gene and brain tissue as the calibrator sample. Each sample contained ~15 peripheral airways microdissected from several precision-cut lung slices (PCLS) from a different mouse (*n* = 5 mice) as described in MATERIALS AND METHODS.

Acute and 'chronic' BA nebulization affects murine airway resistance and compliance. To assess whether the observed effect on airway contractility was also true in vivo, we utilized the Flexivent apparatus, which allows for in vivo intratracheal nebulization of solutions and simultaneous measurement of changes in respiratory parameters, as described in the methods section above. Mice in the acute cohort were subjected to two rounds of 10s nebulization of each BA or vehicle control followed by the nebulization of increasing concentrations of Ach. The BA GLCA (p=0.009), LCA (p=0.034), CDCA (p=0.01), GCA (p=0.008), and GCDCA (p=0.005), showed significant decrease in airway resistance compared to the vehicle control (**Figure 8a**). Simultaneous measurement of airway compliance, which indicates lung expandability, surprisingly showed significant difference GCA(p=0.0198) and GCDCA (p=0.052), with a trending difference in GLCA (p=0.0626), compared to vehicle control (**Figure 8b**).

Mice in the 'chronic' cohort were subjected to measurement in airway resistance one month post daily intranasal instillation of LCA (BA of choice) or vehicle control. After repeated exposure to LCA, airway resistance increased compared to the vehicle control (p=0.057) (**Figure 8c**). However, the targeted metabolomics obtained from patient samples indicated a prevalence of CA, CDCA, GCA, GCDCA, DCA and TCA in the post-transplant airway (Urso et al., 2021). To simulate BA aspiration, we prepared a cocktail of the above BA and administered it daily for 1 and 3 months. While no significant difference was found, a trending difference in resistance and total lung volume can be observed (**Figure 9a,b**). As indicated by our ex-vivo assessments, the resistance is reduced and the total volume is increased upon long-term administration of BA.

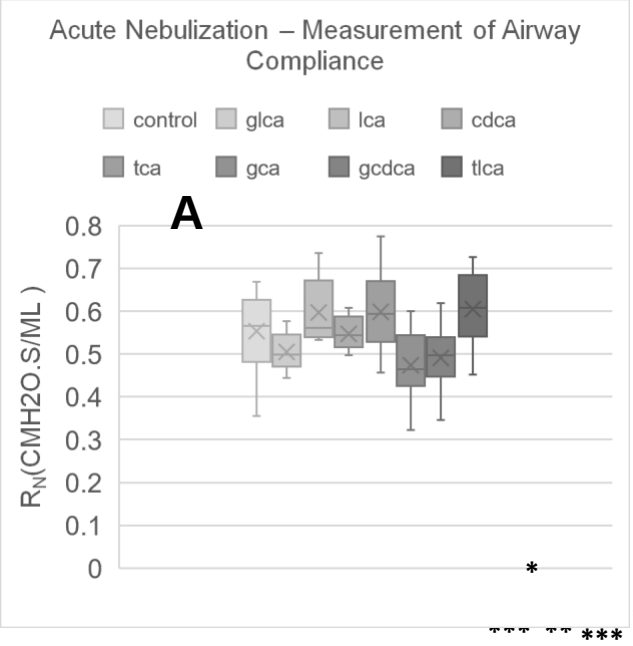

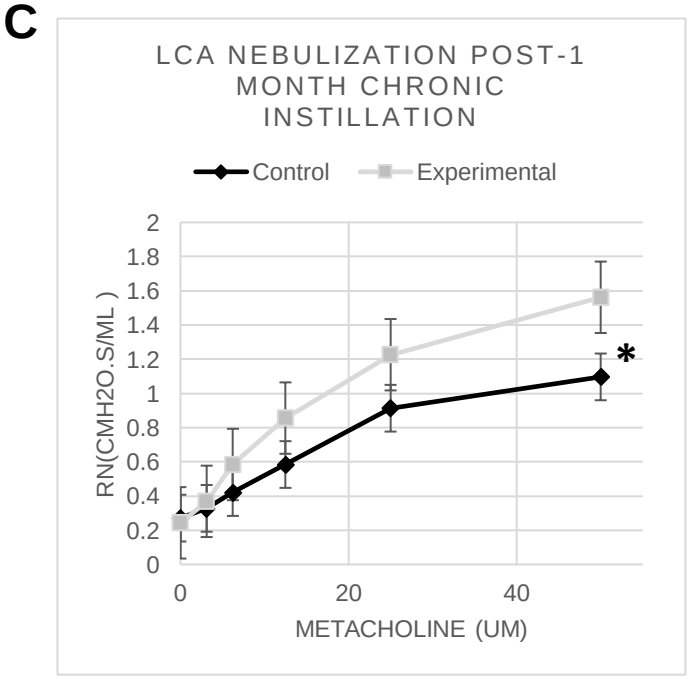

Figure 8. *Relative airway resistance and compliance post-acute and chronic BA treatment.* A-B. Airway resistance and compliance for in vivo acute exposure to BA and vehicle control. C. Airway resistance for in vivo chronic exposure to LCA and vehicle control. Results represent n=30 control mice and n=10 experimental mice (per each BA) (A-B); n=10 mice for both control and experimental (C). Procedure is described in MATERIALS AND METHODS.

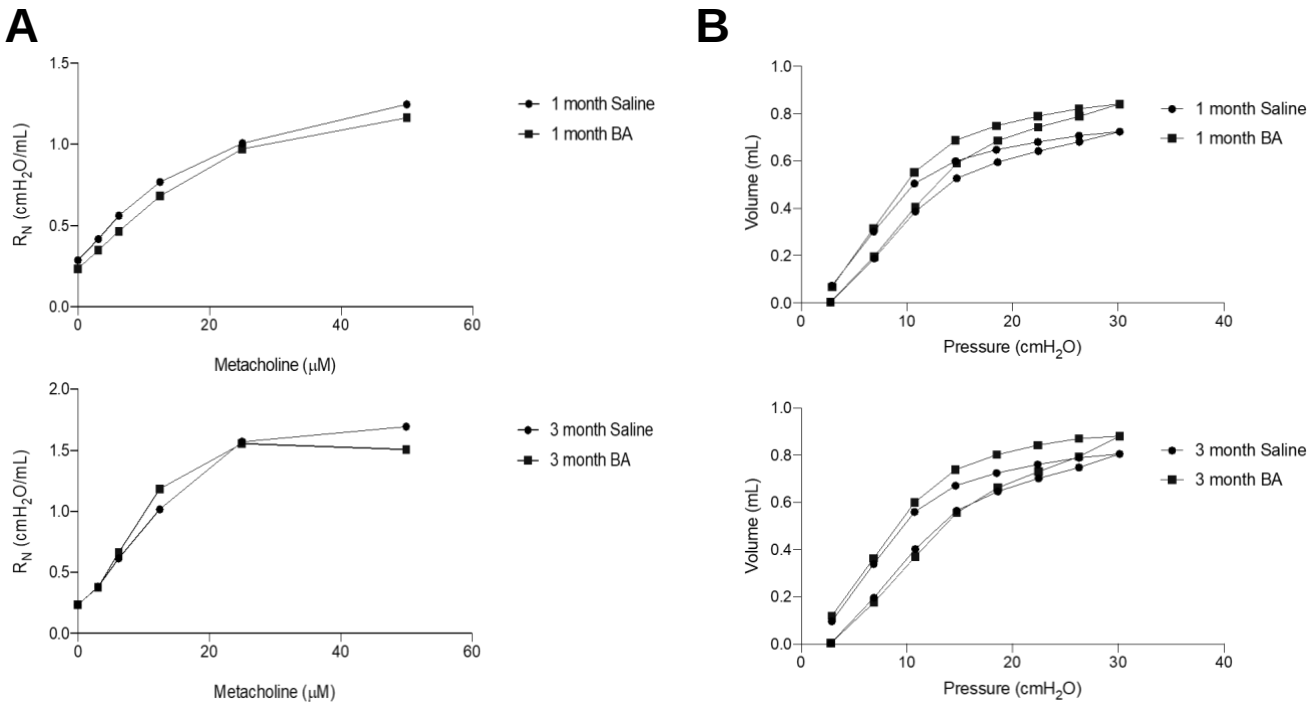

Figure 9. *Chronic BA cocktail instillation in murine model of aspiration.* A. Airway resistance and B. total lung volume for mice instilled with a 4mM BA cocktail including CA, CDCA, GCA, GCDCA, DCA and TCA. Results represent n=10 control mice and n=10 experimental mice (per each cohort). Procedure is described in MATERIALS AND METHODS.

Repeated exposure to BA mildly impacts airway inflammation. As we observed in Figure 8c, repeated LCA instillations promoted an increase in airway resistance over time compared to the vehicle control. To assess whether the increase in resistance was accompanied by inflammatory processes in the BALF and tissue, we instilled two parallel and littermate cohort of mice with LCA for one month and measured BALF cytokines as well as tissue inflammation. No striking difference was observed in the BALF cytokine release between the vehicle control and the LCA experimental cohort except for IL-1α, a protein commonly present in epithelial and mesenchymal cells of healthy subjects and predominantly in the vasculature (**Figure 10a**). Lung sections were stained with hematoxylin and eosin, as well as Masson's Trichrome, to assess changes in inflammation or collagen deposition, which indicated mild inflammation and early organizing pneumonia (**Figure 10b**).

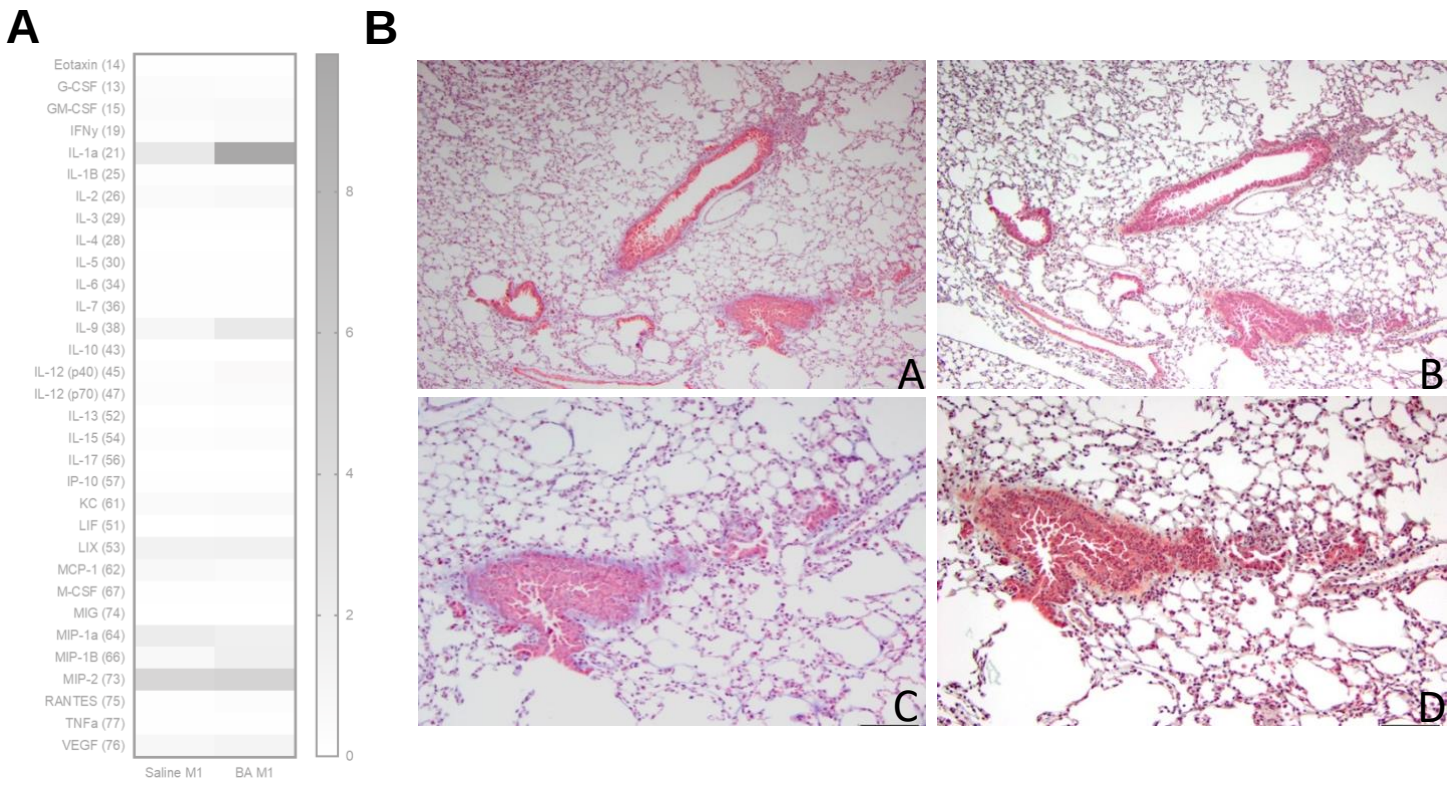

Figure 10. *Inflammatory cytokines and pathology assessment 1-month post LCA treatment.* A. Cytokines for saline (left) and LCA (right) treated mice and B. H&E (A,C) and Masson's trichrome (B,D) for LCA treated mice. Methodologies described in MATERIALS AND METHODS.

Discussion

This study investigates, for the first time, the effects of the 13 BAs detected in BAL and LABW from post-lung transplant patients with DGER aspiration on proximal and peripheral airway contractility in both humans and rodents. We found that BAs had no acute effects on contraction of unstimulated (resting) airways but strongly, dose-dependently, and reversibly relaxed peripheral airways precontracted with ACh in both humans and mice. The secondary BA lithocholic acid and its glycine and taurine conjugates (i.e., LCA, GLCA, and TLCA) as well as the taurine conjugate of deoxycholic acid (TDCA) had the strongest effects on airway relaxation, whereas only CDCA among the primary BAs had small but significant effects at the concentration tested (30 μM). These results are consistent with our observations in the clinical samples described in section one, where conjugated BA exhibited the most prominent effect in patient morbidity, mortality and amount of free lipids in the airway (Urso et al., 2021). The inhibitory effects of BAs were specific for ACh-induced airway constriction, but they did not inhibit constriction induced by noncholinergic bronchoconstrictors. BAs also inhibited airway constriction mediated by endogenous ACh-release in proximal airways of guinea pigs stimulated by EFS, and in this preparation, secondary conjugated BAs (i.e., TLCA) also had stronger effects. Accordingly, we propose that BAs have anticholinergic effects in both peripheral and proximal airways. Furthermore, we found that TC-G 1005, a highly specific agonist for the BA receptor TGR5, failed to relax ACh-precontracted airways. Additionally, the relaxing effect of TLCA was not affected by the genetic deletion of TGR5 in mice. These results suggest that TGR5 is not the receptor mediating the acute effects

of BAs in airway smooth muscle. Finally, we showed that TLCA but not the primary BA GCDCA inhibited ACh-induced inositol phosphate synthesis in human airway smooth muscle cells that overexpress muscarinic M3 receptors. Altogether, our results suggest that select BAs have the potential to inhibit the cholinergic contractile responses of the proximal and peripheral airways, possibly by acting as M3 receptor antagonists. We found that neither primary nor secondary BAs had any acute effects on contraction of unstimulated (resting) airways in peripheral lung slices from human and mice (see Fig. 1). Furthermore, the BAs did not potentiate airway constriction in lung slices exposed to low concentrations of the cholinergic agonist ACh, but instead most secondary BAs caused relaxation. Similarly, pre-exposure of lung slices to secondary BA TLCA reduced the airway constriction stimulated by ACh and had no effects on the contractile response of the airways to the noncholinergic agonist 5-HT (see Fig. 4). Furthermore, primary BAs did not potentiate constriction or cause relaxation of airways precontracted with 5-HT (see Fig. 5). These results suggest that BAs do not cause acute constriction of unstimulated airways or of those exposed to contractile agonists. These results were of interest, as lung transplant patients with chronic BA aspiration from DGER are at increased risk for increased airflow limitation and decreased forced expiratory volume in 1 s (FEV1) (Mertens et al 2011, Mokhlesi et al 2001), and suggest that this association cannot be explained by an acute direct effect on airway smooth muscle.

We found that secondary BAs inhibited cholinergic airway constriction with higher potency than primary BAs. TLCA at 1 μM and 30 μM relaxed airways by ~20% and ~80% respectively, whereas most primary BAs caused no significant airway relaxation at 30 μM in PCLS (see Figs. 1 and 2). Furthermore, the primary BAs caused neither relaxation nor

further contraction of peripheral airways precontracted with the noncholinergic agonist 5-HT (see Fig. 5). These results were interesting, as the most abundant BAs are of the primary category. Yet prandial states and microbial conversion impose a high level of complexity in the measurement of individual BA levels at a given time. In fact, following a meal, total BAs could reach the low millimolar range (0.2–1.0 mM) in the intestine. Ranges as wide as 30 –700 μM DCA or 1– 450 μM LCA have been measured, implying large variability among individuals (Hamilton et al., 2007). Upon aspiration, BAs are diluted in variable volumes of saliva and airway mucus and likely have a differential local distribution along the airway tree. Therefore, no correlation can be noted between BA concentrations in the gastrointestinal system, serum, and in the lung (D'Ovidio et al., 2005c). To note is that total, primary, and secondary BAs breakdowns have been identified in BAL and LABW of patients with lung transplants and terminal disease, with primary BAs being the most abundant (D'Ovidio et al., 2005c, 2006; Mertens et al., 2011; Urso et al., 2018). Assayed as a marker of DGER aspiration in post-lung trans- plant surveillance BAL, BAs have a median of 0.3 μM (25th- 75th percentile range 0–16 μM) in healthy recipients and of 1.6 μM (25th–75th percentile range 0–32 μM) in those with failed allograft (Urso et al., 2018) These values originate from BAL samples that present with a low saline-to-lung-volume ratio and an undefined dilutive magnitude that do not allow for a precise calculation of BA concentration in the airways. Since the concentrations of individual BAs in the liquid phase of the airways are presently unknown, we first performed concentration-response curves for TLCA and CDCA, which showed consistent and substantial contractile responses between 1 and 30 μM. Hence, our choice to use 30 μM to test airway reactivity was determined by our experimental observations, as BAs

concentrations in the airways upon DGER micro-aspirations cannot be accurately estimated. Although a direct com- parison of the BA (e.g., TLCA) concentrations that produced contractile effects in the peripheral airways with their concentration in the patient airways cannot be established, we think our findings are important when considering the possible mechanisms of the association between the presence of BAs in patients with DGER micro-aspirations and the decline in airway function.

TGR5 has been identified as the primary cell membrane receptor that mediates the acute signaling effects of BAs in a variety of cells in several organ systems (Thomas et al., 2008; Bunnett, 2014; Lieu et al., 2014; Mertens et al., 2017; Herman-Edelstein et al., 2018). Upon BAs binding, TGR5 initiates a signaling cascade through Gs by activating adenylyl cyclase and causing elevation of intracellular cAMP. In airway smooth muscle, agonists that cause an increase in intracellular cAMP (e.g., β_2-adrenoceptor agonists) also induce airway relaxation (Hakonarson and Grunstein, 1998). Accordingly, we first hypothesized that cAMP-coupled TGR5 receptors could mediate the BA-induced airway relaxation. In fact, TGR5 receptors have been found expressed in gastric smooth muscle, and activation with a TGR5-selective ligand, oleanolic acid, was found to elevate intracellular cAMP and induce relaxation (Rajagopal et al., 2013). However, we found that this hypothesis was not sup- ported in airway smooth muscle by several of our experimental results. First, the BA-induced inhibition of airway constriction was observed only when the airways were stimulated with ACh but not with other noncholinergic bronchoconstrictors (i.e., 5-HT and caffeine). In contrast, β_2-agonists are known to similarly inhibit airway constriction stimulated by either cholinergic (e.g., ACh, methacholine) or noncholinergic bronchoconstrictors, including 5-HT, endothelin-1 (ET-

1), histamine, and cysteinyl leukotrienes (Jonsson, 1998; Parks et al., 1999; Bai and Sanderson, 2006; Perez-Zoghbi and Sanderson, 2007; Perez-Zoghbi et al., 2010). Yet, receptors for all the latter bronchoconstrictors are all Gq-coupled, suggesting that β_2-agonists act downstream of receptor activation (White et al., 1987; Jonsson, 1998; Parks et al., 1999; Perez-Zoghbi and Sanderson, 2007; Brown et al., 2013). In sharp contrast, because BAs only inhibited airways stimulated by ACh and not by 5-HT or caffeine, we believe that they may be blocking muscarinic receptor activation rather than activating TGR5. Second, TC-G 1005 not causing relaxation suggests that TGR5 receptors may not be functionally expressed in the smooth muscle cells of the peripheral airways. Third, genetic deletion of TGR5 receptors in the TGR5-KO mice did not affect the TLCA-induced airway relaxation. Consequently, our results do not support a role of TGR5 receptors in the airway relaxation induced by BAs.

The nuclear BA receptor farsenoid X receptor alpha (FXR-α) is the mediator of the genomic actions of BAs in hepatocytes and many other cell types (Zhang et al., 2003; Thomas et al., 2008; Lefebvre et al., 2009; Herman-Edelstein et al., 2018) and has been found expressed in the lung (Zhang et al 2003). FXR-α receptors mediate most of the endocrine effects of BAs on glucose and lipid metabolism, including the feedback regulation of BA synthesis (Shapiro et al., 2018). However, the acute airway relaxation induced by BAs occurred quickly, initiating within 1–3 min after exposure, suggesting that it could not be mediated by FXR-α- activated alterations of gene expression. In addition, CDCA and its glycine and taurine conjugates constitute the most potent FXR-α ligands with an EC50 of ~5–10 μM (Makishima et al., 1999; Parks et al., 1999), yet they had little or no effect on airway constriction. Another alternative is that cytotoxicity or inflammatory

cytokines are causing BA-induced airway relaxation. In fact, exposure of an immortalized bronchial epithelial cell line to BAs during 48 h caused cell death and IL-8, IL-6, and GM-CSF release (Aldhahrani et al., 2017). However, because of the brief exposure to BAs and reversibility of their effects in airways, we do not believe such alternatives are applicable in the results we presented. Nevertheless, prolonged exposure of airways to BAs may have additional effects on reactivity that could be mediated by activation of FXR-α receptors in airway smooth muscle or by cytokines, but these alternatives require further investigation. Altogether, our data suggest that neither TGR5 nor FXR-α receptors are involved in the acute effects of BAs on airway contraction.

Muscarinic M3 receptors have been suggested as mediators of the anticholinergic effects of select BAs in secretory and other non-muscle cells. In dispersed chief cells from guinea pig stomach, TLCA, but not TCA or taurine, strongly inhibited pepsinogen secretion induced by the cholinergic agonist carbachol (Raufman et al., 1998). Furthermore, in this preparation, TLCA alone inhibited the binding of the muscarinic receptor radioligand *N*-methyl-[^{3}H] scopolamine to chief cells and induced a small but significant pepsinogen secretion that was inhibited by atropine. These pioneer findings lead to the suggestion that TLCA interact with muscarinic receptors (as partial agonists) in chief cells (Raufman et al., 1998). Subsequent studies by the same group confirmed this hypothesis, showing that LCA, GLCA, TLCA, DCA, GDCA, and TDCA, but not the primary BAs, inhibited *N*-methyl-[^{3}H] scopolamine binding in Chinese hamster ovary (CHO) and human colon cancer cell lines expressing recombinant M3 receptors (Cheng et al., 2002; Raufman et al., 2002). Our results in proximal and peripheral airways along with human airway smooth muscle cells expressing M3 receptors appear to support the

hypothesis that select BAs inhibit cholinergic contractile responses of the airways by interacting with M3 receptors in airway smooth muscle due to the similar selectivity and the concentration-dependence of their relaxation. In sharp contrast, our results do not support that BAs are partial agonists of M3 receptors in airway smooth muscle, as they did not induce significant constriction in peripheral airways. There are several possible reasons why BAs do not induce airway constriction but induce pepsinogen secretion. First, airway smooth muscle cells ex- press both M2 and M3 receptors (Roffel et al., 1987; Maeda et al., 1988), and we found these receptors expressed in the peripheral airways, whereas chief cells express M1 and M3 receptors. The evidence with transgenic mice suggests that both M1- and M3-receptor subtypes mediate pepsinogen secretion (Xie et al., 2005); however, it is unknown which mediate the stimulatory and inhibitory effects of BAs in chief cells. Binding assays in CHO and human colon cancer cells expressing recombinant M3 (but not M1) receptors (Cheng et al., 2002; Raufman et al., 2002; Zhang et al., 2015) support that at least the inhibitory effects of BA are mediated by M3 receptors. If the stimulatory effects of BA in chief cells are mediated by M1 receptors, then the absence of BA-induced airway constriction could be explained by the lack of M1- receptor expression in airway smooth muscle and our inability to detect significant expression of M1 receptors in the peripheral airways despite evident expression of M2 and M3 receptors (see Table 2). Secondly, BAs could be partial agonists for M3 receptors; however, the downstream cell-signaling mechanisms required for airway constriction may differ from those for pepsinogen secretion. In airway smooth muscle, contraction requires the activation of two independent signaling pathways initiated by phospholipase C beta (PLCβ) and RhoA/Rho Kinase (Zhang et al 2015), whereas in chief cells, pepsinogen

secretion is associated only with PLCβ-initiated signaling (Xie et al., 2005). It is possible that BAs alone only partially activate PCLβ signaling to induce secretion, but not the RhoA/Rho Kinase signaling ultimately required for airway smooth muscle contraction. In addition, the lack of BA-induced relaxation in resting airways is consistent with the inability of several other bronchodilators, including β_2-agonists, bitter taste receptor agonists, nitric ox ide, and hydrogen sulfide, to cause relaxation in unstimulated airways (Bai and Sanderson, 2006; Perez-Zoghbi et al., 2010; Castro-Piedras and Perez-Zoghbi, 2013; Tan and Sanderson, 2014).

Lastly, our in vivo data showed a decrease in airway relaxation upon acute BA exposure. While secondary BA were expected to result in reduced airway resistance as per our mechanistic results, primary BA were also surprisingly effective. One explanation could also be the length of the exposure. Metacholine challenges are effective in mice up to a maximal concentration of 50 μM after which the animal perishes. The ex-vivo studies on lung slices were performed over hours of conditioning with Ach prior to BA exposure, which may suggest that primary BA are also ligands to the M3 receptors, yet are easily displaced by ACh, producing no visible relaxation ex-vivo. In addition, the airway microenvironment may impose compensatory strategies upon exposure to extraneous and emulsifying molecules such as BA, which clearly cannot be recapitulated in ex-vivo models. The results we observed after prolonged BA exposure may show precisely the latter. We speculate that while inducing airway relaxation in an acute setting, the prolonged exposure to these amphipathic molecules and sustained relaxation of airways overtime may induce structural changes and compensatory mechanisms stiffening the

tissue, as the physiological impact of prolonged BA aspiration has yet to be clinically described.

Conclusion

In line with previous findings in the pulmonary field, our study on the impact of bile acids in the pathophysiology of reflux asxpiration in lung transplant recipients provides additional data indicate that BA are indeed risk factors for poor outcomes due to their physiochemical properties injuring cellular bilayers, thus liberating airway lipids and facilitating infections. As established markers of aspiration in lung disease, we illustrate that BA detection post-transplant can be exploited as a marker of CLAD development and incite the treating clinician towards alternative action plans for the patient in question. We have specifically identified that primary conjugated BA are particularly deleterious for lung transplant recipients; however, the emulsifying property of this molecular category is extended to all BA and should not deter from pursuing further treatment alternatives. Thus, BA and in particular the conjugated forms can be used as biomarkers of allograft failure and used as diagnostic tools for the placement of preventive strategies.

The impact of BA extends beyond their physiochemical properties, as we found that most secondary BAs, the conjugated forms showing the strongest effect, acutely inhibit the cholinergic constriction of the proximal and peripheral airways in vitro in humans and rodents and that these effects are likely mediated by inhibition of muscarinic M3 receptors in the airway smooth muscle. While these current results alone do not account for the detrimental effects of chronic microaspiration of BAs on transplanted lungs, we think that these novel acute effects of antagonism of muscarinic receptor signaling are an important component of unraveling the likely multifactorial effects of aspirated BAs on multiple cell types in the lung. For example, by inhibiting cholinergic bronchoconstriction, we speculate that aspirated BAs in patients with lung transplants

may further affect the innate defense of the lung, avoiding clearance of bronchial secretions, in turn stimulating inflammatory cytokine release, deranging surfactant protein and lipids, and facilitating airway infections as previously shown (Briganti et al 2016, D'Ovidio et al 2005, D'Ovidio et al 2005, Urso et al 2018). In addition, the simulation of chronic BA aspiration also impacted the resistance and compliance of the murine lungs. Overall, our studies show that BA vest a multifaceted role in the context of aspiration and pulmonary health, and that with the surging establishment of metabolo-spectrometric assays in patient point of care diagnostics, we conclude that these investigative efforts would provide useful information to the treating clinician and significant benefit to the newly implanted organ.

References

Adachi, R., Honma, Y., Masuno, H., Kawana, K., Shimomura, I., Yamada, S., et al. (2005). Selective activation of vitamin D receptor by lithocholic acid acetate, a bile acid derivative. *J Lipid Res* 46, 46–57. doi: 10.1194/jlr.M400294-JLR200.

Ahmed, M., Levy, L., Hunter, S. E., Zhang, K. C., Huszti, E., Boonstra, K. M., et al. (2019). Lung Bile Acid as Biomarker of Microaspiration and Its Relationship to Lung Inflammation. *The Journal of Heart and Lung Transplantation* 38, S255–S256. doi: 10.1016/j.healun.2019.01.635.

Aldhahrani, A., Verdon, B., Ward, C., and Pearson, J. (2017). Effects of bile acids on human airway epithelial cells: implications for aerodigestive diseases. *ERJ Open Res* 3, 00107–02016. doi: 10.1183/23120541.00107-2016.

Alemi, F., Kwon, E., Poole, D. P., Lieu, T., Lyo, V., Cattaruzza, F., et al. (2013a). The TGR5 receptor mediates bile acid–induced itch and analgesia. *Journal of Clinical Investigation* 123, 1513–1530. doi: 10.1172/JCI64551.

Alemi, F., Poole, D. P., Chiu, J., Schoonjans, K., Cattaruzza, F., Grider, J. R., et al. (2013b). The Receptor TGR5 Mediates the Prokinetic Actions of Intestinal Bile Acids and Is Required for Normal Defecation in Mice. *Gastroenterology* 144, 145–154. doi: 10.1053/j.gastro.2012.09.055.

Allaix, M. E., Rebecchi, F., Morino, M., Schlottmann, F., and Patti, M. G. (2017). Gastroesophageal Reflux and Idiopathic Pulmonary Fibrosis. *World J Surg* 41, 1691–1697. doi: 10.1007/s00268-017-3956-0.

Al-Momani, H., Perry, A., Nelson, A., Stewart, C. J., Jones, R., Krishnan, A., et al. (2022). Exposure to bile and gastric juice can impact the aerodigestive microbiome in people with cystic fibrosis. *Sci Rep* 12, 11114. doi: 10.1038/s41598-022-15375-4.

AMONYINGCHAROEN, S., SURIYO, T., THIANTANAWAT, A., WATCHARASIT, P., and SATAYAVIVAD, J. (2015). Taurolithocholic acid promotes intrahepatic cholangiocarcinoma cell growth via muscarinic acetylcholine receptor and EGFR/ERK1/2 signaling pathway. *Int J Oncol* 46, 2317–2326. doi: 10.3892/ijo.2015.2939.

Anisfeld, A. M., Kast-Woelbern, H. R., Lee, H., Zhang, Y., Lee, F. Y., and Edwards, P. A. (2005). Activation of the nuclear receptor FXR induces fibrinogen expression: a new role for bile acid signaling. *J Lipid Res* 46, 458–468. doi: 10.1194/jlr.M400292-JLR200.

Babaei, A., Bhargava, V., Korsapati, H., Zheng, W. H., and Mittal, R. K. (2008). A Unique Longitudinal Muscle Contraction Pattern Associated With Transient Lower Esophageal Sphincter Relaxation. *Gastroenterology* 134, 1322–1331. doi: 10.1053/j.gastro.2008.02.031.

Bai, Y., and Sanderson, M. J. (2006). Airway smooth muscle relaxation results from a reduction in the frequency of Ca2+ oscillations induced by a cAMP-mediated inhibition of the IP3 receptor. *Respir Res* 7, 34. doi: 10.1186/1465-9921-7-34.

Bardhan, K. D., Strugala, V., and Dettmar, P. W. (2012). Reflux Revisited: Advancing the Role of Pepsin. *Int J Otolaryngol* 2012, 1–13. doi: 10.1155/2012/646901.

Biswas Roy, S., Elnahas, S., Serrone, R., Haworth, C., Olson, M. T., Kang, P., et al. (2018). Early fundoplication is associated with slower decline in lung function after lung transplantation

in patients with gastroesophageal reflux disease. *J Thorac Cardiovasc Surg* 155, 2762-2771.e1. doi: 10.1016/j.jtcvs.2018.02.009.

Björkhem, I., Leoni, V., and Meaney, S. (2010). Genetic connections between neurological disorders and cholesterol metabolism. *J Lipid Res* 51, 2489–2503. doi: 10.1194/jlr.R006338.

Blondeau, K., Mertens, V., Vanaudenaerde, B. A., Verleden, G. M., van Raemdonck, D. E., Sifrim, D., et al. (2008). Gastro-oesophageal reflux and gastric aspiration in lung transplant patients with or without chronic rejection. *European Respiratory Journal* 31, 707–713. doi: 10.1183/09031936.00064807.

Brown, S. M., Koarai, A., Sturton, R. G., Nicholson, A. G., Barnes, P. J., and Donnelly, L. E. (2013). A role for M2 and M3 muscarinic receptors in the contraction of rat and human small airways. *Eur J Pharmacol* 702, 109–115. doi: 10.1016/j.ejphar.2013.01.054.

Bunnett, N. W. (2014). Neuro-humoral signalling by bile acids and the TGR5 receptor in the gastrointestinal tract. *J Physiol* 592, 2943–2950. doi: 10.1113/jphysiol.2014.271155.

Cantu, E., Appel, J. Z., Hartwig, M. G., Woreta, H., Green, C., Messier, R., et al. (2004). Early Fundoplication Prevents Chronic Allograft Dysfunction in Patients with Gastroesophageal Reflux Disease. *Ann Thorac Surg* 78, 1142–1151. doi: 10.1016/j.athoracsur.2004.04.044.

Caparrós-Martín, J. A., Flynn, S., Reen, F. J., Woods, D. F., Agudelo-Romero, P., Ranganathan, S. C., et al. (2020). The Detection of Bile Acids in the Lungs of Paediatric Cystic Fibrosis Patients Is Associated with Altered Inflammatory Patterns. *Diagnostics (Basel)* 10. doi: 10.3390/diagnostics10050282.

Castro-Piedras, I., and Perez-Zoghbi, J. F. (2013). Hydrogen sulphide inhibits Ca^{2+} release through $InsP_3$ receptors and relaxes airway smooth muscle. *J Physiol* 591, 5999–6015. doi: 10.1113/jphysiol.2013.257790.

Cheng, K., Chen, Y., Zimniak, P., Raufman, J.-P., Xiao, Y., and Frucht, H. (2002). Functional interaction of lithocholic acid conjugates with M3 muscarinic receptors on a human colon cancer cell line. *Biochimica et Biophysica Acta (BBA) - Molecular Basis of Disease* 1588, 48–55. doi: 10.1016/S0925-4439(02)00115-1.

Cheng, K., Shang, A. C., Drachenberg, C. B., Zhan, M., and Raufman, J.-P. (2017). Differential expression of M3 muscarinic receptors in progressive colon neoplasia and metastasis. *Oncotarget* 8, 21106–21114. doi: 10.18632/oncotarget.15500.

Cheng, K., Xie, G., and Raufman, J.-P. (2007). Matrix metalloproteinase-7-catalyzed release of HB-EGF mediates deoxycholyltaurine-induced proliferation of a human colon cancer cell line. *Biochem Pharmacol* 73, 1001–1012. doi: 10.1016/j.bcp.2006.11.028.

Chiang, J. Y. L., and Ferrell, J. M. (2019). Bile Acids as Metabolic Regulators and Nutrient Sensors. *Annu Rev Nutr* 39, 175–200. doi: 10.1146/annurev-nutr-082018-124344.

Chojnowski, M., Kobylecka, M., and Olesińska, M. (2016). Esophageal transit scintigraphy in systemic sclerosis. *Reumatologia/Rheumatology* 5, 251–255. doi: 10.5114/reum.2016.63666.

Cipriani, S., Mencarelli, A., Chini, M. G., Distrutti, E., Renga, B., Bifulco, G., et al. (2011). The Bile Acid Receptor GPBAR-1 (TGR5) Modulates Integrity of Intestinal Barrier and Immune Response to Experimental Colitis. *PLoS One* 6, e25637. doi: 10.1371/journal.pone.0025637.

D'Aldebert, E., Biyeyeme Bi Mve, M., Mergey, M., Wendum, D., Firrincieli, D., Coilly, A., et al. (2009). Bile Salts Control the Antimicrobial Peptide Cathelicidin Through Nuclear Receptors

in the Human Biliary Epithelium. *Gastroenterology* 136, 1435–1443. doi: 10.1053/j.gastro.2008.12.040.

Dawson, P. A. (2018). "Bile Formation and the Enterohepatic Circulation," in *Physiology of the Gastrointestinal Tract* (Elsevier), 931–956. doi: 10.1016/B978-0-12-809954-4.00041-4.

de Bortoli, N., Ottonello, A., Zerbib, F., Sifrim, D., Gyawali, C. P., and Savarino, E. (2016). Between GERD and NERD: the relevance of weakly acidic reflux. *Ann N Y Acad Sci* 1380, 218–229. doi: 10.1111/nyas.13169.

de Luca, D., Minucci, A., Zecca, E., Piastra, M., Pietrini, D., Carnielli, V. P., et al. (2009). Bile acids cause secretory phospholipase A2 activity enhancement, revertible by exogenous surfactant administration. *Intensive Care Med* 35, 321–326. doi: 10.1007/s00134-008-1321-3.

de Aguiar Vallim, T. Q., Tarling, E. J., and Edwards, P. A. (2013). Pleiotropic Roles of Bile Acids in Metabolism. *Cell Metab* 17, 657–669. doi: 10.1016/j.cmet.2013.03.013.

Donepudi, A. C., Ferrell, J. M., Boehme, S., Choi, H., and Chiang, J. Y. L. (2018). Deficiency of cholesterol 7α-hydroxylase in bile acid synthesis exacerbates alcohol-induced liver injury in mice. *Hepatol Commun* 2, 99–112. doi: 10.1002/hep4.1129.

D'Ovidio, F., and Keshavjee, S. (2006). Gastroesophageal reflux and lung transplantation. *Diseases of the Esophagus* 19, 315–320. doi: 10.1111/j.1442-2050.2006.00603.x.

D'Ovidio, F., Mura, M., Ridsdale, R., Takahashi, H., Waddell, T. K., Hutcheon, M., et al. (2006). The Effect of Reflux and Bile Acid Aspiration on the Lung Allograft and Its Surfactant and Innate Immunity Molecules SP-A and SP-D. *American Journal of Transplantation* 6, 1930–1938. doi: 10.1111/j.1600-6143.2006.01357.x.

D'Ovidio, F., Mura, M., Tsang, M., Waddell, T. K., Hutcheon, M. A., Singer, L. G., et al. (2005a). Bile acid aspiration and the development of bronchiolitis obliterans after lung transplantation. *J Thorac Cardiovasc Surg* 129, 1144–1152. doi: 10.1016/j.jtcvs.2004.10.035.

D'Ovidio, F., Singer, L. G., Hadjiliadis, D., Pierre, A., Waddell, T. K., de Perrot, M., et al. (2005b). Prevalence of Gastroesophageal Reflux in End-Stage Lung Disease Candidates for Lung Transplant. *Ann Thorac Surg* 80, 1254–1260. doi: 10.1016/j.athoracsur.2005.03.106.

D'Ovidio F, Waddell T, Singer LG, Pierre A, De Perrot M, Chaparro C, Hutcheon M, Miller L, Darling G, Keshavjee S. "Spontaneous Reversal of Acid Gastroesophageal Reflux After Lung Transplantation". *JHLT* (2008);27(2): S109.

Duan, H., Ning, M., Chen, X., Zou, Q., Zhang, L., Feng, Y., et al. (2012). Design, Synthesis, and Antidiabetic Activity of 4-Phenoxynicotinamide and 4-Phenoxypyrimidine-5-carboxamide Derivatives as Potent and Orally Efficacious TGR5 Agonists. *J Med Chem* 55, 10475–10489. doi: 10.1021/jm301071h.

Duan, T., Cil, O., Tse, C. M., Sarker, R., Lin, R., Donowitz, M., et al. (2019). Inhibition of CFTR-mediated intestinal chloride secretion as potential therapy for bile acid diarrhea. *The FASEB Journal* 33, 10924–10934. doi: 10.1096/fj.201901166R.

Dumoulin, g. (1982). Aspiration of gastric bacteria in antacid-treated patients: a frequent cause of postoperative colonisation of the airway. *The lancet* 319, 242–245. Doi: 10.1016/s0140-6736(82)90974-6.

Fass, r., boeckxstaens, g. E., el-serag, h., rosen, r., sifrim, D., and Vaezi, M. F. (2021). Gastro-oesophageal reflux disease. *Nat Rev Dis Primers* 7, 55. doi: 10.1038/s41572-021-00287-w.

Felton, J., Hu, S., and Raufman, J.-P. (2018). Targeting M3 Muscarinic Receptors for Colon Cancer Therapy. *Curr Mol Pharmacol* 11, 184–190. doi: 10.2174/1874467211666180119115828.

Fiorucci, S., Biagioli, M., Zampella, A., and Distrutti, E. (2018). Bile Acids Activated Receptors Regulate Innate Immunity. *Front Immunol* 9. doi: 10.3389/fimmu.2018.01853.

Fletcher, J. (2004). Studies of acid exposure immediately above the gastro-oesophageal squamocolumnar junction: evidence of short segment reflux. *Gut* 53, 168–173. doi: 10.1136/gut.2003.022160.

Flynn, C., Montrose, D. C., Swank, D. L., Nakanishi, M., Ilsley, J. N. M., and Rosenberg, D. W. (2007). Deoxycholic acid promotes the growth of colonic aberrant crypt foci. *Mol Carcinog* 46, 60–70. doi: 10.1002/mc.20253.

Frankhuisen, R., van Herwaarden, M. A., Scheffer, R. C., Hebbard, G. S., Gooszen, H. G., and Samsom, M. (2009). Increased intragastric pressure gradients are involved in the occurrence of acid reflux in gastroesophageal reflux disease. *Scand J Gastroenterol* 44, 545–550. doi: 10.1080/00365520902718903.

Freel, R. W., Hatch, M., Earnest, D. L., and Goldner, A. M. (1983). Dihydroxy bile salt-induced alterations in NaCl transport across the rabbit colon. *American Journal of Physiology-Gastrointestinal and Liver Physiology* 245, G808–G815. doi: 10.1152/ajpgi.1983.245.6.G808.

García-Cañaveras, J. C., Donato, M. T., Castell, J. v., and Lahoz, A. (2012). Targeted profiling of circulating and hepatic bile acids in human, mouse, and rat using a UPLC-MRM-MS-validated method. *J Lipid Res* 53, 2231–2241. doi: 10.1194/jlr.D028803.

Ghosh, S. K., Kahrilas, P. J., and Brasseur, J. G. (2008). Liquid in the gastroesophageal segment promotes reflux, but compliance does not: a mathematical modeling study. *American Journal of Physiology-Gastrointestinal and Liver Physiology* 295, G920–G933. doi: 10.1152/ajpgi.90310.2008.

Gipson, K. S., Nickerson, K. P., Drenkard, E., Llanos-Chea, A., Dogiparthi, S. K., Lanter, B. B., et al. (2020). The Great ESKAPE: Exploring the Crossroads of Bile and Antibiotic Resistance in Bacterial Pathogens. *Infect Immun* 88. doi: 10.1128/IAI.00865-19.

Gombart, A. F. (2009). The vitamin D–antimicrobial peptide pathway and its role in protection against infection. *Future Microbiol* 4, 1151–1165. doi: 10.2217/fmb.09.87.

Gombart, A. F., Borregaard, N., and Koeffler, H. P. (2005). Human cathelicidin antimicrobial peptide (CAMP) gene is a direct target of the vitamin D receptor and is strongly up-regulated in myeloid cells by 1,25-dihydroxyvitamin D $_3$. *The FASEB Journal* 19, 1067–1077. doi: 10.1096/fj.04-3284com.

Goyal, R. K., and Chaudhury, A. (2008). Physiology of Normal Esophageal Motility. *J Clin Gastroenterol* 42, 610–619. doi: 10.1097/MCG.0b013e31816b444d.

Gyawali, C. P., Kahrilas, P. J., Savarino, E., Zerbib, F., Mion, F., Smout, A. J. P. M., et al. (2018). Modern diagnosis of GERD: the Lyon Consensus. *Gut* 67, 1351–1362. doi: 10.1136/gutjnl-2017-314722.

HAKONARSON, H., and GRUNSTEIN, M. M. (1998). Regulation of Second Messengers Associated with Airway Smooth Muscle Contraction and Relaxation. *Am J Respir Crit Care Med* 158, S115–S122. doi: 10.1164/ajrccm.158.supplement_2.13tac700.

Hamilton, J. P., Xie, G., Raufman, J.-P., Hogan, S., Griffin, T. L., Packard, C. A., et al. (2007). Human cecal bile acids: concentration and spectrum. *American Journal of Physiology-Gastrointestinal and Liver Physiology* 293, G256–G263. doi: 10.1152/ajpgi.00027.2007.

Harris, S. C., Devendran, S., Méndez- García, C., Mythen, S. M., Wright, C. L., Fields, C. J., et al. (2018). Bile acid oxidation by *Eggerthella lenta* strains C592 and DSM 2243 ^{T}. *Gut Microbes*, 1–17. doi: 10.1080/19490976.2018.1458180.

Hendrick, S. M., Mroz, M. S., Greene, C. M., Keely, S. J., and Harvey, B. J. (2014). Bile acids stimulate chloride secretion through CFTR and calcium-activated Cl^- channels in Calu-3 airway epithelial cells. *American Journal of Physiology-Lung Cellular and Molecular Physiology* 307, L407–L418. doi: 10.1152/ajplung.00352.2013.

Herman-Edelstein, M., Weinstein, T., and Levi, M. (2018). Bile acid receptors and the kidney. *Curr Opin Nephrol Hypertens* 27, 56–62. doi: 10.1097/MNH.0000000000000374.

Herraez, E., Lozano, E., Poli, E., Keitel, V., de Luca, D., Williamson, C., et al. (2014). Role of macrophages in bile acid-induced inflammatory response of fetal lung during maternal cholestasis. *J Mol Med* 92, 359–372. doi: 10.1007/s00109-013-1106-1.

Hershcovici, T., Jha, L. K., Johnson, T., Gerson, L., Stave, C., Malo, J., et al. (2011). Systematic review: the relationship between interstitial lung diseases and gastro-oesophageal reflux disease. *Aliment Pharmacol Ther* 34, 1295–1305. doi: 10.1111/j.1365-2036.2011.04870.x.

Hofmann, A. F. The continuing importance of bile acids in liver and intestinal disease. *Arch Intern Med* 159, 2647–58. doi: 10.1001/archinte.159.22.2647.

Hoshino, M., Sundaram, A., and Mittal, S. K. (2011). Role of the Lower Esophageal Sphincter on Acid Exposure Revisited with High-Resolution Manometry. *J Am Coll Surg* 213, 743–750. doi: 10.1016/j.jamcollsurg.2011.09.002.

Hotta, K., Emala, C. W., and Hirshman, C. A. (1999). TNF-alpha upregulates Gialpha and Gqalpha protein expression and function in human airway smooth muscle cells. *Am J Physiol* 276, L405-11. doi: 10.1152/ajplung.1999.276.3.L405.

Hsu, W.-T., Lai, C.-C., Wang, Y.-H., Tseng, P.-H., Wang, K., Wang, C.-Y., et al. (2017). Risk of pneumonia in patients with gastroesophageal reflux disease: A population-based cohort study. *PLoS One* 12, e0183808. doi: 10.1371/journal.pone.0183808.

Hylemon, P. B., Harris, S. C., and Ridlon, J. M. (2018). Metabolism of hydrogen gases and bile acids in the gut microbiome. *FEBS Lett* 592, 2070–2082. doi: 10.1002/1873-3468.13064.

Ilyaskin, A. v., Diakov, A., Korbmacher, C., and Haerteis, S. (2016). Activation of the Human Epithelial Sodium Channel (ENaC) by Bile Acids Involves the Degenerin Site. *Journal of Biological Chemistry* 291, 19835–19847. doi: 10.1074/jbc.M116.726471.

Ilyaskin, A. v., Diakov, A., Korbmacher, C., and Haerteis, S. (2017). Bile acids potentiate proton-activated currents in *Xenopus laevis* oocytes expressing human acid-sensing ion channel (ASIC1a). *Physiol Rep* 5, e13132. doi: 10.14814/phy2.13132.

Ilyaskin, A. v., Kirsch, S. A., Böckmann, R. A., Sticht, H., Korbmacher, C., Haerteis, S., et al. (2018). The degenerin region of the human bile acid-sensitive ion channel (BASIC) is involved in channel inhibition by calcium and activation by bile acids. *Pflugers Arch* 470, 1087–1102. doi: 10.1007/s00424-018-2142-z.

Inagaki, T., Moschetta, A., Lee, Y.-K., Peng, L., Zhao, G., Downes, M., et al. (2006). Regulation of antibacterial defense in the small intestine by the nuclear bile acid receptor. *Proceedings of the National Academy of Sciences* 103, 3920–3925. doi: 10.1073/pnas.0509592103.

INGENITO, E. P., MORA, R., and MARK, L. (2000). Pivotal Role of Anionic Phospholipids in Determining Dynamic Behavior of Lung Surfactant. *Am J Respir Crit Care Med* 161, 831–838. doi: 10.1164/ajrccm.161.3.9903048.

Inglis, T. J. J., Sherratt, M. J., Sproat, L. J., Hawkey, P. M., and Gibson, J. S. (1993). Gastroduodenal dysfunction and bacterial colonisation of the ventilated lung. *The Lancet* 341, 911–913. doi: 10.1016/0140-6736(93)91208-4.

Ji, C.-G., Xie, X.-L., Yin, J., Qi, W., Chen, L., Bai, Y., et al. (2017). Bile acid receptor TGR5 overexpression is associated with decreased intestinal mucosal injury and epithelial cell proliferation in obstructive jaundice. *Translational Research* 182, 88–102. doi: 10.1016/j.trsl.2016.12.001.

Johnston, N., Dettmar, P. W., Bishwokarma, B., Lively, M. O., and Koufman, J. A. (2007). Activity/Stability of Human Pepsin: Implications for Reflux Attributed Laryngeal Disease. *Laryngoscope* 117, 1036–1039. doi: 10.1097/MLG.0b013e31804154c3.

Jonsson, E. W. (1998). Functional characterisation of receptors for cysteinyl leukotrienes in smooth muscle. *Acta Physiol Scand Suppl* 641, 1–55.

Jooste, E., Zhang, Y., and Emala, C. W. (2005). Rapacuronium Preferentially Antagonizes the Function of M2 versus M3 Muscarinic Receptors in Guinea Pig Airway Smooth Muscle. *Anesthesiology* 102, 117–124. doi: 10.1097/00000542-200501000-00020.

Kahrilas, P. J., Dodds, W. J., Dent, J., Haeberle, B., Hogan, W. J., and Arndorfer, R. C. (1987). Effect of sleep, spontaneous gastroesophageal reflux, and a meal on upper esophageal sphincter pressure in normal human volunteers. *Gastroenterology* 92, 466–471. doi: 10.1016/0016-5085(87)90143-0.

Keely, S. J., Urso, A., Ilyaskin, A. v., Korbmacher, C., Bunnett, N. W., Poole, D. P., et al. (2022). Contributions of bile acids to gastrointestinal physiology as receptor agonists and modifiers of ion channels. *American Journal of Physiology-Gastrointestinal and Liver Physiology* 322, G201–G222. doi: 10.1152/ajpgi.00125.2021.

Klag, T., Thomas, M., Ehmann, D., Courth, L., Mailänder-Sanchez, D., Weiss, T. S., et al. (2018). β-Defensin 1 Is Prominent in the Liver and Induced During Cholestasis by Bilirubin and Bile Acids via Farnesoid X Receptor and Constitutive Androstane Receptor. *Front Immunol* 9. doi: 10.3389/fimmu.2018.01735.

Kliewer, S. A., Goodwin, B., and Willson, T. M. (2002). The Nuclear Pregnane X Receptor: A Key Regulator of Xenobiotic Metabolism. *Endocr Rev* 23, 687–702. doi: 10.1210/er.2001-0038.

Krill, T., Baliss, M., Roark, R., Sydor, M., Samuel, R., Zaibaq, J., et al. (2019). Accuracy of endoscopic ultrasound in esophageal cancer staging. *J Thorac Dis* 11, S1602–S1609. doi: 10.21037/jtd.2019.06.50.

KULLAK-UBLICK, G. A., STIEGER, B., HAGENBUCH, B., and MEIER, P. J. (2000). Hepatic Transport of Bile Salts. *Semin Liver Dis* Volume 20, 273–292. doi: 10.1055/s-2000-9426.

Lajczak-McGinley, N. K., Porru, E., Fallon, C. M., Smyth, J., Curley, C., McCarron, P. A., et al. (2020). The secondary bile acids, ursodeoxycholic acid and lithocholic acid, protect against intestinal inflammation by inhibition of epithelial apoptosis. *Physiol Rep* 8. doi: 10.14814/phy2.14456.

Lee, A. S., Lee, J. S., He, Z., and Ryu, J. H. (2020). Reflux-Aspiration in Chronic Lung Disease. *Ann Am Thorac Soc* 17, 155–164. doi: 10.1513/AnnalsATS.201906-427CME.

Lee, A. S., and Ryu, J. H. (2018). Aspiration Pneumonia and Related Syndromes. *Mayo Clin Proc* 93, 752–762. doi: 10.1016/j.mayocp.2018.03.011.

Lefebvre, P., Cariou, B., Lien, F., Kuipers, F., and Staels, B. (2009). Role of Bile Acids and Bile Acid Receptors in Metabolic Regulation. *Physiol Rev* 89, 147–191. doi: 10.1152/physrev.00010.2008.

Leiva-Juárez, M. M., Urso, A., Costa, J., Stanifer, B. P., Sonett, J. R., Benvenuto, L., et al. (2021). Fundoplication after lung transplantation in patients with systemic sclerosis–related end-stage lung disease. *J Scleroderma Relat Disord* 6, 247–255. doi: 10.1177/23971983211016210.

Lenzig, P., Wirtz, M., and Wiemuth, D. (2019). Comparative electrophysiological analysis of the bile acid-sensitive ion channel (BASIC) from different species suggests similar physiological functions. *Pflugers Arch* 471, 329–336. doi: 10.1007/s00424-018-2223-z.

Lickteig, A. J., Csanaky, I. L., Pratt-Hyatt, M., and Klaassen, C. D. (2016). Activation of Constitutive Androstane Receptor (CAR) in Mice Results in Maintained Biliary Excretion of Bile Acids Despite a Marked Decrease of Bile Acids in Liver. *Toxicological Sciences* 151, 403–418. doi: 10.1093/toxsci/kfw054.

Lieu, T., Jayaweera, G., and Bunnett, N. W. (2014). GPBA: a GPCR for bile acids and an emerging therapeutic target for disorders of digestion and sensation. *Br J Pharmacol* 171, 1156–1166. doi: 10.1111/bph.12426.

Liu, D., Qian, T., Sun, S., and Jiang, J. J. (2021). Laryngopharyngeal Reflux and Inflammatory Responses in Mucosal Barrier Dysfunction of the Upper Aerodigestive Tract. *J Inflamm Res* Volume 13, 1291–1304. doi: 10.2147/JIR.S282809.

Ma, Y., Yang, X., Chatterjee, V., Wu, M. H., and Yuan, S. Y. (2021). The Gut-Lung Axis in Systemic Inflammation. Role of Mesenteric Lymph as a Conduit. *Am J Respir Cell Mol Biol* 64, 19–28. doi: 10.1165/rcmb.2020-0196TR.

Maeda, A., Kubo, T., Mishina, M., and Numa, S. (1988). Tissue distribution of mRNAs encoding muscarinic acetylcholine receptor subtypes. *FEBS Lett* 239, 339–342. doi: 10.1016/0014-5793(88)80947-5.

Makishima, M., Lu, T. T., Xie, W., Whitfield, G. K., Domoto, H., Evans, R. M., et al. (2002). Vitamin D Receptor As an Intestinal Bile Acid Sensor. *Science (1979)* 296, 1313–1316. doi: 10.1126/science.1070477.

Makishima, M., Okamoto, A. Y., Repa, J. J., Tu, H., Learned, R. M., Luk, A., et al. (1999). Identification of a Nuclear Receptor for Bile Acids. *Science (1979)* 284, 1362–1365. doi: 10.1126/science.284.5418.1362.

Masuda, T., Mittal, S. K., Kovacs, B., Smith, M., Walia, R., Huang, J., et al. (2018). Thoracoabdominal pressure gradient and gastroesophageal reflux: insights from lung transplant candidates. *Diseases of the Esophagus* 31. doi: 10.1093/dote/doy025.

McDonnell, M. J., O'Toole, D., Ward, C., Pearson, J. P., Lordan, J. L., de Soyza, A., et al. (2018). A qualitative synthesis of gastro-oesophageal reflux in bronchiectasis: Current understanding and future risk. *Respir Med* 141, 132–143. doi: 10.1016/j.rmed.2018.06.031.

Mekhjian, H. S., Phillips, S. F., and Hofmann, A. F. (1979). Colonic absorption of unconjugated bile acids. *Dig Dis Sci* 24, 545–550. doi: 10.1007/BF01489324.

Mertens, K. L., Kalsbeek, A., Soeters, M. R., and Eggink, H. M. (2017). Bile Acid Signaling Pathways from the Enterohepatic Circulation to the Central Nervous System. *Front Neurosci* 11. doi: 10.3389/fnins.2017.00617.

Mertens, V., Blondeau, K., van Oudenhove, L., Vanaudenaerde, B., Vos, R., Farre, R., et al. (2011). Bile Acids Aspiration Reduces Survival in Lung Transplant Recipients with BOS Despite Azithromycin. *American Journal of Transplantation* 11, 329–335. doi: 10.1111/j.1600-6143.2010.03380.x.

Meyer, K. C. (2015). Gastroesophageal reflux and lung disease. *Expert Rev Respir Med* 9, 383–385. doi: 10.1586/17476348.2015.1060858.

Mikov, M., Fawcett, J. P., Kuhajda, K., and Kevresan, S. (2006). Pharmacology of bile acids and their derivatives: Absorption promoters and therapeutic agents. *Eur J Drug Metab Pharmacokinet* 31, 237–251. doi: 10.1007/BF03190714.

Moschetta, A., Portincasa, P., Debellis, L., Petruzzelli, M., Montelli, R., Calamita, G., et al. (2003). Basolateral Ca2+-dependent K+-channels play a key role in Cl-secretion induced by taurodeoxycholate from colon mucosa. *Biol Cell* 95, 115–122. doi: 10.1016/S0248-4900(03)00011-X.

Mosińska, P., Szczepaniak, A., and Fichna, J. (2018). Bile acids and FXR in functional gastrointestinal disorders. *Digestive and Liver Disease* 50, 795–803. doi: 10.1016/j.dld.2018.05.016.

Mroz, M. S., and Harvey, B. J. (2019). Ursodeoxycholic acid inhibits ENaC and Na/K pump activity to restore airway surface liquid height in cystic fibrosis bronchial epithelial cells. *Steroids* 151, 108461. doi: 10.1016/j.steroids.2019.108461.

Mukherjee, S., Trice, J., Shinde, P., Willis, R. E., Pressley, T. A., and Perez-Zoghbi, J. F. (2013). Ca2+ oscillations, Ca2+ sensitization, and contraction activated by protein kinase C in small airway smooth muscle. *Journal of General Physiology* 141, 165–178. doi: 10.1085/jgp.201210876.

Mungan, Z., and Pinarbasi Simsek, B. (2020). Which drugs are risk factors for the development of gastroesophageal reflux disease? *The Turkish Journal of Gastroenterology* 28, S38–S43. doi: 10.5152/tjg.2017.11.

Nehring, J. A., Zierold, C., and DeLuca, H. F. (2007). Lithocholic acid can carry out *in vivo* functions of vitamin D. *Proceedings of the National Academy of Sciences* 104, 10006–10009. doi: 10.1073/pnas.0703512104.

Neujahr, D. C., Uppal, K., Force, S. D., Fernandez, F., Lawrence, C., Pickens, A., et al. (2014). Bile Acid Aspiration Associated With Lung Chemical Profile Linked to Other Biomarkers of Injury After Lung Transplantation. *American Journal of Transplantation* 14, 841–848. doi: 10.1111/ajt.12631.

Nicodème, F., Pipa-Muniz, M., Khanna, K., Kahrilas, P. J., and Pandolfino, J. E. (2014). Quantifying esophagogastric junction contractility with a novel HRM topographic metric, the EGJ-Contractile Integral: normative values and preliminary evaluation in PPI non-responders. *Neurogastroenterology & Motility* 26, 353–360. doi: 10.1111/nmo.12267.

Okwara, N. C., and Chan, W. W. (2021). Sorting out the Relationship Between Esophageal and Pulmonary Disease. *Gastroenterol Clin North Am* 50, 919–934. doi: 10.1016/j.gtc.2021.08.006.

Orr, W. (2000). Proximal migration of esophageal acid perfusions during waking and sleep. *Am J Gastroenterol* 95, 37–42. doi: 10.1016/S0002-9270(99)00728-5.

Parks, D. J., Blanchard, S. G., Bledsoe, R. K., Chandra, G., Consler, T. G., Kliewer, S. A., et al. (1999). Bile acids: natural ligands for an orphan nuclear receptor. *Science* 284, 1365–8. doi: 10.1126/science.284.5418.1365.

Peleman, C., Camilleri, M., Busciglio, I., Burton, D., Donato, L., and Zinsmeister, A. R. (2017). Colonic Transit and Bile Acid Synthesis or Excretion in Patients With Irritable Bowel Syndrome–Diarrhea Without Bile Acid Malabsorption. *Clinical Gastroenterology and Hepatology* 15, 720-727.e1. doi: 10.1016/j.cgh.2016.11.012.

Peng, Z., Heath, J., Drachenberg, C., Raufman, J.-P., and Xie, G. (2013). Cholinergic muscarinic receptor activation augments murine intestinal epithelial cell proliferation and tumorigenesis. *BMC Cancer* 13, 204. doi: 10.1186/1471-2407-13-204.

Perez-Zoghbi, J. F., Bai, Y., and Sanderson, M. J. (2010). Nitric oxide induces airway smooth muscle cell relaxation by decreasing the frequency of agonist-induced Ca2+ oscillations. *Journal of General Physiology* 135, 247–259. doi: 10.1085/jgp.200910365.

Perez-Zoghbi, J. F., and Sanderson, M. J. (2007). Endothelin-induced contraction of bronchiole and pulmonary arteriole smooth muscle cells is regulated by intracellular Ca^{2+} oscillations and Ca^{2+} sensitization. *American Journal of Physiology-Lung Cellular and Molecular Physiology* 293, L1000–L1011. doi: 10.1152/ajplung.00184.2007.

Pols, T. W. H., Nomura, M., Harach, T., lo Sasso, G., Oosterveer, M. H., Thomas, C., et al. (2011a). TGR5 activation inhibits atherosclerosis by reducing macrophage inflammation and lipid loading. *Cell Metab* 14, 747–57. doi: 10.1016/j.cmet.2011.11.006.

Pols, T. W. H., Noriega, L. G., Nomura, M., Auwerx, J., and Schoonjans, K. (2011b). The bile acid membrane receptor TGR5 as an emerging target in metabolism and inflammation. *J Hepatol* 54, 1263–1272. doi: 10.1016/j.jhep.2010.12.004.

Portincasa, P., Bonfrate, L., de Bari, O., Lembo, A., and Ballou, S. (2017). Irritable bowel syndrome and diet. *Gastroenterol Rep (Oxf)* 5, 11–19. doi: 10.1093/gastro/gow047.

Rajagopal, S., Kumar, D. P., Mahavadi, S., Bhattacharya, S., Zhou, R., Corvera, C. U., et al. (2013). Activation of G protein-coupled bile acid receptor, TGR5, induces smooth muscle relaxation via both Epac- and PKA-mediated inhibition of RhoA/Rho kinase pathway. *American Journal of Physiology-Gastrointestinal and Liver Physiology* 304, G527–G535. doi: 10.1152/ajpgi.00388.2012.

Raufman, J.-P., Chen, Y., Cheng, K., Compadre, C., Compadre, L., and Zimniak, P. (2002). Selective interaction of bile acids with muscarinic receptors: a case of molecular mimicry. *Eur J Pharmacol* 457, 77–84. doi: 10.1016/S0014-2999(02)02690-0.

Raufman, J.-P., Dawson, P. A., Rao, A., Drachenberg, C. B., Heath, J., Shang, A. C., et al. (2015). *Slc10a2* -null mice uncover colon cancer-promoting actions of endogenous fecal bile acids. *Carcinogenesis* 36, 1193–1200. doi: 10.1093/carcin/bgv107.

Raufman, J.-P., Zimniak, P., and Bartoszko-Malik, A. (1998). Lithocholyltaurine interacts with cholinergic receptors on dispersed chief cells from guinea pig stomach. *American Journal of Physiology-Gastrointestinal and Liver Physiology* 274, G997–G1004. doi: 10.1152/ajpgi.1998.274.6.G997.

Reen, F. J., Flynn, S., Woods, D. F., Dunphy, N., Chróinín, M. N., Mullane, D., et al. (2016). Bile signalling promotes chronic respiratory infections and antibiotic tolerance. *Sci Rep* 6, 29768. doi: 10.1038/srep29768.

Rhee, P.-L., Liu, J., Puckett, J. L., and Mittal, R. K. (2002). Measuring esophageal distension by high-frequency intraluminal ultrasound probe. *American Journal of Physiology-Gastrointestinal and Liver Physiology* 283, G886–G892. doi: 10.1152/ajpgi.00107.2002.

Ridlon, J. M., Harris, S. C., Bhowmik, S., Kang, D.-J., and Hylemon, P. B. (2016). Consequences of bile salt biotransformations by intestinal bacteria. *Gut Microbes* 7, 22–39. doi: 10.1080/19490976.2015.1127483.

Roffel, A. F., in't Hout, W. G., de Zeeuw, R. A., and Zaagsma, J. (1987). The M2 selective antagonist AF-DX 116 shows high affinity for mnscarine receptors in bovine tracheal membranes. *Naunyn Schmiedebergs Arch Pharmacol* 335, 593–595. doi: 10.1007/BF00169130.

Romero, F., Shah, D., Duong, M., Penn, R. B., Fessler, M. B., Madenspacher, J., et al. (2015). A Pneumocyte–Macrophage Paracrine Lipid Axis Drives the Lung toward Fibrosis. *Am J Respir Cell Mol Biol* 53, 74–86. doi: 10.1165/rcmb.2014-0343OC.

Rosen, R., Johnston, N., Hart, K., Khatwa, U., and Nurko, S. (2012). The presence of pepsin in the lung and its relationship to pathologic gastro-esophageal reflux. *Neurogastroenterology & Motility* 24, 129-e85. doi: 10.1111/j.1365-2982.2011.01826.x.

Ruiz de León San Juan, A. (2018). Lung transplantation and esophageal dysfunction. *Revista Española de Enfermedades Digestivas* 110. doi: 10.17235/reed.2018.5693/2018.

Russell, D. W. (2003). The Enzymes, Regulation, and Genetics of Bile Acid Synthesis. *Annu Rev Biochem* 72, 137–174. doi: 10.1146/annurev.biochem.72.121801.161712.

Said, A. H., Hu, S., Abutaleb, A., Watkins, T., Cheng, K., Chahdi, A., et al. (2017). Interacting post-muscarinic receptor signaling pathways potentiate matrix metalloproteinase-1 expression and invasion of human colon cancer cells. *Biochemical Journal* 474, 647–665. doi: 10.1042/BCJ20160704.

Sandhu, K. v., Sherwin, E., Schellekens, H., Stanton, C., Dinan, T. G., and Cryan, J. F. (2017). Feeding the microbiota-gut-brain axis: diet, microbiome, and neuropsychiatry. *Translational Research* 179, 223–244. doi: 10.1016/j.trsl.2016.10.002.

Savarino, V., Marabotto, E., Zentilin, P., Furnari, M., Bodini, G., de Maria, C., et al. (2020). Pathophysiology, diagnosis, and pharmacological treatment of gastro-esophageal reflux disease. *Expert Rev Clin Pharmacol* 13, 437–449. doi: 10.1080/17512433.2020.1752664.

Shapiro, H., Kolodziejczyk, A. A., Halstuch, D., and Elinav, E. (2018). Bile acids in glucose metabolism in health and disease. *Journal of Experimental Medicine* 215, 383–396. doi: 10.1084/jem.20171965.

Staudinger, J., Liu, Y., Madan, A., Habeebu, S., and Klaassen, C. D. (2001). Coordinate regulation of xenobiotic and bile acid homeostasis by pregnane X receptor. *Drug Metab Dispos* 29, 1467–72.

Stenman, L. K., Holma, R., Eggert, A., and Korpela, R. (2013). A novel mechanism for gut barrier dysfunction by dietary fat: epithelial disruption by hydrophobic bile acids. *American Journal of Physiology-Gastrointestinal and Liver Physiology* 304, G227–G234. doi: 10.1152/ajpgi.00267.2012.

Stovold, R., Forrest, I. A., Corris, P. A., Murphy, D. M., Smith, J. A., Decalmer, S., et al. (2007). Pepsin, a Biomarker of Gastric Aspiration in Lung Allografts. *Am J Respir Crit Care Med* 175, 1298–1303. doi: 10.1164/rccm.200610-1485OC.

Su, K.-C., Wu, Y.-C., Chen, C.-S., Hung, M.-H., Hsiao, Y.-H., Tseng, C.-M., et al. (2013). Bile acids increase alveolar epithelial permeability via mitogen-activated protein kinase, cytosolic phospholipase A_2, cyclooxygenase-2, prostaglandin E_2 and junctional proteins. *Respirology* 18, 848–856. doi: 10.1111/resp.12086.

Swann, J. R., Want, E. J., Geier, F. M., Spagou, K., Wilson, I. D., Sidaway, J. E., et al. (2011). Systemic gut microbial modulation of bile acid metabolism in host tissue compartments. *Proceedings of the National Academy of Sciences* 108, 4523–4530. doi: 10.1073/pnas.1006734107.

Sweet, M. P., Patti, M. G., Hoopes, C., Hays, S. R., and Golden, J. A. (2009). Gastro-oesophageal reflux and aspiration in patients with advanced lung disease. *Thorax* 64, 167–173. doi: 10.1136/thx.2007.082719.

Tabei, I., Kubo, H., Yano, F., and Inada, H. (2003). The Effect of Viscosity Regulating Solution for Enteral Nutrition Against Gastro Esophageal Reflux. *The Japanese Journal of Gastroenterological Surgery* 36, 71–77. doi: 10.5833/jjgs.36.71.

TAMHANKAR, A., PETERS, J., PORTALE, G., HSIEH, C., HAGEN, J., BREMNER, C., et al. (2004). Omeprazole does not reduce gastroesophageal reflux: new insights using multichannel intraluminal impedance technology. *Journal of Gastrointestinal Surgery* 8, 888–896. doi: 10.1016/j.gassur.2004.08.001.

Tan, X., and Sanderson, M. J. (2014). Bitter tasting compounds dilate airways by inhibiting airway smooth muscle calcium oscillations and calcium sensitivity. *Br J Pharmacol* 171, 646–662. doi: 10.1111/bph.12460.

Taranto, M. P., Perez-Martinez, G., and Font de Valdez, G. (2006). Effect of bile acid on the cell membrane functionality of lactic acid bacteria for oral administration. *Res Microbiol* 157, 720–5. doi: 10.1016/j.resmic.2006.04.002.

Thomas, C., Pellicciari, R., Pruzanski, M., Auwerx, J., and Schoonjans, K. (2008). Targeting bile-acid signalling for metabolic diseases. *Nat Rev Drug Discov* 7, 678–693. doi: 10.1038/nrd2619.

Tobey, N., Carson, J., Alkiek, R., and Orlando, R. (1996). Dilated intercellular spaces: A morphological feature of acid reflux-- damaged human esophageal epithelium. *Gastroenterology* 111, 1200–1205. doi: 10.1053/gast.1996.v111.pm8898633.

Townsend, E. A., and Emala, C. W. (2013). Quercetin acutely relaxes airway smooth muscle and potentiates β-agonist-induced relaxation via dual phosphodiesterase inhibition of PLCβ and PDE4. *American Journal of Physiology-Lung Cellular and Molecular Physiology* 305, L396–L403. doi: 10.1152/ajplung.00125.2013.

Townsend, E. A., Zhang, Y., Xu, C., Wakita, R., and Emala, C. W. (2014). Active components of ginger potentiate β-agonist-induced relaxation of airway smooth muscle by modulating cytoskeletal regulatory proteins. *Am J Respir Cell Mol Biol* 50, 115–24. doi: 10.1165/rcmb.2013-0133OC.

Tripathi, M., Streutker, C. J., and Marginean, E. C. (2018). Relevance of histology in the diagnosis of reflux esophagitis. *Ann N Y Acad Sci* 1434, 94–101. doi: 10.1111/nyas.13742.

Urso, A., Briganti, D. F., Costa, J., Nandakumar, R., Robbins, H., Shah, L., et al. (2018). Bile Acid Aspiration is Associated with Airway Infections: A Targeted Metabolomic Approach. *The Journal of Heart and Lung Transplantation* 37, S462. doi: 10.1016/j.healun.2018.01.1201.

Urso, A., Leiva-Juárez, M. M., Briganti, D. F., Aramini, B., Benvenuto, L., Costa, J., et al. (2021). Aspiration of conjugated bile acids predicts adverse lung transplant outcomes and correlates with airway lipid and cytokine dysregulation. *The Journal of Heart and Lung Transplantation* 40, 998–1008. doi: 10.1016/j.healun.2021.05.007.

Vaezi, M. F., Brunton, S., Mark Fendrick, A., Howden, C. W., Atkinson, C., Pelletier, C., et al. (2022). Patient journey in erosive oesophagitis: real-world perspectives from US physicians and patients. *BMJ Open Gastroenterol* 9, e000941. doi: 10.1136/bmjgast-2022-000941.

Vakil, N., van Zanten, S. v., Kahrilas, P., Dent, J., and Jones, R. (2006). The Montreal Definition and Classification of Gastroesophageal Reflux Disease: A Global Evidence-Based Consensus. *Am J Gastroenterol* 101, 1900–1920. doi: 10.1111/j.1572-0241.2006.00630.x.

Vakil, N., Vieth, M., Wernersson, B., Wissmar, J., and Dent, J. (2017). Diagnosis of gastro-oesophageal reflux disease is enhanced by adding oesophageal histology and excluding epigastric pain. *Aliment Pharmacol Ther* 45, 1350–1357. doi: 10.1111/apt.14028.

van de Peppel, I. P., Bodewes, F. A. J. A., Verkade, H. J., and Jonker, J. W. (2019). Bile acid homeostasis in gastrointestinal and metabolic complications of cystic fibrosis. *Journal of Cystic Fibrosis* 18, 313–320. doi: 10.1016/j.jcf.2018.08.009.

van Meer, G., Voelker, D. R., and Feigenson, G. W. (2008). Membrane lipids: where they are and how they behave. *Nat Rev Mol Cell Biol* 9, 112–124. doi: 10.1038/nrm2330.

Verleden, S. E., Vos, R., Mertens, V., Willems-Widyastuti, A., de Vleeschauwer, S. I., Dupont, L. J., et al. (2011). Heterogeneity of chronic lung allograft dysfunction: Insights from protein expression in broncho alveolar lavage. *The Journal of Heart and Lung Transplantation* 30, 667–673. doi: 10.1016/j.healun.2010.12.008.

Volpe, B. T., and Binder, H. J. (1975). Bile salt alteration of ion transport across jejunal mucosa. *Biochimica et Biophysica Acta (BBA) - Biomembranes* 394, 597–604. doi: 10.1016/0005-2736(75)90145-5.

Wang, H., He, Q., Wang, G., Xu, X., and Hao, H. (2018). FXR modulators for enterohepatic and metabolic diseases. *Expert Opin Ther Pat* 28, 765–782. doi: 10.1080/13543776.2018.1527906.

Wang, T.-T., Nestel, F. P., Bourdeau, V., Nagai, Y., Wang, Q., Liao, J., et al. (2004). Cutting Edge: 1,25-Dihydroxyvitamin D $_3$ Is a Direct Inducer of Antimicrobial Peptide Gene Expression. *The Journal of Immunology* 173, 2909–2912. doi: 10.4049/jimmunol.173.5.2909.

Ward, J. B. J., Mroz, M. S., and Keely, S. J. (2013). The bile acid receptor, TGR5, regulates basal and cholinergic-induced secretory responses in rat colon. *Neurogastroenterology & Motility* 25, 708–711. doi: 10.1111/nmo.12148.

Wedegaertner, P. B., Chu, D. H., Wilson, P. T., Levis, M. J., and Bourne, H. R. (1993). Palmitoylation is required for signaling functions and membrane attachment of Gq alpha and Gs alpha. *J Biol Chem* 268, 25001–8.

White, J. P., Mills, J., and Eiser, N. M. (1987). Comparison of the effects of histamine H1- and H2-receptor agonists on large and small airways in normal and asthmatic subjects. *Br J Dis Chest* 81, 155–169. doi: 10.1016/0007-0971(87)90134-3.

Wiemuth, D., Lefèvre, C. M. T., Heidtmann, H., and Gründer, S. (2014). Bile acids increase the activity of the epithelial Na+ channel. *Pflugers Arch* 466, 1725–1733. doi: 10.1007/s00424-013-1403-0.

Wilshire, C. L., Salvador, R., Sepesi, B., Niebisch, S., Watson, T. J., Litle, V. R., et al. (2013). Reflux-Associated Oxygen Desaturations: Usefulness in Diagnosing Reflux-Related Respiratory Symptoms. *Journal of Gastrointestinal Surgery* 17, 30–38. doi: 10.1007/s11605-012-2065-5.

Woodland, P., and Sifrim, D. (2010). The refluxate: The impact of its magnitude, composition and distribution. *Best Pract Res Clin Gastroenterol* 24, 861–871. doi: 10.1016/j.bpg.2010.09.002.

Woods, D. F., Flynn, S., Caparrós-Martín, J. A., Stick, S. M., Reen, F. J., and O'Gara, F. (2021). Systems Biology and Bile Acid Signalling in Microbiome-Host Interactions in the Cystic Fibrosis Lung. *Antibiotics* 10, 766. doi: 10.3390/antibiotics10070766.

Wu, Y.-C., Hsu, P.-K., Su, K.-C., Liu, L.-Y., Tsai, C.-C., Tsai, S.-H., et al. (2009). Bile Acid Aspiration in Suspected Ventilator-Associated Pneumonia. *Chest* 136, 118–124. doi: 10.1378/chest.08-2668.

Xie, G., Drachenberg, C., Yamada, M., Wess, J., and Raufman, J.-P. (2005). Cholinergic agonist-induced pepsinogen secretion from murine gastric chief cells is mediated by M_1 and M_3 muscarinic receptors. *American Journal of Physiology-Gastrointestinal and Liver Physiology* 289, G521–G529. doi: 10.1152/ajpgi.00105.2004.

Xie, W., Radominska-Pandya, A., Shi, Y., Simon, C. M., Nelson, M. C., Ong, E. S., et al. (2001). An essential role for nuclear receptors SXR/PXR in detoxification of cholestatic bile acids. *Proceedings of the National Academy of Sciences* 98, 3375–3380. doi: 10.1073/pnas.051014398.

Yerian, L., Fiocca, R., Mastracci, L., Riddell, R., Vieth, M., Sharma, P., et al. (2011). Refinement and Reproducibility of Histologic Criteria for the Assessment of Microscopic Lesions in Patients with Gastroesophageal Reflux Disease: the Esohisto Project. *Dig Dis Sci* 56, 2656–2665. doi: 10.1007/s10620-011-1624-z.

Zhang, C. Y. K., Ahmed, M., Huszti, E., Levy, L., Hunter, S. E., Boonstra, K. M., et al. (2020). Bronchoalveolar bile acid and inflammatory markers to identify high-risk lung transplant recipients with reflux and microaspiration. *The Journal of Heart and Lung Transplantation* 39, 934–944. doi: 10.1016/j.healun.2020.05.006.

Zhang, J., Huang, W., Qatanani, M., Evans, R. M., and Moore, D. D. (2004). The Constitutive Androstane Receptor and Pregnane X Receptor Function Coordinately to Prevent Bile Acid-induced Hepatotoxicity. *Journal of Biological Chemistry* 279, 49517–49522. doi: 10.1074/jbc.M409041200.

Zhang, W., Huang, Y., Wu, Y., and Gunst, S. J. (2015). A novel role for RhoA GTPase in the regulation of airway smooth muscle contraction. *Can J Physiol Pharmacol* 93, 129–136. doi: 10.1139/cjpp-2014-0388.

Zhang, Y., Kast-Woelbern, H. R., and Edwards, P. A. (2003). Natural Structural Variants of the Nuclear Receptor Farnesoid X Receptor Affect Transcriptional Activation. *Journal of Biological Chemistry* 278, 104–110. doi: 10.1074/jbc.M209505200.

Zhangxue, H., Min, G., Jinning, Z., Yuan, S., li, W., Huapei, S., et al. (2012). Glycochenodeoxycholate induces rat alveolar epithelial type II cell death and inhibits

surfactant secretion in vitro. *Free Radic Biol Med* 53, 122–128. doi: 10.1016/j.freeradbiomed.2012.04.027.

Zhao, Y. D., Yun, H. Z. H., Peng, J., Yin, L., Chu, L., Wu, L., et al. (2014). De novo synthesize of bile acids in pulmonary arterial hypertension lung. *Metabolomics* 10, 1169–1175. doi: 10.1007/s11306-014-0653-y.